

**ALMA MATER STUDIORUM-UNIVERSITA' DI BOLOGNA**

**DOTTORATO DI RICERCA IN**

**SCIENZE BIOTECNOLOGICHE, BIOCOMPUTAZIONALI,  
FARMACEUTICHE E FARMACOLOGICHE**

**Ciclo XXXIII**

**Settore Concorsuale: 05/G1**

**Settore Scientifico Disciplinare: BIO/14**

**Modeling Alzheimer disease with iPSCs and mouse model  
for the identification of risk factors, new targets, and  
potential therapeutical strategies**

*Presentata da:* **Dott.ssa Agnese Graziosi**

**Coordinatore Dottorato**

Prof.ssa Maria Laura Bolognesi

**Supervisore**

Prof.ssa Patrizia Hrelia

**Co-supervisore**

Dott.ssa Fabiana Morroni

*Esame finale anno 2021*

“Qual è stato e qual è il motore della tua vita?  
Cos’è che ti spinge sempre a superarti?”

“Il motore della mia vita è la curiosità sono un’appassionata degli esseri umani e tutte le volte che vedo qualcosa che non ho mai visto è come se fossi ferro con un magnete, mi attrae tantissimo. Non sopporto i contesti noiosi, le persone che non sanno cambiare e la frase che odio di più è “si è fatto sempre così”.

Michela Murgia

<b>1</b>	<b>Abstract .....</b>	<b>1</b>
<b>2</b>	<b>Introduction .....</b>	<b>4</b>
	<b>2.1 Neurodegenerative disease.....</b>	<b>4</b>
	<b>2.2 Alzheimer’s disease.....</b>	<b>5</b>
	2.2.1 Epidemiology .....	6
	2.2.2 Risk factors.....	7
	2.2.3 Brain Changes Associated with Alzheimer’s Disease .....	10
	2.2.4 Diagnosis.....	12
	<b>2.3 Pathophysiology of AD.....</b>	<b>13</b>
	2.3.1 Amyloid.....	13
	2.3.2 Amyloid hypothesis implementation.....	14
	2.3.3 Tau hypothesis.....	16
	2.3.4 ApoE.....	17
	<b>2.4 Neuroinflammation.....</b>	<b>17</b>
	<b>2.5 Models to study AD.....</b>	<b>19</b>
	2.5.1 Animal Models.....	20
	2.5.2 The promises of new technologies for human disease models: iPSC and CRISPR/CAS technique	21
	<b>2.6 Treatments for AD.....</b>	<b>25</b>
	2.6.1 Cholinesterase inhibitors .....	25
	2.6.2 Anti-NMDA .....	26
	2.6.3 Neuroprotection .....	26
	2.6.3.1 Ferulic Acid.....	27
	2.6.4 Multi-target-directed ligands strategy.....	28
	2.6.4.1 Feruloyl-donepezil hybrids.....	29
<b>3</b>	<b>Project Purpose .....</b>	<b>31</b>
	<b>SECTION ONE.....</b>	<b>35</b>
<b>4</b>	<b>Aim Section One.....</b>	<b>36</b>
<b>5</b>	<b>Materials and Methods.....</b>	<b>39</b>
	<b>5.1 Reagents .....</b>	<b>39</b>
	<b>5.2 Animals.....</b>	<b>39</b>
	<b>5.3 Experimental design.....</b>	<b>40</b>
	<b>5.4 A<math>\beta</math><sub>1-42</sub> oligomers preparation and injection .....</b>	<b>41</b>
	<b>5.5 Donepezil hydrochloride and PQM130 preparations .....</b>	<b>41</b>
	<b>5.6 Behavioral analysis.....</b>	<b>42</b>
	<b>5.7 Morris Water Maze (MWM).....</b>	<b>42</b>
	<b>5.8 Y-Maze test.....</b>	<b>43</b>
	<b>5.9 Tissue preparation for immunohistochemistry and neurochemical analysis .....</b>	<b>43</b>
	<b>5.10 Determination of caspase-9 and -3 activations .....</b>	<b>43</b>
	<b>5.11 Determination of cellular redox status .....</b>	<b>44</b>
	<b>5.12 Determination of glutathione (GSH) content .....</b>	<b>44</b>
	<b>5.13 Western blotting .....</b>	<b>45</b>

5.14	Immunohistochemistry .....	45
5.15	Hematoxylin/eosin staining.....	45
5.16	Anti-Glial fibrillary acidic protein (GFAP) staining .....	46
5.17	Quantitative images analysis.....	46
5.18	RNA preparation and gene expression analysis .....	47
5.19	Statistical analysis .....	48
<b>6</b>	<b>Results .....</b>	<b>49</b>
6.1	PQM130 ameliorates cognitive deficits in mice .....	49
6.2	Effects of PQM130 on hippocampal cell death.....	51
6.3	PQM130 antagonizes oxidative stress in mice .....	54
6.4	PQM130 regulates GSK3 $\beta$ and ERK1/2 protein expressions in mice .....	56
6.5	PQM130 reduces neuroinflammation and astrocytic activation in mice.....	57
6.6	PQM130 modulates synaptic plasticity in mice.....	58
<b>7</b>	<b>Discussion .....</b>	<b>61</b>
	<b>SECTION TWO.....</b>	<b>66</b>
<b>8</b>	<b>Aim of the study.....</b>	<b>67</b>
<b>9</b>	<b>Materials and Methods.....</b>	<b>70</b>
9.1	ABCA7 Isogenic iPSC Lines Generation.....	70
9.1.1	Colony inspection .....	71
9.1.2	Karyotyping.....	71
9.1.3	Genomic variant analysis for genome-edited iPSCs .....	71
9.2	Astrocyte Differentiation.....	72
9.3	RNA-seq analysis of iPSC-derived cell lines .....	73
9.4	Amyloid $\beta$ up-take.....	73
9.5	Cholesterol Assay.....	74
9.6	Transferrin and EGF uptake assay.....	74
9.7	Lipid droplet analysis .....	75
9.8	Immunostaining analysis.....	75
9.9	Fluorescence microscopy .....	75
9.10	Quantification and statistical analysis .....	75
<b>10</b>	<b>Results .....</b>	<b>76</b>
10.1	Generation of human isogenic ABCA7 Y622* iPSCs .....	76
10.2	Generation of ABCA7 Y622* astrocytes .....	78
10.3	Gene expression and Gene set enrichment analysis of ABCA7 Y622* astrocytes.....	79
10.4	Effects of ABCA7 Y622* mutation on A $\beta$ clearance capacity.....	85
10.5	Effects of ABCA7 Y622* mutation on early endocytosis .....	86

10.6	Effects of ABCA7 Y622* mutation on lipids transport.....	87
10.7	Effects of ABCA7 Y622* mutation on intracellular lipid homeostasis .....	88
11	<i>Discussion</i> .....	90
12	<i>Conclusion</i> .....	95
13	<i>Bibliography</i> .....	98

# 1 Abstract

Neurodegeneration defines a set of pathological conditions characterized by the progressive and consistent loss of Central Nervous system functions. Alzheimer's disease (AD) is the most common neurodegenerative disease in older people. Because of the complex nature of AD, a combined pharmacological approach is needed to control neurodegenerative processes and manage the main symptoms. Donepezil is the first-line acetylcholinesterase inhibitor used for AD treatment. In the first part of this study, the experimental activity has been oriented to evaluate and characterize molecular and cellular mechanisms that contribute to neurodegeneration induced by the A $\beta$  oligomers and potential neuroprotective effects of the hybrids feruloyl-donepezil compound called PQM130 (Figure 1). The neuroprotective effects of PQM130 were also examined compared to donepezil in a murine AD model, obtained by intracerebroventricular (i.c.v.) injection of A $\beta_{1-42}$  oligomers (A $\beta_{1-42}$ O). The intraperitoneal administration of PQM130 (0.5-1 mg/kg) after i.c.v. A $\beta_{1-42}$ O injection improved learning and memory, protecting mice against the decline in spatial cognition. Moreover, it reduced oxidative stress, induced cell survival, and protein synthesis through the modulation of glycogen synthase kinase 3 $\beta$  (GSK3 $\beta$ ) and extracellular signal-regulated kinases (ERK1/2), and increased the brain derived neurotrophic factor (BDNF) and synaptophysin levels in mice hippocampus. Additionally, PQM130 treatment decreased A $\beta$ O-induced neuronal apoptosis, via the caspase pathway, and neuroinflammation. Interestingly, PQM130 modulated different pathways than donepezil, and it is more effective in counteracting A $\beta_{1-42}$ O damage. Therefore, our findings highlighted that PQM130 is a potent multi-functional agent against AD and could act as a promising neuroprotective compound for anti-AD drug development.

The second part of the experimental activity, carried out at the Massachusetts Institute of Technology (MIT), was focused on studying a loss of function variants of ABCA7 (Figure 2). ABCA7 regulates lipid metabolism and critically controls phagocytic function in macrophages, contributing to immune responses along with the host defense system. Genome-wide association studies (GWAS) have identified mutations in the

ABCA7 gene, which confer increased risk for late-onset AD. However, the mechanism by which ABCA7 can contribute to AD is not clear. To investigate the functions of ABCA7, CRISPR/Cas9 technology has been used to engineer human iPSCs and to carry the genetic variant Y622\*, which results in a premature stop codon, causing ABCA7 loss-of-function. From iPSCs, astrocytes have been generated. This study revealed the effects of ABCA7 loss in astrocytes. ABCA7 Y622\* mutation can induce dysfunctional endocytic trafficking, impairing A $\beta$  clearance. Loss of ABCA7 expression is involved in other aspects of AD pathogenesis, such as lipid dysregulation and cell homeostasis, all changes that could bring to synaptic susceptibility and neurodegeneration.

Based on the results, it has been confirmed that ABCA7 plays a crucial role in maintaining lipid compositions, thus regulating endocytic trafficking, which can significantly contribute to AD pathology. The results provide a better understanding of the role of ABCA7 in AD and pave the way to develop novel therapeutic strategies for ABCA7-associated AD pathology or AD itself. Though further experimental studies are needed to confirm the PQM130 neuroprotective role and ABCA7 function in AD, the results presented in this study provide a better understanding of AD's pathophysiology, show a new therapeutic approach to treat AD, and illustrate an innovative and different methodology for studying the disease.

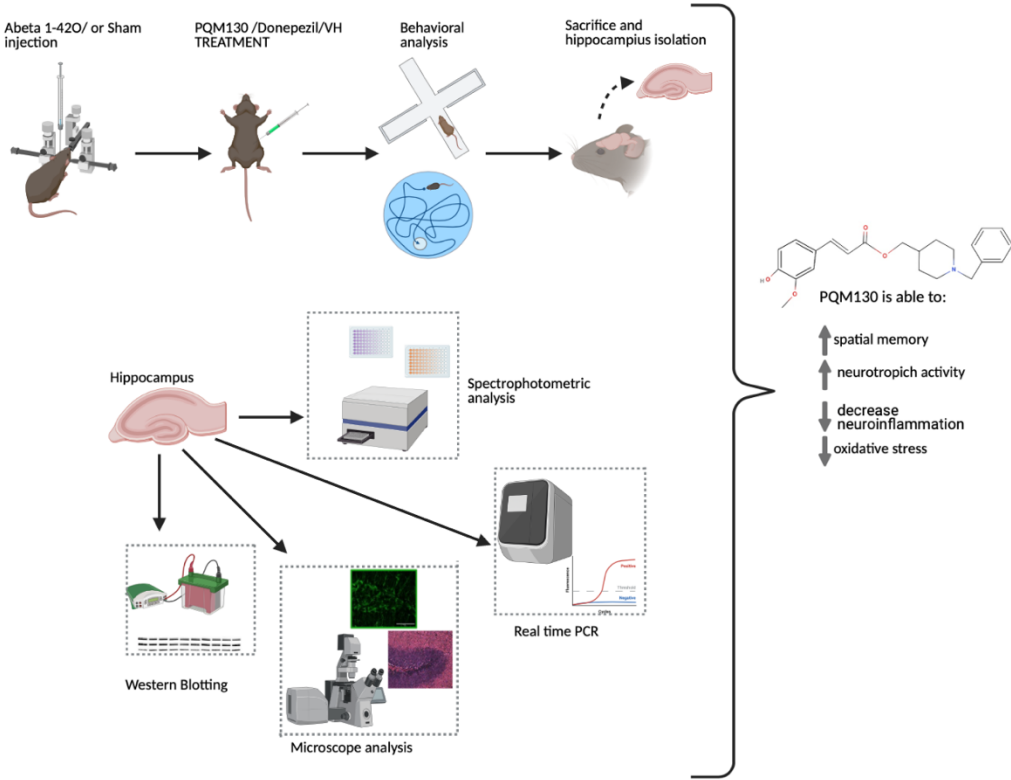


Figure 1 Graphical abstract Section One

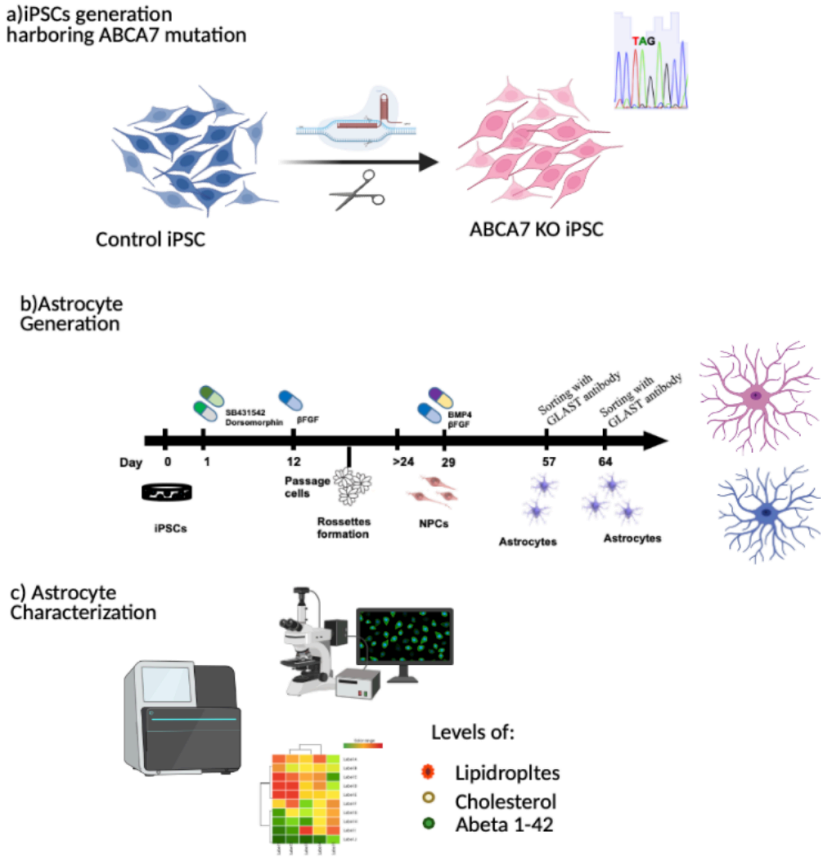


Figure 2 Graphical abstract Section two

## 2 Introduction

### 2.1 Neurodegenerative disease

The term "neurodegeneration" refers to a group of pathologies characterized by the slow and progressive loss of neurons in the central nervous system (CNS), responsible for both functional alterations and dementia. Clinical manifestations caused by neuronal damage are represented by mnemonic alterations, motor difficulties, cognitive and behavioral disorders.<sup>1</sup>

Brain degeneration in these diseases is determined by environmental factors and human genetic, and multiple cellular and molecular events, such as increased oxidative stress, inflammatory responses, trafficking dysregulation, and the formation of protein deposits and aggregates.<sup>2</sup>

Within risk factors for neurodegeneration, the aging process has by far the most influence.

To develop successful treatments, it is essential to consider the basic mechanisms of ageing and their role in the onset and progression of neurodegenerative disease. It is tempting, consequently, to look at neurodegenerative diseases as a manifestation of enhanced ageing. Contrariwise, ageing is a major risk factor for neurodegeneration.<sup>3</sup>

These diseases are a central problem not only for patients but also for the entire health system. As life expectancy increases, the elderly population is more likely to develop them.<sup>4</sup> Over the past decade, neurodegenerative diseases have been the subject of strong interest from all over the scientific world; however, so far, only palliative cares are available that are unable to slow or stop the progression of these pathologies.<sup>1</sup>

The most common neurodegenerative diseases are Alzheimer disease (AD) and Parkinson disease (PD), predominantly observed in elderly individuals. Common age-related neurodegenerative diseases and their estimated incidences are reported in Figure 3.<sup>5</sup>

Disease	Prevalence	Major symptoms	Risk factors	Neuropathological hallmarks
Alzheimer disease	5.7 million in the USA in 2018 (REF. <sup>3</sup> )	Impairment of learning and memory, speech difficulties	Age, family history, genetics, history of head trauma, female gender, vascular risk factors, environmental factors <sup>195–198</sup>	A $\beta$ plaques, neurofibrillary tangles, neuronal loss, neuroinflammation
Parkinson disease	2–3% of the global population aged >65 years in 2017 (REF. <sup>19</sup> )	Muscle rigidity, tremors, alterations in speech and gait	Environmental factors, genetics, male gender, ethnicity, age, psychiatric symptoms <sup>199,200</sup>	$\alpha$ -Synuclein-containing Lewy bodies and loss of dopaminergic neurons, grey matter atrophy <sup>201</sup>
Amyotrophic lateral sclerosis	0.6 cases per million globally in 2016 (REF. <sup>202</sup> )	Progressive motor defects, with muscle weakness, atrophy and spasms	Physical activity, familial aggregation, environmental and occupational exposure (for example, to pesticides, solvents or heavy metals), smoking, head injury, genetics <sup>202</sup>	TAR DNA-binding protein 43 aggregation
Huntington disease	5–7 per 100,000 white people in 2007 (REF. <sup>203</sup> )	Chorea, dystonia, loss of coordination, cognitive decline, behavioural difficulties	Genetic mutation in <i>HTT</i> , inheritance	Striatal atrophy, neuronal loss, psychiatric symptoms <sup>204,205</sup>
Dementia with Lewy bodies	1.3 million in the USA in 2014 (REF. <sup>206</sup> )	Visual hallucinations, movement disorders, cognitive problems, sleep difficulties, depression	Age >50 years, male gender, family history <sup>206</sup>	Lewy bodies and Lewy neurites
Ataxia telangiectasia	From 1 in 40,000 to 1 in 100,000 live births worldwide in 2016 (REF. <sup>207</sup> )	Cerebellar degeneration, immunodeficiency, radiation sensitivity, diabetes, cancer predisposition	Genetics (mutations in <i>ATM</i> gene)	Ataxia and telangiectasias
Cockayne syndrome	2–3 per million globally in 2008 (REF. <sup>208</sup> )	Growth failure, neurological disorders, photosensitivity, eye disorders, premature ageing	Genetics (mutations in <i>CSA</i> or <i>CSB</i> gene)	Growth retardation and neurodegeneration

Figure 3. Age-related neurodegenerative diseases from “Ageing as a risk factor for neurodegenerative disease”, Yujun Hou et al., *Nature reviews*, 2019.

## 2.2 Alzheimer’s disease

First described by Alois Alzheimer, AD is characterized by progressive cognitive decline, affecting short-term memory, but later also language, mood, movement, and physiological functions. In 1906, Alois Alzheimer recognized neuritic plaques and neurofibrillary tangles (NFTs) as neuropathologic features in certain patients' brains, and the illness was called Alzheimer's disease.<sup>6</sup> In the 1980s, amyloid  $\beta$ -peptide (A $\beta$ ) and hyperphosphorylated tau (pTau) were claimed as significant components of, correspondingly, neuritic plaques and NFTs of AD.<sup>7</sup>

AD is the most common cause of dementia. It is a heterogeneous and multifactor disease that is challenging to discriminate from other forms of dementia, such as vascular dementia, dementia with Lewy bodies, mixed dementia, and frontotemporal dementia. Understanding of AD has grown over the last 35 years. Before 2011, it was a clinical diagnosis that could only be confirmed by an autopsy.<sup>8</sup> Then, thanks to the identification of biomarkers, a premortem diagnosis became possible.<sup>9</sup> Now, AD is considered to be a long, degenerative process with a preclinical stage in which A $\beta$  and pTau start to aggregate but cognition abilities are preserved, followed by neurodegeneration and mild cognitive impairment (MCI), which can progress to clinical AD.<sup>10</sup>

Drug treatment that changes the course of the disease is perhaps the most unaddressed need for AD patients. Despite billions of dollars invested into clinical trials, a new AD drug has not been approved by the FDA since 2003.<sup>11 12</sup> Besides, no drugs have been approved to treat MCI. As of November 2020, more than 130 new molecular were in clinical trials for AD.<sup>13</sup> Though many AD drugs have failed in late-stage clinical trials, there is hope that at least one may receive regulatory agency approval soon.

## 2.2.1 Epidemiology

Worldwide, around 50 million people have dementia, 60% of them living in low- and middle-income countries. There are approximately 10 million new cases every year. At the moment, around 5-8% of the world's elderly population have dementia. The total number of people with dementia is projected to reach 82 million in 2030 and 152 in 2050 (Figure 4). AD is the most common form of dementia and may contribute to 60-70% of cases (World Health Organization, 2020).

The increase in incidence will not be homogeneous. Even if they have a huge number of patients, the developed countries will have a smaller increase in cases than the developing countries. The increased incidence in underdeveloped countries may be related to the concomitant increase in life expectancy.<sup>14</sup>

Most AD cases have a late onset, age is one of the main risk factors with a sharp increase after 65 years old.<sup>5</sup> Also, the incidence of AD among male and female is not the same. The risk of developing AD is three times higher in women than in men, even if this data could be misleading since they live longer<sup>15</sup> (Figure 5).

Among 65 years or older people diagnosed with AD, the mean survival is 4 to 8 years but can reach 20 years.<sup>16</sup> About 40% of patients with AD have severe dementia that requires treatments in a nursing home. A person living with AD between age 70 and 80 years is expected to have severe dementia for 4 years and live in a nursing home for most of that time.<sup>17</sup>

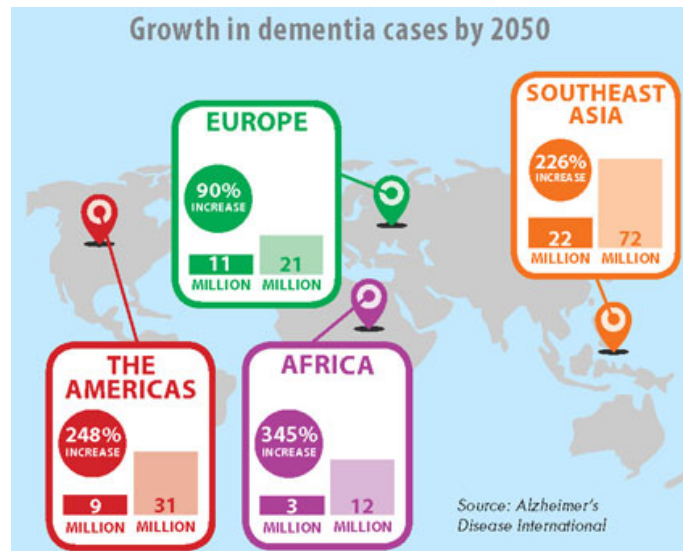


Figure 4. Growth dementia cases by 2050. Alzheimer's disease international 2013.

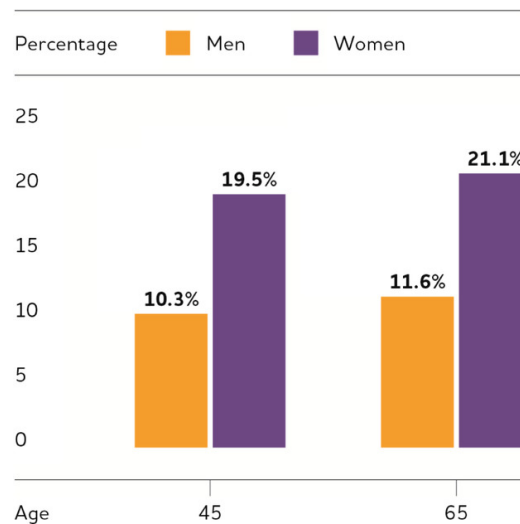


Figure 5. Percentage of AD among men and women by age in the USA.<sup>16</sup>

## 2.2.2 Risk factors

Risk factors can be divided into unmodifiable and modifiable.

Age is the most important among immutable risk factors, numerous studies have estimated that about 15% of patients are between 65 and 74 years of age, while 44% between 75 and 84.<sup>18</sup> Aging is a risk factor, but it is not necessary nor sufficient to cause AD. Besides aging itself, the other main unmodifiable risk factor for AD is the genetic background.

Based on its age of onset, AD is classified into early onset AD (EOAD, onset < 65 years), accounting for 1–5% of all cases, and late-onset AD (LOAD, onset ≥ 65 years),

accounting for >95% of affected.<sup>19</sup> EOAD is also called familial AD. EOAD and LOAD from a clinical point of view are indistinguishable except for a faster progression of the disease in the patient with EOAD.

Three genes are responsible for these familial types of AD: the gene coding for presenilin 1 (*PSEN1*) in chromosome 14, the gene coding for presenilin 2 (*PSEN2*) in chromosome 14, and the one coding for amyloid beta precursor protein (APP) in chromosome 21.<sup>20</sup> All of these genes encode for proteins involved in APP lysis and A $\beta$  generation. PSEN1 and APP mutations exhibit high penetrance (around 100%), which means that everyone harboring that mutation will develop AD. Instead, PSEN 2 mutation has a penetrance near 95%.<sup>21</sup>

Contrariwise, the genes involved in LOAD do not have such a clear correlation.

First-degree relatives of LOAD patients have twice the life-time risk expected of individuals without a first-degree relative affected by AD. Moreover, in monozygotic than in dizygotic co-twins, LOAD occurs more often, indicating a significant genetic contribution to this condition of ~60-80 percent.<sup>19</sup>

The genetic polymorphism in the apolipoprotein E (APOE) gene: the APOE  $\epsilon$ 4 allele, is one of the main risk factors for LOAD.<sup>22</sup> Comparing to  $\epsilon$ 3/ $\epsilon$ 3 carriers, the presence of one  $\epsilon$ 4 allele increase the risk of developing AD three times, whereas homozygous  $\epsilon$ 4 allele carriers develop AD up to 12 times more than individuals who do not have this allele.<sup>23</sup> Approximately 20–25% of the general population carries one or more  $\epsilon$ 4 alleles, whereas 50–65% of people with AD are  $\epsilon$ 4 carriers. In addition, the presence of at least one  $\epsilon$ 4 allele has been associated with reduced age at onset.<sup>24</sup> By contrast, some protection is provided by the rarer  $\epsilon$ 2 allele.<sup>22</sup> The risk of developing AD is reduced by half in  $\epsilon$ 2 allele individuals, delays its clinical onset, and reduces the formation of neuropathological changes usually reported in AD.<sup>25</sup>

APOE is a multifunctional protein that transports cholesterol and is involved in amyloid fibrils' genesis and plays a key role in the deposition of A $\beta$  in amyloid plaques.<sup>26</sup>

Whereas APOE  $\epsilon$ 4 is the strongest known genetic factor for sporadic AD, it is not necessary nor sufficient to cause AD, and it is not the only genetic risk factor.

Multiple susceptible loci have been found in many different genes, thanks to Genome-wide association studies (GWAS). These studies began with a limited sample size of

1,086 individuals in 2007, capable of recognizing only the APOE locus. In 2013, a meta-analysis of all existing GWAS was conducted by the International Genomics of Alzheimer's Project (IGAP) using data from 74 046 people, which until 2018 was the largest Alzheimer's disease GWAS. Twenty four susceptibility loci for AD were found in populations with European ancestry in this meta-analysis.<sup>27</sup> Three new GWAS in AD were released in 2018 and 2019.<sup>28,29,30</sup>

In total, 40 AD susceptibility loci reached genome-wide significance in at least one of the GWAS. Discovering 40 risk loci does not mean discovering 40 risk genes. Functional genomics studies have identified common or rare functional variants in APOE, CR1, BIN1, TREM2, CLU, SORL1, ADAM10, ABCA7, CD33, SPI1, and PILRA. While GWAS has made considerable progress in characterizing the genetic architecture of AD, a large amount remains to be done to identify functional genetic variants and biological mechanisms underlying the genetic loci correlation with AD.<sup>31</sup> Interestingly, it has been assumed that EOAD and LOAD have different patterns in the pathogenesis of A $\beta$  peptide deposition with a focus on overproduction and emphasis on decreased clearance in EOAD and LOAD, respectively.<sup>32</sup>

Increased attention is paid to modifiable risk factors, including alcohol consumption, blood pressure, diabetes, education, inflammation, hormonal therapy, hypercholesterolemia, especially if not monitored.<sup>33</sup>

Another risk factor for AD is head injuries. Many studies demonstrated that head injury could increase the risk of developing AD from twice to four times in moderate or severe damage.<sup>34</sup>

In summary, both EOAD and LOAD have a significant genetic component. However, susceptibility to AD development is seen as a dynamic interaction between environmental, lifestyle, and genetic influences, contributing to today's definition of AD as a multifactorial disease.<sup>34</sup>

### 2.2.3 Brain Changes Associated with Alzheimer's Disease

AD is a slow and progressive disorder caused by the gradual loss of neuronal function responsible for controlling capabilities. Two of the main changes present in an AD patient's brain, mainly in the neocortical area and in the hippocampus, are A $\beta$  plaques outside cells and NFTs of pTau inside cells, with atrophy and inflammation (Figure 6).<sup>7</sup> The presence of these aggregates could cause the activation of immune system cells, microglia, and astrocytes. Chronic inflammation is probably caused by the microglia not able to clear all the aggregates.<sup>35</sup>

The structure of NFTs has been extensively studied in the past few decades, and much has been known about their components. Ultrastructurally, the NFT is composed of abnormal fibrils measuring 10 nm in diameter that occur in pairs and are wound in a helical fashion with a regular periodicity of 80 nm.

Because of that, such structures are called paired helical filaments. Microtubule-associated tau protein is the main component of these tangles. It is essential to consider that tau protein in the NFTs is abnormally phosphorylated. Besides tau protein, other proteins are aggregated in the tangles such as ubiquitin, cholinesterases and A $\beta$ .<sup>36</sup>

The NFT's distribution is predictable, mainly in the entorhinal cortex, the CA1 and subicular regions of the hippocampus, the amygdala, and the deeper layers (layers III, V, and superficial VI) of the neocortex. It seems that the abundance and the distribution of tangles are correlated with the degree of dementia and the duration of illness, suggesting a pivotal role of these structures in AD.<sup>37</sup> However, it is also evident that other variables contribute to the disease's development and progression. It should be kept in mind that this neuropathological lesion may also appear in other disorders, like dementia or Parkinson disease.

Neuritic or senile plaque is the other pathological marker of AD. Neuritic plaques have a central core of A $\beta$ . A $\beta$  is originated from APP after the action of two secretases. Based on which type of secretases cut APP, it is possible to obtain longer or shorter peptides. Longer peptides with 42 or 43 amino acids tend to be deposited in the plaque, while shorter ones with 40 amino acids are more soluble than longer ones. The central core of senile plaques is made of a different type of protein, as APOE.<sup>38</sup>

Even if these two types of lesions, NFTs and neuritic plaques, are neuropathological markers of AD, only looking at these parameters is difficult to discriminate between elderly patients with AD from people of the same age without dementia.<sup>39</sup>

Neurodegeneration in AD starts 20 to 30 years before developing clinical symptoms during the so-called preclinical AD. AD develops along three phases continuum: preclinical disease, MCI, and clinically apparent dementia. While cognitive impairment progress over time, the progression of biomarkers occurs before the onset of symptoms. During MCI, minor symptoms appear without interfering with everyday activities. MCI is not necessarily the precursor of AD, it may be a natural aging process, or it could be due to other causes of dementia. Just 10-15% of patients with MCI develop AD every year.<sup>40</sup>

AD severity is characterized as mild, moderate, or severe, depending mainly on the ability to perform day-to-day tasks. In mild disease, patients may still drive and work but are likely to require assistance. In moderate AD, patients may have difficulties communicating and performing daily living activities, such as bathing and dressing. They may exhibit changes in personality and behavior. In severe AD, patients need substantial assistance with multiple activities, and probable require around-the-clock care. These patients may become bedbound because of damage to areas of the brain involved in movements.<sup>41</sup>

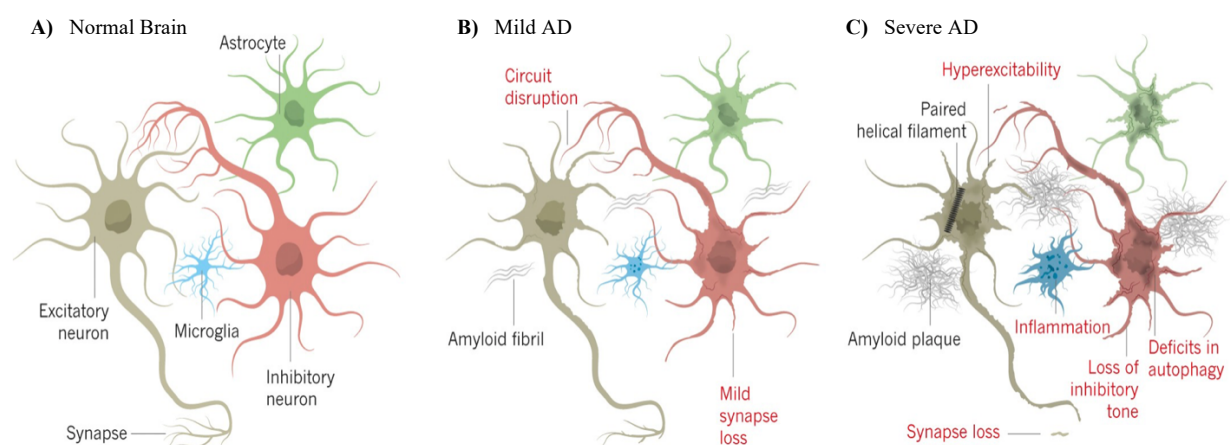


Figure 6. Representations of neurons and glial cells synaptic connections and functional circuits in normal brain, mild AD, and severe AD. A) Normal brain. B) Amyloid- $\beta$  fibrils starts to deposit in the extracellular space and contribute to early circuit dysfunction and the initiation of inflammatory processes. C) amyloid- $\beta$  plaques grow as NFTs inside the cells, inflammation and synapses reach an irreversible stage. Modified picture from Rebecca G. Canter et al.<sup>42</sup>

## 2.2.4 Diagnosis

Even if it is crucial an early and accurate diagnosis, an estimated 29% to 76% of patients with dementia in primary care are undiagnosed.<sup>43</sup> Clinical guidelines for a diagnosis of AD include a history of cognitive decline with a gradual onset and progressive course and documented cognitive deficiency in at least one field (attention, executive function, learning and memory, language, perceptual motor function).<sup>16</sup>

A correct diagnosis is based on cognitive and neurological examination and preferably involves information from close contacts about the patient's cognitive status.<sup>1</sup> The diagnostic evaluation may also include blood tests and magnetic resonance imaging to certificate neurodegeneration and exclude other forms of dementia and neurodegenerative diseases. Neuropsychological testing may be useful, but they are time consuming and may not be commonly available.<sup>44</sup>

Current diagnostic biomarkers that differentiate AD from other forms of dementia include brain imaging and cerebrospinal fluid (CSF) biomarkers. FDA-approved A $\beta$  positron emission tomography (PET).<sup>45</sup> It has been found that A $\beta$  PET was highly sensitive and specific for A $\beta$  pathology of AD and may increase classification accuracy.<sup>44</sup> Biomarkers play a crucial role in identifying eligible patients in clinical trials evaluating disease-modifying drugs for AD. It is under investigation, and it may be ready soon, a diagnostic imaging agent that identifies AD-associated tau pathology. PET and CSF biomarkers for A $\beta$  are invasive, expensive, time consuming, cause adverse effects, and are not broadly available. Biomarkers in clinical development may address these limitations. For example, a blood test for plasma ptau181 able to predict tau and A $\beta$  pathologies, identify AD across the clinical continuum, and differentiate it from other neurodegenerative diseases, is in validation studies.<sup>46</sup>

AD is a serious public health problem because patients are disabled and are relying on others for a considerable part of the disease. An early diagnosis is useful for medical care costs, patients and their families. Unfortunately, there are many obstacles to the early detection of AD because of a lack of evaluation instruments, training, time, and infrastructure, as previously described.

## 2.3 Pathophysiology of AD

### 2.3.1 Amyloid

Over the past years, extensive research efforts have been made to explain this peptide's underlying biology and its function in AD pathophysiology. A $\beta$  is produced by consecutive cleavage of APP by  $\beta$ -secretase and  $\gamma$ -secretase.<sup>47</sup> The  $\beta$ -secretase enzyme (BACE1) cleaves APP at the N-terminus of the A $\beta$  sequence, generating APP- $\beta$  and the membrane bound C99 fragment.<sup>48</sup> After BACE1 cut, the  $\gamma$ -secretase complex binds to fragment C99 and, in an intramembranous layer, cleaves the epsilon site releasing C-terminal fragment (CTF) and A $\beta$ 48. The complex keeps cutting along the remaining C-terminal end producing sequentially shorter peptides until the A $\beta$  peptide is released from the complex; they are usually 38, 40 and 42 amino acids in length (Figure 7).

The  $\gamma$ -secretase complex consists of four protein subunits: presenilin (PSEN), presenilin enhancer (PEN), APH and Nicastrin. There are multiple isoforms of PSEN (PSEN1/PSEN2).<sup>49</sup> A $\beta$  is produced predominantly in endosomes, and its release from neurons is modulated by presynaptic<sup>50</sup> and postsynaptic<sup>51</sup> activities. A $\beta$  peptides are likely to assemble into beta-sheet conformations in the form of oligomers, protofibrils, and fibrils found in the AD brain. Due to the increased hydrophobicity of A $\beta$ <sub>1-42</sub>, it has a higher tendency for aggregation.<sup>52</sup>

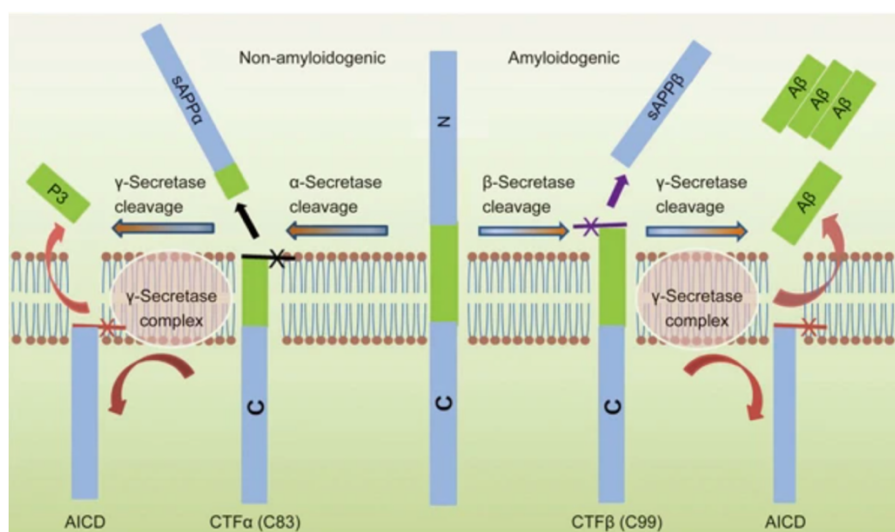


Figure 7. Human APP proteolytic pathways. Image from Chen et al.<sup>53</sup>

Assuming that deposition of A $\beta$  in the brain is the initiating step of AD pathogenesis, leading to subsequent tau deposition, neuron and synaptic loss, and cognitive decline, Hardy and Higgins proposed the amyloid cascade hypothesis in 1992.<sup>54</sup> Albeit portions have been revised or supplemented over time this hypothesis has been the leading model of AD pathogenesis since its first publication.<sup>55</sup>

The hypothesis is corroborated by the fact that in genetic forms of AD, as EOAD, Down syndrome or APP locus duplication, is reported an increase of A $\beta$ 42/40 ratio, a rise of A $\beta$  production, and deposition of NFTs, and it is possible to see typical AD pathology features.<sup>56</sup> Also, a rare APP mutation A673T is considered protective against AD because of decreased A $\beta$  production.<sup>57</sup> In addition, the most potent genetic risk factor for LOAD seems to increase risk via inducing A $\beta$  deposition and clearance alteration.<sup>58</sup> Although genetic evidence indicates the significance of the A $\beta$  aggregation in initiating the AD cascade, it seems evident that A $\beta$  is necessary but not sufficient, and other factors play a crucial role. For instance, there is a slight correlation between the level of amyloid deposition and the grade of cognitive impairment.<sup>59</sup> Finally, no amyloid-targeting treatment has managed to limit AD's progression, despite massive investment by the pharmaceutical industry in anti-amyloid therapies and numerous phase 3 clinical trials. These data imply that even if amyloid accumulation is central to initiate the pathological process, other events like neuroinflammation and tau accumulation may be the main drivers of neurodegeneration.

### 2.3.2 Amyloid hypothesis implementation

One implementation of the amyloid hypothesis is the one proposed by Bart De Strooper and Eric Karran.<sup>60</sup> They hypothesized a "biochemical phase", a "cellular phase" and a "clinical phase". The "biochemical phase" is characterized by qualitative changes more than quantitative. In the "biochemical phase" starts the deposition of amyloid plaques and neuronal tangles, cells are subjected to proteopathic stress. These aggregates interact with proteins and membranes of different cells type, altering signaling and functions. First of all, they bind APP and tau disturbing the standard function of these proteins in neurotransmission.<sup>61</sup>

It is a loop where the proteostatic network, compromised by age, could increase proteins' accumulation; conversely, protein aggregates might alter the process responsible for protein folding and aggregates clearance.<sup>62</sup> The lysosomal and endosomal systems play a pivotal role in this phase. In AD brains, several studies reported an increase in phagosomes, especially in the disorder's early stage.<sup>63</sup> It should be clear that this "biochemical phase" is a slow, gradual process, in any way overwhelming or irreversible. Processes activated in this phase are physiological and can be cell-dependent. Inflammatory responses are necessary to sustain homeostasis. Only when these compensating mechanisms turn into chronic, irreversible, and pathological processes that the disease progresses inevitably.<sup>60</sup> The transition from an early reversible to a chronic irreversible cellular response is critical in disease development. The stress of the "biochemical phase" results in the "cellular phase" of AD. Specifically, the cellular phase is characterized by dysfunction of the neurovascular unit, abnormal neuronal network activity, and compromised astrocyte and microglia functions. The "clinical phase" of the disease is initiated when the cellular reaction can no longer maintain homeostasis.<sup>60</sup> The clearance system is complex and involves different cells type. The blood brain barrier is made of endothelial cells and astroglia. Gap junctions allow passage of A $\beta$  and tau, making the glia barrier relatively easy to cross. However, the endothelial barrier is not permeable and passage of A $\beta$  and tau is regulated by specialized transport proteins as LDL receptor and ABC transporter, allowing egress to the circulation. The astroglia population seems to have a central role in the cellular phase of AD, and its responsibility for the disease is under investigation. The metabolic function of astroglia is well documented. Astroglia and oligodendrocytes synthesize brain cholesterol and secrete APOE packed together by ATP-binding cassette transporters. Cholesterol, produced by astroglia, is necessary for synaptogenesis. As suggested in GWAS, lipoprotein metabolism seems strongly associated with risk for AD.<sup>64</sup> Astroglia is well furnished to monitor neuronal activity and is fundamental to overall brain function. Astrocytes are involved in A $\beta$  catabolism, and A $\beta$  could affect their metabolic phenotypes. Astrogliosis in AD has been reported since Louis Alzheimer himself. It is a physiological response and until a certain point its function is protective; however, in AD, it could defect A $\beta$  clearance.<sup>65</sup>

In conclusion, this extension proposes that the accumulation of cerebral amyloid and tau pathology is a slow, gradual process tolerated by CNS cells. The disease is only manifest clinically when cellular homeostatic mechanisms fail, leading to impaired clearance of aggregated pathologic protein, increased cellular stress, and a complex breakdown of intercellular physiologic functions that lead to neurodegeneration.

### 2.3.3 Tau hypothesis

As mentioned before, NFTs, have a primary role in neurodegeneration during AD. Tau protein is encoded by microtubule associated protein tau (MAPT) gene on chromosome 17, is primarily expressed by neurons, and is spliced to form 6 distinct isoforms (0N3R, 0N4R, 1N3R, 1N4R, 2N3R, and 2N4R). Although tau's physiological role in the CNS is not entirely clear, numerous studies have documented essential roles in microtubule assembly, stabilization of neuronal axons, and regulation of microtubule transport.<sup>66</sup> Tau protein is subject to numerous post-translational modifications, like phosphorylation, acetylation, glycation, nitration, ubiquitination, and truncation.<sup>67</sup> Tau can be phosphorylated at 85 different residues.<sup>68</sup> In the majority of cases, aberrant phosphorylation results in decreased binding affinity for microtubules.<sup>69</sup> This disassembly increases the cytosolic pool of tau and is supposed to promote aggregation and fibrillization. Hyperphosphorylated tau is also redirected from the axonal compartment to the somatodendritic compartment, impairing synaptic function.<sup>70</sup> Unlike A $\beta$ , the stage of tau pathology is well associated with the development of cognitive impairment.<sup>59</sup> The so called primary age-related tauopathy (PART) is the accumulation of tau in the entorhinal cortex and medial temporal lobes without cognitive decline.<sup>71</sup> Cognitive deficiency in AD is only noted when tau spreads from the entorhinal cortex into the neocortex in neuropathological studies.<sup>72</sup> Only the presence or accumulation of tau seems to predict cognitive impairment.<sup>73</sup> These results contributed to the theory that cognitive impairment and neurodegeneration in AD are primarily driven by the development and distribution of tau pathology. Tau is usually a soluble protein that is unfolded, but in some conditions can aggregate into oligomers and fibrils. NFTs contain an insoluble form of tau

aggregated into beta-sheet-containing amyloid fibrils, known as paired helical filaments (PHF).<sup>69</sup> What then, promotes tau aggregation in the disease? Numerous studies suggest a prion-like mechanism of propagation of protein misfolding.<sup>74</sup> Many scientists have demonstrated the "prion-like" ability of aggregated human tau fibrils to self-propagate and spread trans-synaptically to remote anatomically connected brain regions inducing further seeding and aggregation.<sup>75</sup> Thus, prion-like seeding and spreading may represent a mechanism whereby tau pathology propagates from the entorhinal cortex to the neocortex in AD, generating cognitive impairment.<sup>76</sup>

### 2.3.4 ApoE

ApoE protein is an apolipoprotein whose essential function is to act as a lipid-binding protein in lipoprotein particles and transport and distribute lipids to target sites. ApoE is present mainly in the liver and brain. In the brain, ApoE is expressed mostly in astrocytes and lesser also in microglia. ApoE appears to enhance AD risk by increasing amyloid pathology.<sup>77</sup> A $\beta$  present in plaques is bound to ApoE.<sup>78</sup> Although the interaction between ApoE and A $\beta$  is not completely clear nor the mechanism of reduction of A $\beta$  clearance. More than direct interactions with A $\beta$ , it seems that ApoE regulates the clearance of A $\beta$  by competitively binding to A $\beta$  receptors, such as LDLR-related protein 1 (LRP1) on the surface of astrocytes, blocking A $\beta$  uptake. In fact, Verghese et al. reported that ApoE KO mice exhibit the highest clearance rates since there is no competition with A $\beta$  receptors.<sup>58</sup> Possible routes of A $\beta$  clearance include astrocytic uptake<sup>79</sup>, microglial phagocytosis<sup>80</sup>, or blood-brain barrier transport.<sup>81</sup>

## 2.4 Neuroinflammation

Inflammation is central to the initiation and progression of age-related neurodegenerative diseases,<sup>82</sup> and it has been demonstrated to affect the expression of Brain-Derived Neurotrophic Factor (BDNF) within the brain<sup>83</sup>. In the CNS, cellular infiltration in response to inflammation is weaker and delayed than in other tissues, however microglia, and the expression and release of classical inflammatory mediators,

such as cytokines, can be induced rapidly.<sup>84,85</sup> Nuclear factor (erythroid-derived 2)-like 2 (Nrf2) and nuclear factor- $\kappa$ B (NF- $\kappa$ B) are two interconnected regulators of cellular responses to oxidative stress and inflammation, respectively.<sup>86</sup> Chronic oxidative stress increases homeostasis's loss during aging, particularly involving the regulatory systems and the immune response. This condition induces inflammation, which then raises oxidative stress, producing a vicious cycle. A recent study found that elevated levels of oxidative stress biomarkers are associated with high levels of inflammatory cytokines, both of which are due to poor cognitive performance in elderly patients.<sup>87</sup> Nrf2 is considered to be the key regulator of cellular response to oxidative and toxic shocks, modulating the expression of hundreds of genes involved in the immune and inflammatory responses, cell metabolism and metabolic control, and even cognitive impairment.<sup>88</sup> The regulation of Nrf2 is complex and controlled not only by the repressor protein Kelch ECH associating protein 1 (Keap1) but also by other signaling pathways, including glycogen synthase kinase 3 (GSK3), NF- $\kappa$ B, NOTCH, and AMP kinase.<sup>89,90</sup> Due to the role of Nrf2 deregulation in neurodegenerative diseases, Nrf2 inducers are currently under investigation.

Neuroinflammation is characterized by oxidative stress, glial cell activation, leukocyte recruitment, and inflammatory mediators' release.<sup>91</sup> Microglia are the primary innate immune cells in the CNS and represent the first line of defense.<sup>92</sup> On the other hand, when microglia become overactivated or reactive, it can induce detrimental neurotoxic effects by releasing numerous cytotoxic elements.<sup>93</sup> Additionally, the release of proinflammatory cytokines and other soluble factors by activated microglia can significantly influence the subsequent activation of astrocytes.<sup>94</sup> Upon activation, astrocytes upregulate several neurotrophic factors (e.g., BDNF) that protect against cell injuries.<sup>95</sup>

Neurotrophins (NTs) are responsible for proliferation, differentiation, growth, migration and synaptic formation. NTs are factors secreted by different brain cells, such as microglia, oligodendrocytes, astrocytes, and neurons. Their activity is mediated by the binding to specific transmembrane receptors, the tropomyosin receptor tyrosine kinases (Trk receptors) and the p75 NT receptor. The NT family comprehends BDNF. The role of NTs for the survival of developing neurons is now well known.<sup>96</sup> However,

in the last decades, the research's focus has moved on their function as mediators of neural and synaptic plasticity in the adult brain. The broad spectrum of BDNF activities depends on its complex genetic structure that has been characterized in detail.<sup>97</sup> BDNF gene contains multiple promoters that drive the expression of several transcripts bearing different noncoding exons. Interestingly, different isoforms of BDNF are expressed in different subcellular compartments.<sup>98</sup> The synthesis of the mature BDNF is a complex process, involving different precursor isoforms and different possible pathways to reach the mature form. Binding with BDNF, TrkB starts to dimerize and phosphorylate. Once phosphorylated, TrkB activates a series of intracellular pathways: promotes antiapoptotic and prosurvival synaptic plasticity activities by the phosphatidylinositol 3-kinase/protein kinase B- (PI3K/Akt-) pathways;<sup>99</sup> enhances dendritic growth and branching, by the PI3K/Akt/mammalian target of rapamycin (mTOR) cascade;<sup>100</sup> regulates protein synthesis during neuronal differentiation through the mitogen-activated protein kinase (MAPK)/Ras signaling cascade.<sup>101</sup>

## 2.5 Models to study AD

Significant resources have been spent over decades to combat different neurological disorders; however, many of them remain relatively intractable. This failure is partly because these brain disorders are not well understood, and this makes the search for an effective therapy very difficult. Many experiments have focused on animal models, using rodents, rabbits, and other species to explain disease's development and pathways. Animal models have provided essential and fundamental knowledge in neuroscience and enormous resources to understand potential disease processes since they share certain genetic similarities with humans. On another side, when researching human neurological disorders, animal models show many weaknesses. First, it is challenging to engineer genomes in animals. Second, some mutations and some cells are not even present in animal models. Protein expression levels are different as disease's mechanism, and the interspecies differences could make animal models useless to study some diseases.<sup>102</sup> Third, another significant obstacle is represented by the fact that clinical trials' outcome depends heavily on animal experiments. Although a

considerable amount of money has been invested in discovering therapeutic strategies for AD, animal models with weakness, as described above, struggled to reproduce the essential pathophysiological features of human disease, leading to inadequate clinical translation regardless of financial investment.

Another primary concern in the study of brain disorder is the characteristics of the brain itself. Among all human organs, the brain is the most complicated one. It contains 10 to 100 billion neurons, resulting in 100 trillion synaptic networks. It is strictly compartmentalized but also highly interconnected. The use of post-mortem brain tissues is extremely useful, but it gives only a picture of the alteration, not information on the timing and mechanism involved in neurodegeneration. In addition to the difficulties in using human brain tissues, there are ethical considerations and limiting access to human brains. In this regard, it is not a surprise if the understating of brain functions and development remain vague. Such limits of *in vivo* animal models and limited understanding of diseases have all pointed to the need for new models that fit human biology more closely and serve as a resource for therapeutic treatments.

### 2.5.1 Animal Models

Animal models should mimic neurodegeneration features and help in understanding behavioral, physiological, and pathological mechanisms. There are different types of animal models, but none of them could reproduce AD in all of its characteristics.<sup>103</sup>

Since discovering the genes associated with AD, several knocking and transgenic knockout models have been developed for the genes involved in it, such as those coding for APP, tau, PS1 and PS2. Mice are the most widespread species due to their easy manipulation and accessibility.<sup>103</sup>

There are also AD models that can be used to assess dementia and memory deficits. Like non-human primates, several animals spontaneously develop the pathology with cognitive dysfunctions similar to those observed in humans.<sup>104</sup> These models are valuable tools that can be used to reveal the natural physiopathology of the disease since they do not require invasive techniques or the use of particular substances.

Animal models of AD could also be made by the induction of lesions in specific brain areas or by the intracranial inoculation of chemicals. The exogenous substances injected in healthy rodents are many, such as heavy metals, sodium azide, neurotoxins, and the exogenous A $\beta$  protein. These models serve to explore the role of specific neuronal pathways in the pathogenesis and progression of AD without representing the disease as a whole.<sup>103</sup> A $\beta$  plaques are a distinctive aspect of AD, and several studies have shown that the direct infusion of oligomer A $\beta_{1-42}$  in the brains of wild-type mice manages to mimic the acute effects and neuronal death observed in humans.<sup>104</sup> An additional advantage of using wild-type mice comes from avoiding the appearance of compensation or side effects due to the gene mutations introduced.<sup>105</sup>

The injection of A $\beta$  peptide in the brain is mainly used to evaluate the neuroinflammation process since it stimulates microglia activation. The injection of oligomers could be intracerebroventricular (i.c.v.), intrahippocampal, or in other brain structures. Several studies have shown that i.c.v. injection of A $\beta_{1-40}$  or A $\beta_{1-42}$  induces significant neuronal death and simulate dysfunction as well as oxidative stress, resulting in increased levels of reactive oxygen species (ROS) and glutathione (GSH) in the cortex and hippocampus. Imbalance of the cellular redox state also results in mitochondrial dysfunctions that can lead to the initiation of the apoptotic process.<sup>106</sup>

With i.c.v. injection, the injected substance can reach both hemispheres homogeneously, using cerebrospinal fluid, and the inflammation and damage in the injection site are reduced.<sup>4</sup>

In conclusion, the injection i.c.v. of peptides A $\beta_{1-42}$  into mice, despite the intrinsic limitations that reside in each experimental models, represents a valid tool not only for the study of the early stages of AD but also to evaluate the neuroprotective action of compounds capable of counteracting the pathways involved in the AD.<sup>106</sup>

## 2.5.2 The promises of new technologies for human disease models: iPSC and CRISPR/CAS technique

Recent technologies figure out a new way to improve our biological and pathological knowledge. In 2007, a Nobel prize-winning study of induced Pluripotent Stem Cells

(iPSCs) by the Yamanaka group revolutionized how to study neural cells, suggesting potential solutions to unsolved issues.<sup>107</sup> Technical developments in stem cell biology allow redirecting iPSCs into any cell types found in the body. In particular, with numerous differentiation protocols, it is possible to generate multiple different types of brain cells in a dish to investigate the cellular biology that may lead to disease.<sup>108</sup>

Another transformative discovery is the adaptation of clustered, regularly interspaced short palindromic repeats (CRISPR) and CRISPR-associated (Cas) genes as genetic manipulation tools. This system was discovered from studies on the adaptive immune system of bacteria and archaea.<sup>109</sup> Prokaryotes utilize this CRISPR system to defend themselves against invading foreign nucleic acids. Successful adaptation of this system to a genome-editing tool for the human genome creates a comfortable and precise means to modulate the genome to study the effects of targeted mutations.<sup>109</sup>

The use of genome edited iPSCs allows researchers to study multiple differentiated cells and the impact of a specific genetic background on a disease. Genome editing technology, such as the CRISPR/Cas9 system, is utilized in order to generate isogenic controls for disease iPSCs by correcting the disease variant and introducing rare disease-associated mutations (where patient samples are not always readily available) into healthy iPSCs lines.

With isogenic lines, only the disease-associated difference is studied, as the genetic background of the lines should be identical. In the past years, protocols to differentiate iPSCs into microglia-like cells, oligodendrocytes, astrocytes, neurons, and organoids have been implemented and optimized to model the effects of AD risk gene mutations on brain cells function. However, despite the increased use of this technology, there are possible downsides to which careful attention should be directed to make precise conclusions. First, likely, each clone of human iPSC lines generated in the same way from the same individual could have different properties from each other. Some studies show that each generated pluripotent stem cell-line is affected mainly by methodological and environmental factors, such as timing and methods of derivation, and the set of culture media.<sup>110-112</sup> Second, it seems to exist pronounced effects of genetic background over environmental effects for differentiation.<sup>110</sup> In support of that, sibling lines were hierarchically clustered together regardless of deriving methods in

transcriptional profiling analysis from a broad set of human embryonic stem cells (hESCs).<sup>110</sup>

Many methods have been used to minimize risks arising from the concerns described above. Assays such as genome-wide transcription analysis or epigenomic analysis to evaluate iPSCs' pluripotency, quantitative and quality control are useful to determine whether a generated line is suitable for a particular application.<sup>113,114</sup>

CRISPR/Cas system is a genome-editing tool creating a double strand break by site-specific nucleases. Despite its precise genetic editing capability at a single-nucleotide level, there is a significant concern surrounding the "off-target" effects. Nuclease can induce unwanted mutations elsewhere ("off-target") besides the target site.<sup>115,116</sup> Even if several studies showed that "off-target" mutations were found at a shallow frequency, however, exome sequencing or whole genome sequencing needs to be applied to evaluate "off-target" nuclease activities. Because it is unlikely that multiple clones will have the same off-target effect is essential to use different clones. Another concern on this technology rises from a potential risk derived from clonal selection after mutagenesis.<sup>115,116</sup> Since the clonal isolation step itself impose risks for unexpected mutations, multiple clones to validate any phenotypes observed would be necessary. Moreover, before creating an isogenic line, the parental cell line needs to be assured that it does not show any atypical pathological phenotypes.

A hybrid approach using two groundbreaking technologies will further improve the understanding of AD biology. Combining these technologies, it is possible to model the disease in two different ways, one is to add one or more risk alleles to the undiagnosed background, the other is to remove one or multiple suspected mutations from a pathological background. As previously mentioned, thanks to GWAS, plentiful risk variants for many different disease states have been identified.<sup>117-119</sup> First approach using a healthy background can directly test the effects of rare variant mutations identified from GWAS in AD, but no human samples are available. Subtracting approach, removing a variant of interest can also test its causative effects on the conditions. Furthermore, one advantage of the second approach is to require no consideration of a potential risk of a protective background. In a situation where a

parental cell line already has a protective genetic background, no pathological manifestation can be invoked by introducing a risk variant into a genome.

Once established, which iPSC lines should be used to model the disease, the next step is to determine how to differentiate iPSCs into cell types of interest. While several different protocols have been published for different brain cells, these protocols need to be carefully checked and validated based on experimental purposes and needs, such as the ability to generate adequate cell numbers, differentiated cell type consistency, and heterogeneity of generated cell types.

Essential criteria in the selection of protocols are their efficiency in generating specific cells. Although studies such as immunocytochemistry and electrophysiology involve a relatively small number of cells, different examinations require studying a large number of cells.<sup>120</sup>

The generated cells' quality can then be verified in various ways: by immunocytochemistry, by transcriptional profiling, and by functional assays. Although the method of immunocytochemistry is frequently used for rapid evaluation, it is not unusual that signatures of gene expression defining cell type are not available for interest. Then, it would be an ideal option to perform functional assays.

Previous studies have shown that various types of cells in the brain contribute independently to the disease's progression.<sup>121,122</sup> So, it is necessary to have a population of cells as pure as possible. An additional purification step may reduce unintentional effects through fluorescent activated cell sorting (FACS) or magnetic separation using appropriate surface markers to reduce cellular heterogeneity.<sup>123,124</sup>

In conclusion, iPSCs are a promising *in vitro* platform for functional studies and disease drug discovery. It allows us unique access to human substrates that can mitigate the crucial limitations of animal models in reproducing human phenotypes. On the other hand, iPSC-based technologies often pose many problems to be addressed. As previously said. Consequently, a better disease modeling method can be provided by combining iPSC-based models with other technologies.

## 2.6 Treatments for AD

Four FDA approved medicines for the management of cognitive impairment and dysfunction in symptomatic AD are currently available. These include three cholinesterase inhibitors (ChEIs; donepezil, rivastigmine and galantamine) and memantine, an uncompetitive N-methyl-D-aspartate (NMDA) receptor modulator. Despite the pharmaceutical industry's efforts, no effective disease modifying treatment exist today. More than 20 compounds have finished large phase 3 double-blind randomized control trials in cohorts of patients at various AD stages, and none has demonstrated any efficacy in slowing cognitive decline or improving global functioning. The need for diverse approaches to clinical trial design in AD, an alternative way to study the disease, and a new pharmaceutical approach is demonstrated by these numerous trial failures.

### 2.6.1 Cholinesterase inhibitors

During AD pathogenesis, cholinergic neurons are lost, causing a general cholinergic deficit.<sup>125</sup> This loss of cholinergic input is supposed to contribute to early attention and memory dysfunction in AD. ChEIs can reverse this deficiency by increasing synaptic levels of acetylcholine and by inhibiting of acetylcholinesterase enzyme (AChE), which catalyzes acetylcholine degradation. Three ChEIs are currently approved for use in mild-to-moderate AD: donepezil, rivastigmine and galantamine.

Meta-analyses measuring both cognitive performance and global functioning have verified their symptomatic benefit in AD.<sup>126</sup> They differ primarily in their pharmacokinetic profiles (donepezil has a slightly longer half-life than the others and is administered once a day) and formulation (rivastigmine is available as a transdermal patch with continuous release) but not in overall efficacy. However, the overall effect size is modest, and there is no effect on long-term disease progression.

## 2.6.2 Anti-NMDA

Memantine is an uncompetitive NMDA receptor modulator that inhibits glutamate mediated neurotoxicity that develops as neurons die during AD progression.<sup>127</sup> In pathological condition as AD, NMDA receptors are overactivated with a continuous calcium ( $\text{Ca}^{2+}$ ) permeability and excitotoxicity. Memantine works by blocking the channel of NMDA receptors.

Meta-analysis confirms memantine's efficacy in moderate-to-severe AD on cognition processes, activities of daily living, and neuropsychiatric symptoms.<sup>128</sup> However, as with ChEI, the effect size is relatively small, and the medication does not affect long-term disease progression. This drug is on the first line for the treatment of AD. In most cases, it is a well-tolerated drug and is also used in combination with ChEI to act on two sides, inhibiting the excessive activity of glutamate on the one hand and stimulating the cholinergic system on the other.<sup>129</sup>

## 2.6.3 Neuroprotection

Excitotoxicity, oxidative stress, inflammation, and neuronal defeat seem closely related to AD's evolution and progression. In this scenario, an intervention able to slow down or halt the pathology evolution could be crucial in treating AD. A neuroprotective approach interfering with the inflammatory reaction and oxidative stress may positively moderate the gradual impairment of the patients' quality of life. Neuroprotection could work in association with the endogenous defenses, reducing ROS formation or restoring the antioxidant GSH system and slowing down the progressive neuronal death. A preventive strategy that simultaneously targets multiple risk factors and disease mechanisms at an early stage is most likely to be effective to slow/halt the progression of neurodegenerative diseases, considering their complex multifactorial nature.<sup>130</sup> Agonistic action on Trk receptors, activation of the extracellular signal-regulated kinase (ERK), PI3Kinase/Akt and CREB pathways, activation of the Nrf2 pathway, and upregulation of antioxidant and detoxification enzymes, as well as several other mechanisms, underlie the neurotrophic action of different neuroprotective compounds.

A better understanding of the neurotrophic effects and the molecular mechanisms of action of these compounds could help design better agents for the management of neurodegenerative diseases and other disorders of the nervous system.<sup>131</sup>

Therefore, recent works have underlined the protective role of several food components, including micro- and macronutrients in the prevention and management of AD.<sup>132</sup> Several researchers have explored the role of single food components, as well as lifestyle habits and inappropriate diets in facilitating the development of AD and its clinical progression.

Neuroprotection is undoubtedly one of the most exciting fields where identified new pharmacological treatment for neurodegenerative disease. In conclusion, several efforts are being made in research to find neuroprotective compounds capable of maintaining the integrity and neuronal functions in an ongoing neurodegenerative process to prevent or slow its progression.<sup>133</sup>

#### 2.6.3.1 Ferulic Acid

Ferulic acid ([E]-3-[4-hydroxy-3-methoxy-phenyl] prop-2-enoic acid) is a phenolic acid group usually found in plant tissues.<sup>134</sup> Phenolic acids have multiple biological properties and are secondary metabolites of varying chemical structures. From a chemical structure point of view, they can be divided into derivatives of cinnamic and benzoic acid. Ferulic acid is the most common cinnamic acid derivative. Ferulic acid is mostly found in whole grains, spinach, parsley, grapes, rhubarb, and cereal seeds, mainly wheat, oats, rye, and barley. One of the most important characteristics of phenolic acids, especially cinnamic acid derivatives, is their antioxidant activity, which depends primarily on the number of hydroxyl and methoxy groups attached to the phenyl ring.<sup>135</sup> Ferulic acid is considered to be a superior antioxidant. Ferulic acid is more easily absorbed into the body and stays in the blood longer than any other phenolic acids.<sup>136</sup> The antioxidant action mechanism of ferulic acid is complex, mainly based on the inhibition of the formation of ROS or nitrogen and the neutralization of free radicals.<sup>137</sup> Ferulic acid is a free radical scavenger and an inhibitor of enzymes that catalyze free radical generation and an enhancer of scavenger enzyme activity. It is

directly related to its chemical structure.<sup>138</sup> The mechanism of antioxidative activity of ferulic acid is the ability to form stable phenoxyl radicals, which makes it challenging to initiate a complex cascade of reactions that leads to free radicals being produced. This compound may also act as a hydrogen donor, an essential aspect for protecting cell membrane lipid acids from undesired lipids peroxidation. Ferulic acid has low toxicity and possesses many physiological functions, including anti-inflammatory, antimicrobial and anticancer (for instance, lung, breast, colon and skin cancer). It also demonstrated antidiabetic effects and immunostimulant properties, and it can reduce nerve cell damage and may help repair damaged cells. In pharmaceuticals and food, it has been used extensively.<sup>135</sup>

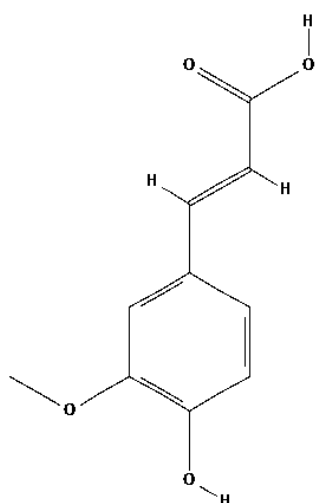


Figure 8. Ferulic Acid Chemical Structure.

## 2.6.4 Multi-target-directed ligands strategy

AD is a complex condition for which effective therapeutic treatments are required immediately. Among the various drug discovery methods, a very promising modern approach consists of designing multi-target-directed ligands (MTDLs). This method has been developed for the treatment of disorders with complex pathological mechanisms. One such disorder is Alzheimer's disease (AD), currently the most common multifactorial neurodegenerative disease.

Over the past two decades, this approach has been progressively employed in AD drug discovery, and many publications have highlighted the advantage of the MTD approach over classical target-specific drugs (TSDs) and their combinations. MTDLs are agents that are synthesized to interact with more than one target responsible for determining the pathogenesis of a specified disease. Theoretically, the same therapeutic effect can also be reached by combination therapy including several TSDs. An MTD approach is supposed to be superior to combination therapy in an ideal situation because it maintains all the benefits of combination therapy with some added advantages. For example, with MTDLs, there should be no risk of drug-drug interactions, and the risk of drug-drug interactions with other medications is also lower. The risk of adverse effects would also be lower by merely reducing polypharmacy. Another advantage is improved compliance by the patient because of a simplification of the dosage regimen. The last issue can also be solved in some cases by using a fixed-dose combination of several TSDs in one medical preparation. However, such a combination of drugs is disadvantaged by the diverse pharmacokinetics of each component and requires further attention in the dosing. Lastly, even though the FDA supports clinical trials for drug combinations, MTDLs development requires fewer clinical trials than combinational therapy involving several TSDs.

#### 2.6.4.1 Feruloyl-donepezil hybrids

ChEIs and NMDA are the current treatment for AD-related symptoms with limited efficacy and no disease correction. Donepezil is a highly centrally selective, reversible, and non-competitive ChEIs and now the most commonly prescribed AD treatment. Clinical trials with donepezil reported modest but reproducible improvements in cognition and global functioning in treated patients compared to placebo. However, these results were not lasting, as cognitive performance tended to decrease in patients over time.<sup>139</sup>

Evidence indicated that one molecule with multiple targets could be the winning strategy for treating complex diseases with the consequent failure of the TSDs approach.<sup>140</sup> The MTDL approach recommends the development of new scaffolds with

two or more pharmacophoric entities associated in a single molecule, which could interact with numerous molecular targets concurrently. Considering the MTDL idea, donepezil is, at the moment, the main inspiration among all the compounds used for the design of novel drugs.<sup>141–144</sup> Another scaffold widely used to develop new MTDLs for AD is curcumin and its metabolites as ferulic acid. Curcumin is an abundant polyphenol found in *Curcuma longa* rhizomes.<sup>145,146</sup> Polyphenol has potent antioxidant and anti-inflammatory features and contributes to reducing oxidative damage, inflammation,<sup>147</sup> and accumulation of amyloids, with an additional capability to chelate biometals. Curcumin and Ferulic acid have been tested in animal models, showing multiple positive results for AD treatment. In particular, it can reduce A $\beta$ -mediate inflammatory response and oxidative stress.<sup>148</sup>

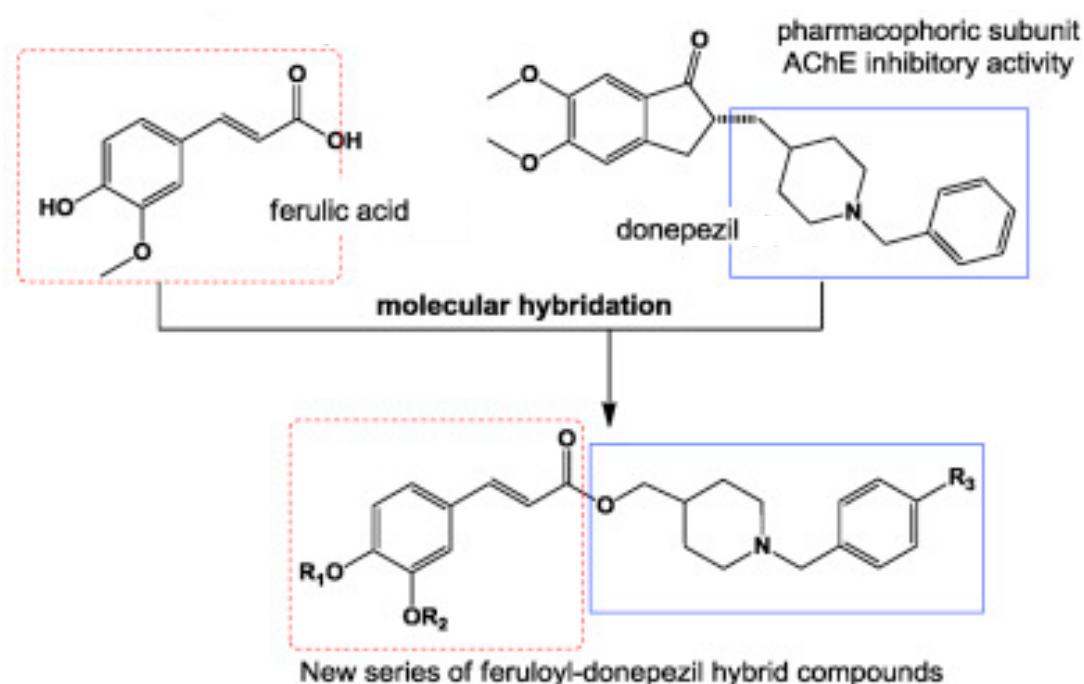


Figure 9. Design of a new series of feruloyl-donepezil hybrid compounds.<sup>148</sup>

### 3 Project Purpose

Neurodegeneration defines a set of pathological conditions characterized by the progressive and consistent loss of CNS functions. Neurodegenerative diseases are recognized as highly debilitating conditions, frequently linked to aging, and for which there are only symptomatic treatments that can initially reduce their symptoms but not restore the correct neuronal function. Although their etiopathology is yet to be clarified, chronic neurodegenerative diseases have a multifactorial nature. In this regard, several studies in the biochemical, pharmacological and toxicological fields have highlighted the involvement of multiple cellular and molecular factors, such as increased oxidative stress, mitochondrial dysfunction, and protein aggregates' deposition.<sup>149</sup> AD is the most frequently diagnosed neurodegenerative disease and is the leading cause of dementia in the elderly.<sup>16</sup>

AD's complex nature requires a combined pharmacological approach to control neurodegenerative processes and the management of the main symptoms. The ideal neuroprotective strategy, made with a single or cocktail of drugs with multiple pharmacological properties associated with the traditional symptomatic therapy, should block or at least slow down the neurodegenerative course with a protection mechanism, recovery, or neuronal repair. In this regard, many studies have shown that some multifunctional bioactive compounds are effective in reducing and/or blocking neuronal death. In particular, it has been estimated that these compounds express their neuroprotective effects through their antioxidant and anti-inflammatory activities and the modulation of genes able to promote cell survival.

The current project aims to identify risk factors and the main mechanisms involved in AD. A particular interest has been addressed to memory impairment, oxidative stress, neuroinflammation, and synaptic plasticity to outline neuroprotective strategies capable of preventing or slowing neurodegenerative diseases related to aging.

In the first part, the experimental activity has been oriented to evaluate and characterize molecular and cellular mechanisms that contribute to neurodegeneration induced by the A $\beta$  oligomers and potential neuroprotective effects of a multifunctional bioactive molecule called PQM130. PQM130 is part of a new series of molecular hybrids feruloyl-donepezil based on the combination of the pharmacophoric N-benzylpiperidine subunit from donepezil and the subunit feruloyl, present in ferulic acid.<sup>150,151</sup> The neuroprotective effects of the multitarget ligand PQM130 were examined also compared to donepezil in a murine AD model, obtained by i.c.v. injection of A $\beta$ <sub>1-42</sub> oligomers (A $\beta$ <sub>1-42</sub>O). After clarifying the mechanisms underlying the damage induced by A $\beta$ , the possible neuroprotective pathways aimed to contain the neurodegeneration, were evaluated with an integrated approach of behavioral tests and biochemical and immunohistochemical analyses. Cognitive impairment has been investigated using a battery of behavioral tests to analyze the hippocampus-dependent learning and memory, such as the Y-maze test and the Morris water maze test. The parameters of neuronal death, the neuroinflammatory response, as well as the activation of caspases and biochemical pathways involved in cell survival have been estimated through western blotting and by immunoenzymatic and immunohistochemical techniques.

Although animal models simulate neurodegeneration characteristics and facilitate the observation of pathological and behavioral changes that characterize AD, *in vitro* models allow accurate and more reproducible control of physiopathological mechanisms. Cells are easier to engineer compared to mice. Some mutation or even some cells are not even present in animal models, the protein expression level is different like disease's mechanism, making animal models useless to study some aspect of a disease. Both experimental models are required to study AD and to develop new therapies. However, none of them can perfectly reproduce the disease's pathogenesis, so the possibility of combining different approaches will undoubtedly increase the scientific value of research results.

The second part of the experimental activity was conducted at the Massachusetts Institute of Technology (MIT) under the supervision of Professor Li-Huei Tsai, and the project was focused on studying how to develop an *in vitro* model of AD using the innovative CRISPR/Cas9 system and iPSC. The Tsai laboratory, where this second part of the project has been executed, use CRISPR/Cas9 genome editing to introduce rare disease-associated mutations (where patient samples are not always readily available) into healthy iPSCs lines.

Among all the mutations associated with AD reported by GWAS studies, this study was focused on ABCA7. ABCA7 is a member of the A subfamily of ABC proteins,<sup>152</sup> which regulates lipid metabolism and critically controls phagocytic function in macrophages, contributing to immune responses and the host defense system.<sup>153</sup> GWA studies have identified mutations and single-nucleotide polymorphisms (SNPs) in the ABCA7 gene, which confer increased risk for LOAD.<sup>154</sup> However, the mechanism by which ABCA7 can contribute to AD is not clear. The role of ABCA7 in lipid metabolism and phagocytosis suggests that an alteration in ABCA7 expression could increase AD incidence in multiple ways. To probe the functions of ABCA7, including the effects of AD-associated mutations, CRISPR/Cas9 technology was used to engineer isogenic human iPSCs to carry the genetic variant loss-of-function ABCA7 Y622\* mutation. This mutation has been associated with increased AD risk in an Icelandic population.<sup>155</sup> From these isogenic cell lines, multiple neural cell types were generated, including astrocytes, microglia, and oligodendrocytes precursor cells (OPC). Using different assays, including those assessing lipid homeostasis defects, endocytosis and phagocytosis, the cellular defects present were characterized due to the ABCA7 mutation. Among all the brain cells generated, astrocytes have been characterized, because of their crucial role in brain homeostasis, supporting both neurons and microglia activities.

This project's results can help comprehend the A $\beta$ <sub>1-42</sub> damage in AD better, develop innovative therapeutic strategies to counteract the evolution of the neurodegenerative process, and understand the genetic background that could

increase AD's risk. This project was able to study the disease under different aspects, using two different models, to understand better various features of AD and other chronic neurodegenerative pathologies of the elderly, characterized by physiopathological and molecular alterations common to AD.

# SECTION ONE

## 4 Aim Section One

The aim of the study was to investigate the neuroprotective activity of the multitarget ligand PQM130 (Figure 10), which is the most promising compound of a new series of group compounds synthesized by Professor Viegas Jr and his collaborators.<sup>148</sup>

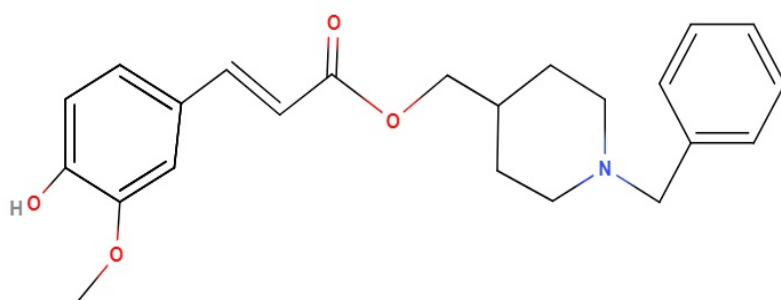


Figure 10 PQM130 chemical structure.

PQM130 is part of a new series of molecular hybrids feruloyl-donepezil synthesized by combing the pharmacophoric N-benzylpiperidine, subunit from donepezil responsible for its AchE selectivity, and the subunit feruloyl present in ferulic acid and curcumin. Ferulic acid contains one phenolic ring, and it is one of the metabolites of the curcuma. Its neuroprotective activities are addressed to the phenolic ring.<sup>150,151</sup> The multitarget ligand PQM130 has already been investigated for several biological properties relevant for AD, including antioxidant activity, neuroprotection against ROS and A $\beta$ -induced toxicity, metal-chelating properties and *in vivo* anti-inflammatory effects.<sup>156</sup>

PQM130 showed an interesting pharmacokinetic profile from the *in silico* evaluation of the absorption, distribution, metabolism, elimination (ADME) parameters, using the software QikProp 3.1 (Schrödinger, LLC, New York, NY, USA; Table 1). As a potential treatment for AD, it is necessary to know if the

compound can pass through the blood brain barrier. Interestingly, ADME data of PQM130 showed good human absorption and blood-brain barrier transposition in accordance with the software reference parameters. A similar *in silico* approach was adopted to evaluate the PQM130 safety, using the VEGA platform (<https://www.vegahub.eu/>; Mario Negri Institute for Pharmacological Research, Milan, Italy), which includes various QSAR models. It has been reported the absence of mutagenic and carcinogen effects of PQM130.

The *in vitro* and *in vivo* assays demonstrated that PQM130 showed multiple desirable effects, consistent with the intended MTDLs approach.

Table 1 *In silico* ADME data from QikPro 3.1 software (Schrödinger) for PQM130

ADME parameter	Description of predicted parameters	PQM130	Reference value*
<b>Reactive FG</b>	Number of reactive functional groups; the specific groups are listed in the jobname.out file. The presence of these groups can lead to false positives in HTS assays and to decomposition, reactivity, or toxicity problems <i>in vivo</i> . See Appendix 5 of the QikProp User Manual for a complete list	1	0 – 2
<b>CNS</b>	Predicted CNS activity on a –2 (inactive) to +2 (active) scale	1	-2 – +2
<b>mol_MW</b>	molecular weight	381.471	130 – 725
<b>donorHB</b>	Estimated number of hydrogen bonds that would be donated by the solute to water molecules in an aqueous solution. Values are averages taken over a number of configurations, so they can be non-integer	1	0 – 6
<b>acceptHB</b>	Estimated number of hydrogen bonds that would be accepted by the solute from water molecules in an aqueous solution. Values are averages taken over a number of configurations, so they can be non-integer	5.5	2.0 – 20.0
<b>QPlogPo/w</b>	Predicted octanol/water partition coefficient	4.356	-2 – 6.5
<b>QPlogS</b>	Predicted aqueous solubility, log S. S in mol dm <sup>-3</sup> is the concentration of the solute in a saturated solution that is in equilibrium with the crystalline solid	-5.118	-6.5 – 0.5
<b>QPlogHERG</b>	Predicted IC50 value for blockage of HERG K <sup>+</sup> channels	-7.39	< -5
<b>QPPCaco</b>	Predicted apparent Caco-2 cell permeability in nm/sec. Caco-2 cells are a model for the gut-blood barrier. QikProp predictions are for non-active transport	275.881	< 25 poor >500 great
<b>QPlogBB</b>	Predicted brain/blood partition coefficient	-0.688	-3 – 1.2
<b>QPlogKhsa</b>	Prediction of binding to human serum albumin	0.708	-1.5 – 1.5

<b>Hum Oral Absorp</b>	Predicted qualitative human oral absorption	3	1: low 2: medium 3: high
<b>% Hum Oral Absorp</b>	Predicted human oral absorption on 0 to 100% scale	96.134	>80%: high <25%: poor
<b>PSA</b>	Van der Waals surface area of polar nitrogen and oxygen atoms.	70.453	7.0 – 200.0
<b>Rule of Five</b>	Number of violations of Lipinski's rule of five. The rules are: mol_MW < 500, QPlogPo/w < 5, donorHB ≤ 5, acceptHB ≤ 10. Compounds that satisfy these rules are considered drug-like.	0	Max 4
<b>Rule of Three</b>	Number of violations of Jorgensen's rule of three. The three rules are: , QPlogS > -5.7, QPPCaco > 22 nm/s, # Primary Metabolites < 7. Compounds with fewer (and preferably no) violations of these rules are more likely to be orally available.	0	Max 3

In the present study, the neuroprotective effects of the multitarget ligand PQM130 were further examined compared to the control group and donepezil in a murine AD model. The mouse model was obtained by i.c.v. injection of A $\beta$ <sub>1-42</sub>O to take advantage of the high amount of cerebrospinal fluid that allows a wide spread of the peptide and reduces the risk of inflammatory reactions in the injury site. An i.c.v. injection of A $\beta$ <sub>1-42</sub>O in the mouse brain increases ROS, neurodegeneration, neuroinflammation, and memory impairment. We investigated its role in modulating synaptic plasticity through BDNF and synaptophysin levels in the hippocampus of mice. Neuroprotection activity was studied analyzing the modulation of glycogen synthase kinase 3 beta (GSK 3 $\beta$ ) and extracellular signal-regulated kinases (ERK1/2). Considering ROS production during AD, we also valued the antioxidant activity, measuring ROS formation and GSH levels. Additionally, we examined the neuroinflammation and neuronal apoptosis via the caspase pathway.

# 5 Materials and Methods

## 5.1 Reagents

A $\beta$ <sub>1-42</sub> peptides were purchased by AnaSpec (Fremont, CA, USA). Aprotinin, bovine serum albumin (BSA), CHAPS, 2'7'-dichlorodihydrofluorescein diacetate (DCFH-DA), dimethyl sulfoxide, 5-5'-dithiobis (2-nitrobenzoic acid), dithiothreitol, donepezil hydrochloride, EDTA, eosin, ethanol, glycerol, hematoxylin, hepes pH 7.4, hexafluoroisopropanol, leupeptin,  $\beta$ -mercaptoethanol, sodium chloride, sodium fluoride, sodium orthovanadate, sucrose, sulfosalicylic acid, Triton-X 100, tris pH 7.5, xylen, and primary antibodies anti-synaptophysin and anti- $\beta$ -actin were provided from Sigma-Aldrich (Saint Louis, MO, USA). Paraformaldehyde solution (4%) was provided from Santa Cruz Biotechnology (Dallas, TX, USA) and NP-40 from Roche Diagnostic (Risch, Switzerland). Caspases substrates were purchased by Alexis Biochemicals (San Diego, CA, USA). Primary antibodies phospho-GSK3 $\alpha/\beta$  (Ser21/9) and GSK3 $\alpha/\beta$ , phospho-p44/42 MAPK (ERK1/2, Thr202/Tyr204) and p44/42 MAPK, anti-GFAP were provided from Cell Signaling Technologies Inc. (Danvers, MA, USA). Secondary anti-mouse and anti-rabbit antibodies were purchased by GE Healthcare (Piscataway, NJ, USA) and fluorescein from Life Technologies (Carlsbad, CA, USA). Bradford assay solution, ECL, TBS, and tween20 were purchased from Bio-Rad Laboratories S.r.L. (Hercules, CA, USA). Normal Goat Serum (NGS) was provided from Wako Pure Chemical Industries (Osaka, Japan). All experiment reagents were reagent grade and commercially available.

## 5.2 Animals

Male C57Bl/6 (9 weeks old, 25–30 g body weight at the beginning of the experiment; Harlan, Milan, Italy) mice were housed under 12h light/12h dark cycle (lights on from 7:00 a.m. to 7:00 p.m.) with free access to food and water in a temperature- and humidity-controlled room. Briefly, procedures on mice were carried out according to the European Communities Council Directive 2010/63/EU and the current Italian Law

on the welfare of the laboratory animal (D.Lgs. n.26/2014). The animal protocol was approved by the Italian Ministry of Health (Authorizazion No. 291/2017-PR) and by the corresponding committee at the University of Bologna. Care was taken to minimize the number of experimental animals and to take measures to limit their suffering. Mice were allowed to acclimatize for at least 1 week before the start of experiments.

### 5.3 Experimental design

The experimental protocol was based on the unilateral stereotaxic i.c.v. injection of A $\beta$ <sub>1-42</sub>. Animals were randomly divided into five major groups (n=10/group) as follows: sham/VH; A $\beta$ /VH; A $\beta$ /DON; A $\beta$ /PQM130 0.5 mg/kg; A $\beta$ /PQM130 1.0 mg/kg. Four groups received an i.c.v. injection of A $\beta$ <sub>1-42</sub>O, while the other received the same amount of saline solution (sham group). One hour after the brain lesion, we started intraperitoneal (i.p.) administration of 1 mg/kg of donepezil hydrochloride (DON, Sigma-Aldrich), 0.5 or 1 mg/kg of PQM130 or vehicle (VH, saline) in both lesioned and sham mice. The dose injected was selected on the basis of previous studies<sup>156,157</sup>. We injected mice everyday once a day for 10 days. At the end of the treatment, mice underwent behavioral assessment. After the behavioral assessment, animals were deeply anesthetized and sacrificed by cervical dislocation to perform immunohistochemistry, neurochemical, and molecular analysis (Figure 11).

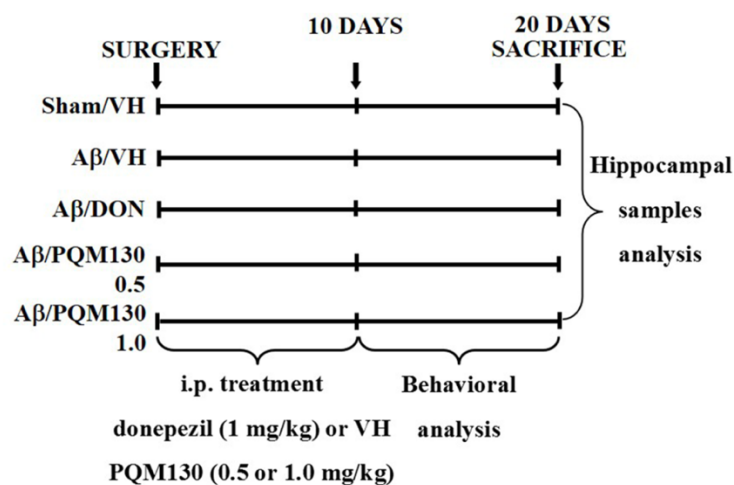


Figure 11 Experimental design

## 5.4 A $\beta$ <sub>1-42</sub> oligomers preparation and injection

A $\beta$ <sub>1-42</sub> peptides (AnaSpec) were firstly dissolved in hexafluoroisopropanol to 1 mg/ml, sonicated, incubated at room temperature for 24 h and lyophilized. The resulting unaggregated A $\beta$ <sub>1-42</sub> film was dissolved with sterile dimethyl sulfoxide to a final concentration of 1 mM and stored at -20°C until use. The A $\beta$ <sub>1-42</sub> aggregation to oligomeric form was prepared as described previously by Tarozzi et al.<sup>158</sup> Briefly, A $\beta$ <sub>1-42</sub> stock was diluted into phosphate buffer saline at 40  $\mu$ M and incubated at 4°C for 48 h to enhance oligomer formation.<sup>159,160</sup> Six  $\mu$ L of A $\beta$ <sub>1-42</sub>O (40  $\mu$ M) were injected i.c.v., using a stereotaxic mouse frame (myNeuroLab, Leica-Microsystems Co, St. Louis, MO, USA) and a 10  $\mu$ L Hamilton syringe, at a rate of 0.5 mL/min. The needle was left in place for 3 min after the injection before slow retraction, followed by cleaning and suturing of the wound. Sham mice received the equivalent volume of saline into the ventricle. The injection was performed at the following co-ordinates: AP: +0.22, ML: +1.0, DV: -2.5, with a flat skull position.

## 5.5 Donepezil hydrochloride and PQM130 preparations

Donepezil hydrochloride was purchased by Sigma-Aldrich and PQM130 (purity 98% by HPLC) was synthesized and provided by Professor Claudio Viegas Jr by the PeQuiM- Laboratory of Research in Medicinal Chemistry, Institute of Chemistry, Federal University of Alfenas (Alfenas, MG, Brazil). Briefly, the powders were solubilized and aliquoted in sterilized saline (donepezil) or in dimethyl sulfoxide (PQM130). Aliquots were conserved at -20°C until the use. Every day of treatment, the work solutions were prepared at the concentration of 0.1 mg/mL (donepezil and PQM130) and 0.05 mg/mL (PQM130) in sterilized saline. Animals were daily i.p. injected with 1 mg/kg solution (donepezil and PQM130) or 0.5 mg/kg (PQM130) for 10 days.

## 5.6 Behavioral analysis

All tests were carried out between 9.30 a.m. and 3.30 p.m. Animals were transferred to the experimental room at least 1 h before the test in order to let them acclimatize to the test environment. All scores were assigned by the same observer who was unaware of the animal treatment.

## 5.7 Morris Water Maze (MWM)

The test was carried out as described previously.<sup>161</sup> Briefly, the apparatus used for the MWM task was a circular plastic tank (1.0 m diameter, 50 cm height) filled with water and milk maintained at 22°C. The maze was located in a room containing several simple visual, extra-maze cues that were constant throughout the study. A transparent platform was set inside the tank and its top was submerged 1.5 cm below the water surface in the center of one of the four quadrants of the maze. The movements of the animal in the tank were monitored with a video tracking system (EthoVision, Noldus, The Netherlands). For each training trial, the mouse was put into the pool at one of the four positions, the sequence of the starting position being selected randomly. The platform was located in a constant position throughout the test period in the middle of one quadrant. In each training session, the latency to escape onto the hidden platform was recorded. If a mouse failed to find the platform within 60 s, it was manually guided to the platform and allowed to remain there for 10 s. After the trial, each mouse was placed in a holding cage under a warming lamp for 25 s until the start of the next trial. Training was conducted for 5 days, four times a day. On day 6, a single probe trial was performed, which consisted of a 60 s free swim in the pool without the platform. The parameters measured during the probe trial included escape latency, frequency in the platform zone, and time spent in the opposite quadrant to the platform zone.

## 5.8 Y-Maze test

Spatial working memory performance was assessed by recording spontaneous alternation behavior in Y-maze as described by Sarter et al.<sup>162</sup> Briefly, each arm of the maze (Ugo Basile® S.r.L., Gemonio (VA), Italy) was 35 cm long, 15 cm high and 5 cm wide and converged to an equal 120° angle. Each mouse was placed at the end of A arm and allowed to freely move through the maze during 5 min. An alternation was defined as entries in all three arms on consecutive occasions. The number of maximum alternations was therefore the total number of arm entries minus two and the percentage of alternation was calculated as (actual alternations/maximum alternations) × 100.<sup>163</sup>

## 5.9 Tissue preparation for immunohistochemistry and neurochemical analysis

Twenty days after Aβ<sub>1</sub>–42O injection, mice were deeply anesthetized and sacrificed by cervical dislocation. The brains were removed and the left hemisphere of each animal was immersed in a 4% fixative solution of paraformaldehyde (Santa Cruz Biotechnology) for 48 h. Right hemispheres were rapidly removed, and the hippocampi were dissected in an ice-cold plastic dish. Samples were then snap-frozen in liquid nitrogen, and kept at –80°C until analysis.

For the protein extraction, tissues were homogenized in lysis buffer (50 mM Tris, pH 7.5, 0.4% NP-40, 10% glycerol, 150 mM NaCl, 10 µg/mL aprotinin, 20 µg/mL leupeptin, 10 mM EDTA, 1 mM sodium orthovanadate, 100 mM sodium fluoride), and the cytoplasmic fraction was kept at –20°C until use. Cytoplasmic protein concentration was determined by the Bradford method.<sup>164</sup>

## 5.10 Determination of caspase-9 and -3 activations

Caspase-9 and -3 enzyme activities were determined using a protocol adapted by Movsesyan et al.<sup>165</sup>. The assay is based on the hydrolysis of the p-nitroaniline (pNA) moiety by caspases. Briefly, tissue lysates were incubated with assay buffer (50 mmol/L

Hepes, pH 7.4; 0.2% CHAPS; 20% sucrose; 2 mmol/L EDTA; and 10 mmol/L dithiothreitol) and a 50 mmol/L concentration of chromogenic pNA specific substrate (caspase-9, Ac-Leu-Glu-His-Asp-pNA; caspase-3, Z-Asp-Glu-Val-Asp-pNa; Alexis Biochemicals). In a final volume of 100  $\mu$ L (containing 60  $\mu$ g of protein), each test sample was incubated for 3 h at 37°C. The amount of chromogenic pNA released was measured with a microplate reader (GENios, TECAN®) at 405 nm. Values are expressed as the mean  $\pm$  SEM of optical density (OD) of each experimental group.

## 5.11 Determination of cellular redox status

The redox status, in terms of reactive oxygen species (ROS) formation, was measured as described previously,<sup>166</sup> based on the oxidation of DCFH-DA to 2'7'-dichlorofluorescein (DCF). Briefly, the reaction mixture (60  $\mu$ L) containing 2 mg/mL of DCFH-DA was incubated for 30 min to allow the DCFH-DA to be incorporated into any membrane bound vesicles and the diacetate group to be cleaved by esterases. After 30 min of incubation, the conversion of DCFH-DA to the fluorescent product DCF was measured using a microplate reader (GENios, TECAN®, Mannedorf, Switzerland) with excitation at 485 nm and emission at 535 nm. Background fluorescence (conversion of DCFH-DA in the absence of homogenate) was corrected by the inclusion of parallel blanks. Values were normalized to protein content and expressed as the mean  $\pm$  SEM of fluorescence intensity arbitrary units (UF) of each experimental group.

## 5.12 Determination of glutathione (GSH) content

GSH content was assessed using the protocol described earlier.<sup>167</sup> Briefly, aliquots of 50  $\mu$ L of samples were precipitated with 100  $\mu$ L of sulfosalicylic acid (4%). The samples were kept at 4°C for at least 1 h and then subjected to centrifugation at 3000 rpm for 10 min at 4°C. A volume of 25  $\mu$ L of the assay mixture and 50  $\mu$ L of 5-5'-dithiobis (2-nitrobenzoic acid) (4 mg/mL in phosphate buffer, 0.1 M, pH 7.4) was made up to a total volume of 500  $\mu$ L. The yellow color that developed was read immediately at 412 nm (GENios, TECAN®) and results were calculated using a standard calibration

curve. Values were normalized to protein content and expressed as the mean  $\pm$  SEM of GSH mmol/mg protein of each experimental group.

## 5.13 Western blotting

Samples (30  $\mu$ g proteins) were separated on 4-15% SDS polyacrylamide gels (Bio-rad Laboratories S.r.L.) and electroblotted onto 0.45  $\mu$ m nitrocellulose membranes. Membranes were incubated overnight at 4°C with primary antibody recognizing phospho-GSK3 $\alpha/\beta$  (Ser21/9), phospho-p44/42 MAPK (ERK1/2, Thr202/Tyr204), (1:1000; Cell Signaling Technology Inc), or anti-synaptophysin (1:1000; Sigma-Aldrich). Membranes were washed with TBS-T (TBS +0.05% Tween20), and then incubated with a horseradish peroxidase linked anti-rabbit or anti-mouse secondary antibody (1:2000; GE Healthcare). Immunoreactive bands were visualized by enhanced chemiluminescence (ECL; Bio-rad Laboratories). The same membranes were stripped and reprobed with GSK3 $\alpha/\beta$ , p44-42 MAPK (1:1000; Cell Signaling Technology Inc.) or anti- $\beta$ -actin (1:1000; Sigma-Aldrich). Data were analyzed by densitometry, using Quantity One software (Bio-Rad Laboratories® S.r.L.). Values were normalized and expressed as the mean  $\pm$  SEM of the densitometry in each experimental group.

## 5.14 Immunohistochemistry

Fixed brains were sliced on a vibratome (Leika Microsystems, Milan, Italy) at 40  $\mu$ m thickness and staining was assessed using the protocol described earlier.<sup>168</sup>

## 5.15 Hematoxylin/eosin staining

Hematoxylin/eosin (H&E) staining was performed as described by Fischer et al.<sup>169</sup> Briefly, selected sections were mounted on slides and dried before dipping them in 100%, 95% and 70% ethanol (Sigma-Aldrich). Slices were washed and stained with hematoxylin for 8 min and then incubated for 10 min in tap water to promote the change to violet coloration. Subsequently, slices were washed in distilled water and then dipped

10 times in 80% ethanol before being immersed in 25% eosin solution (in ethanol 80%) for 1 min. Finally, slices were dehydrated in 95% and 100% ethanol solutions for 5 min before being fixed in xylene.

## 5.16 Anti-Glial fibrillary acidic protein (GFAP) staining

The immunofluorescence staining was performed as described earlier.<sup>161</sup> After deparaffinization slices were washed in phosphate buffer and then incubated in TBS-A (TBS 0,1 % Triton-X 100) and then TBS-B (TBS-A 2% di BSA) to minimize non-specific absorption. Sections were then incubated overnight at 4°C with a mouse anti-GFAP primary antibody (1:300; Cell Signaling Technology Inc.) in TBS-B with 3% Normal Goat Serum (NGS, Wako Pure Chemical Industries). Twenty-four hours later, slices were washed with TBS-A and TBS-B before the incubation with secondary anti-mouse antibody (1:200; Fluorescein, Life Technologies) in TBS-B with 3% NGS. To verify the binding specificity, some sections were also incubated with only primary antibody (no secondary) or with the secondary antibody (no primary). In these situations, no positive staining was found in the sections, indicating that the immunoreactions were positive in all experiments carried out.

## 5.17 Quantitative images analysis

Image analysis was performed by a blinded investigator, using an AxioImager M1 microscope (Carl Zeiss, Oberkochen, Germany) and a computerized image analysis system (AxioCam MRc5, Carl Zeiss) equipped with dedicated software (AxioVision Rel 4.8, Carl Zeiss). After defining the boundary of the hippocampus at low magnification (2.5X objective), H&E or GFAP staining were evaluated by densitometry of five different sections for each sample analyzed at a higher magnification (10X, 20X or 40X objective). Quantification and morphological analysis were performed with the ImageJ software.

## 5.18 RNA preparation and gene expression analysis

Total RNA was isolated from the snap frozen hippocampus tissue samples using Pure link RNA mini kit (Ambion, Thermo Fisher Scientific, Carlsbad, CA, USA), as previously described.<sup>167</sup> Briefly, hippocampal samples were homogenized in Lysis buffer with 1%  $\beta$ -mercaptoethanol by a homogenizer SHM1 (Stuart, Bibby Scientific LTD, Staffordshire, UK) on ice. Homogenized samples were added to an equal volume of 70% ethanol and mixed. The solution was passed through a filter cartridge, containing a clear silica-based membrane to which the RNA binds, and washed with Wash Buffer I and Wash Buffer II. RNA was finally eluted with RNase-free water and stored at  $-80^{\circ}\text{C}$ . RNA was quantified by spectrophotometric analysis and reverse transcribed using High Capacity cDNA Reverse Transcription kit (Applied biosystem, Thermo Fisher Scientific).

The mRNA encoding for the mouse nuclear factor (erythroid-derived 2)-like 2 (Nrf2), GSH reductase (GR), tumor protein 53 (TP53) and the actin (ACTB) as internal reference were quantified by Taqman RT-PCR with a 7900HT Fast Real-Time PCR system (Applied Biosystem). Samples were run in 96-well format in triplicate. The specific Taqman gene expression assays (Applied Biosystem) were: Nrf2 (Mm0047784\_m1), GSTP1 (Mm04213618\_gH), GR (Mm00439154\_m1), TP53 (Mm01731290\_g1) and ACTB (Mm00607939\_s1).

To assess mRNA levels of different BDNF transcripts (total form, long 3'UTR form, exon IV, exon VI) and synaptophysin, samples were processed for RT-PCR reaction and subsequently analyzed by qRT-PCR instrument (CFX384 Real-Time system, Bio-Rad Laboratories S.r.l.) using the iScript one-step RT-PCR kit for probes (Bio-Rad Laboratories S.r.l.). Samples were run in 384-well format in triplicate as multiplexed reactions with a normalizing internal control (ACTB). The primers and probes sequences were respectively: total BDNF (Fwd: AAGTCTGCATTACATTCCTCGA, Rev: GTTTTCTGAAAGAGGGACAGTTTAT, Probe: TGTGGTTTGTGCGTTGCCAAG), long 3'UTR BDNF (Fwd: GTTGTCATTGCTTTACTGGCG, Rev: AATTTTCTCCATCCCTACTCCG, Probe:

AATCTACCCCTCCCATTCCCCGT), BDNF exon IV (Fwd: AGCTGCCTTGATGTTTACTTTG, Rev: CGTTTACTTCTTTTCATGGGCG, Probe: AGGATGGTCATCACTCTTCTCACCTGG), BDNF exon VI (Fwd: GGACCAGAAGCGTGACAAC, Rev: ATGCAACCGAAGTATGAAATAACC, Probe: ACCAGGTGAGAAGAGTGATGACCATCC), Synaptophysin (Fwd: CCTGTCCGATGTGAAGATGG, Rev: AGGTTTCAGGAAGCCAAACAC, Probe: ACACATGCAAGGAACTGAGGGACC), and ACTB (Fwd: ACCTTCTACAATGAGCTGCG, Rev: CTGGATGGCTACGTACATGG, Probe: TCTGGGTCATCTTTTCACGGTTGGC).

Each RT-PCR run followed the manufacturer's conditions: an incubation at 50 °C for 10 min (RNA retrotranscription), followed by a step at 95 °C for 5 min (TaqMan polymerase activation). After this initial step, 39 cycles of PCR were performed. Each PCR cycle consisted of heating the samples at 95 °C for 10 sec to enable the melting process, and then for 30 sec at 60 °C for the annealing and extension reactions. A comparative cycle threshold (Ct) method was used to calculate the relative target gene expression versus the control group. Specifically, fold change for each target gene relative to ACTB was determined by the  $2^{-\Delta(\Delta Ct)}$  method, where  $\Delta Ct = Ct_{\text{target}} - Ct_{\beta\text{-actin}}$ ;  $\Delta(\Delta Ct) = Ct_{\text{exp. group}} - Ct_{\text{control group}}$  and Ct is the threshold cycle. For graphical clarity, the obtained data were then expressed as percentage versus Sham/VH, which has been set at 100%.

## 5.19 Statistical analysis

Data were analyzed with the PRISM 9 software (GraphPad Software, La Jolla, CA, USA) and expressed as mean  $\pm$  SEM of each experimental group. The difference between groups was analyzed one-way ANOVA with Bonferroni post hoc test. A difference was considered statistically significant when a p value was less than 0.05.

## 6 Results

### 6.1 PQM130 ameliorates cognitive deficits in mice

The mice's behavioral performance using the MWM test was evaluated to assess the protective effect of PQM130 against A $\beta$ <sub>1-42</sub>O-induced spatial memory deficits in mice. During the MWM training phase, all mice learned the platform location, as revealed by a decrease in the latency. On the fourth and fifth day of training, the treated groups (A $\beta$ /DON and A $\beta$ /PQM130) showed a significantly lower escape latency than those in the A $\beta$ /VH group ( $p < 0.05$ ; Figure 12A). The mice in the A $\beta$ /VH group took significantly more time to find the hidden platform than the sham group, confirming that A $\beta$ <sub>1-42</sub>O could induce short-term memory impairment in mice. The swimming speed was also evaluated, but there was no significant difference among different groups throughout the training days.

The platform was removed in the probe trial, and the mice were allowed to swim freely. The mice in the A $\beta$ /VH group took more time to locate the original position of the removed platform as compared to the sham group. A $\beta$ /VH group exhibited more flawed memory in the probe test. It is clear a longer latency before entering the target zone, less frequency passage in the platform area, and more time spent swimming in the opposite quadrant (Figure 12 B-D). Interestingly, A $\beta$ /DON and A $\beta$ /PQM130 mice performed better than A $\beta$ /VH, even though significantly only in time spent in the opposite quadrant (donepezil  $p < 0.01$ ; PQM130  $p < 0.05$  and  $p < 0.01$ , respectively).

To further confirm the protective effect of PQM130 against the cognitive damage induced by i.c.v. injection of A $\beta$ <sub>1-42</sub>O, Y-maze test was performed. Y-maze test, which evaluates spatial working memory, showed that the A $\beta$ /VH group exhibited a significantly lower alternation behavior than the sham group ( $p < 0.05$ , Figure 13), confirming deficits in remembering which arm was explored. This alternation behavior deficit was significantly ameliorated in the A $\beta$ /DON and A $\beta$ /PQM130 groups (donepezil  $p < 0.001$ ; PQM130  $p < 0.05$  and  $p < 0.001$ , respectively), confirming that DON

and PQM130 were effective in enhancing spatial working memory during the early stage of AD development.

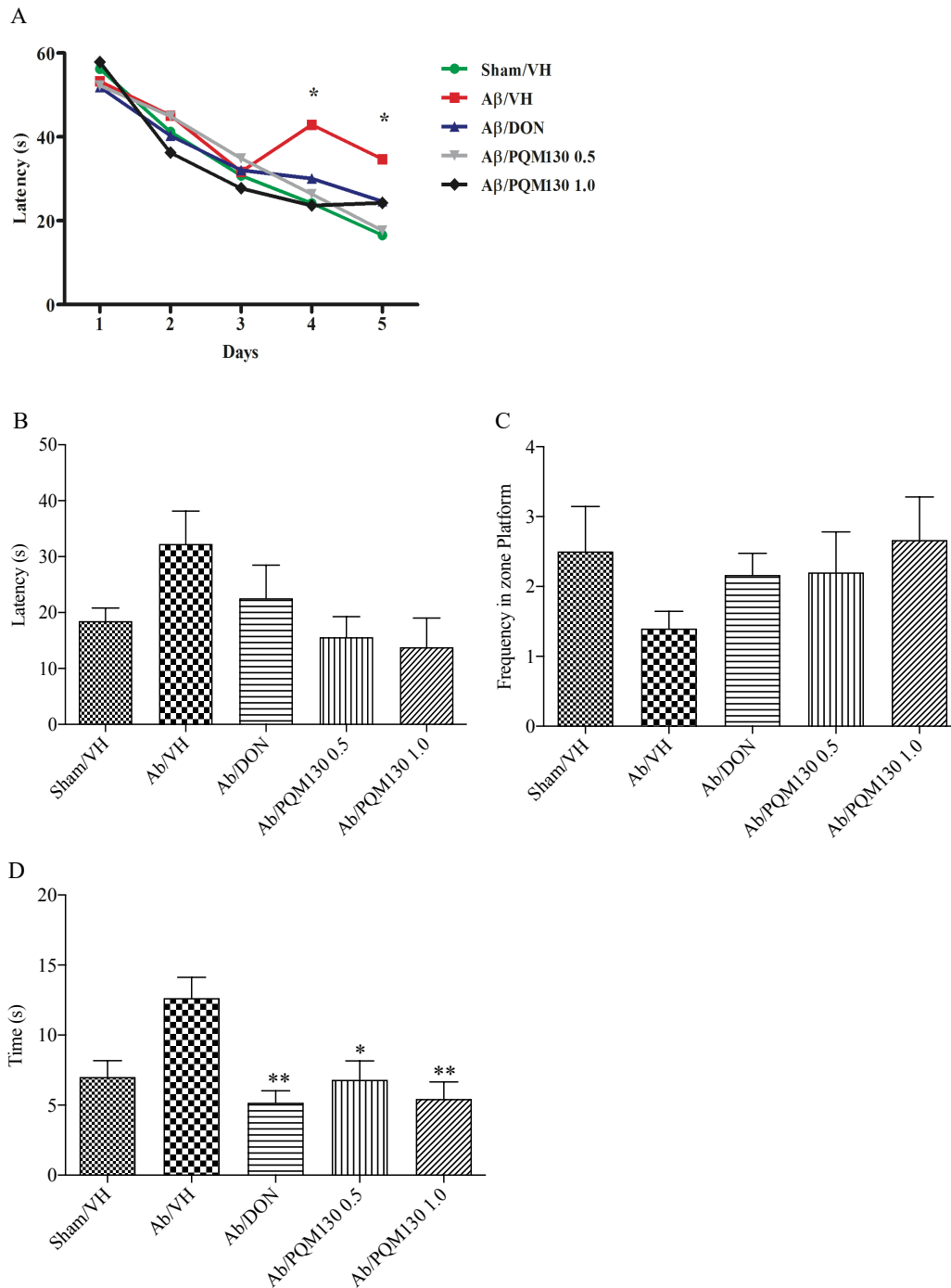


Figure 12 Effects of donepezil and PQM130 treatments (0.5 or 1.0 mg/kg) on the performance in the training (A) and probe trials (B-D) of the MWM test in  $A\beta_{1-42}$ -injected mice. The training trials were carried out for 5 days (four per day) the probe trial was performed on day 6. Escape latency (B), the frequency in the platform zone (C), and time spent in the opposite quadrant to the platform zone (D) were recorded in the probe test. Values are expressed as mean  $\pm$  SEM ( $n=10$ ) (A: \* $p<0.05$  vs.  $A\beta/VH$  group; D: \* $p<0.05$  and \*\* $p<0.01$  vs.  $A\beta/VH$ ; ANOVA, post hoc test Bonferroni).

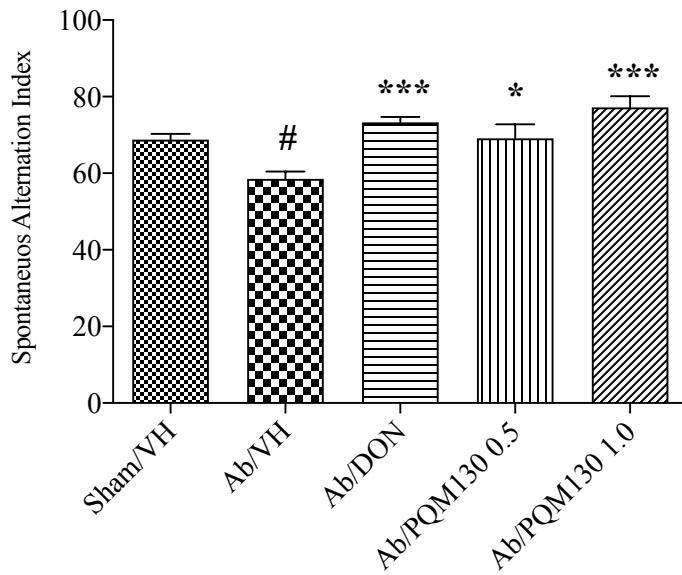


Figure 13 Effects of donepezil and PQM130 treatments (0.5 or 1.0 mg/kg) on the performance in the Y-maze test in  $A\beta_{1-42}O$ -injected mice. The spontaneous alternation was recorded in a 5 minutes trial. Values are expressed as mean  $\pm$  SEM ( $n=10$ ) (# $p<0.05$  vs. Sham/VH, \* $p<0.05$  and \*\*\* $p<0.001$  vs. Ab/VH; ANOVA, post hoc test Bonferroni).

## 6.2 Effects of PQM130 on hippocampal cell death

Next, the pathologic changes in different areas of the hippocampus through H&E-stained sections were examined. In  $A\beta$ /VH mice, H&E staining exhibited irregular and sparse neuronal arrangements in the CA1, CA3, DG regions of the hippocampus.

Unsurprisingly, neuropathological changes, including neuron loss and nucleus shrinkage or disappearance, were found in the hippocampus in  $A\beta_{1-42}O$ -injected mice (Figure 14 A). Interestingly, PQM130 treatment but not donepezil alleviated neuronal injury status compared with the saline treated  $A\beta$  group ( $p<0.01$ , Figure 14 B).

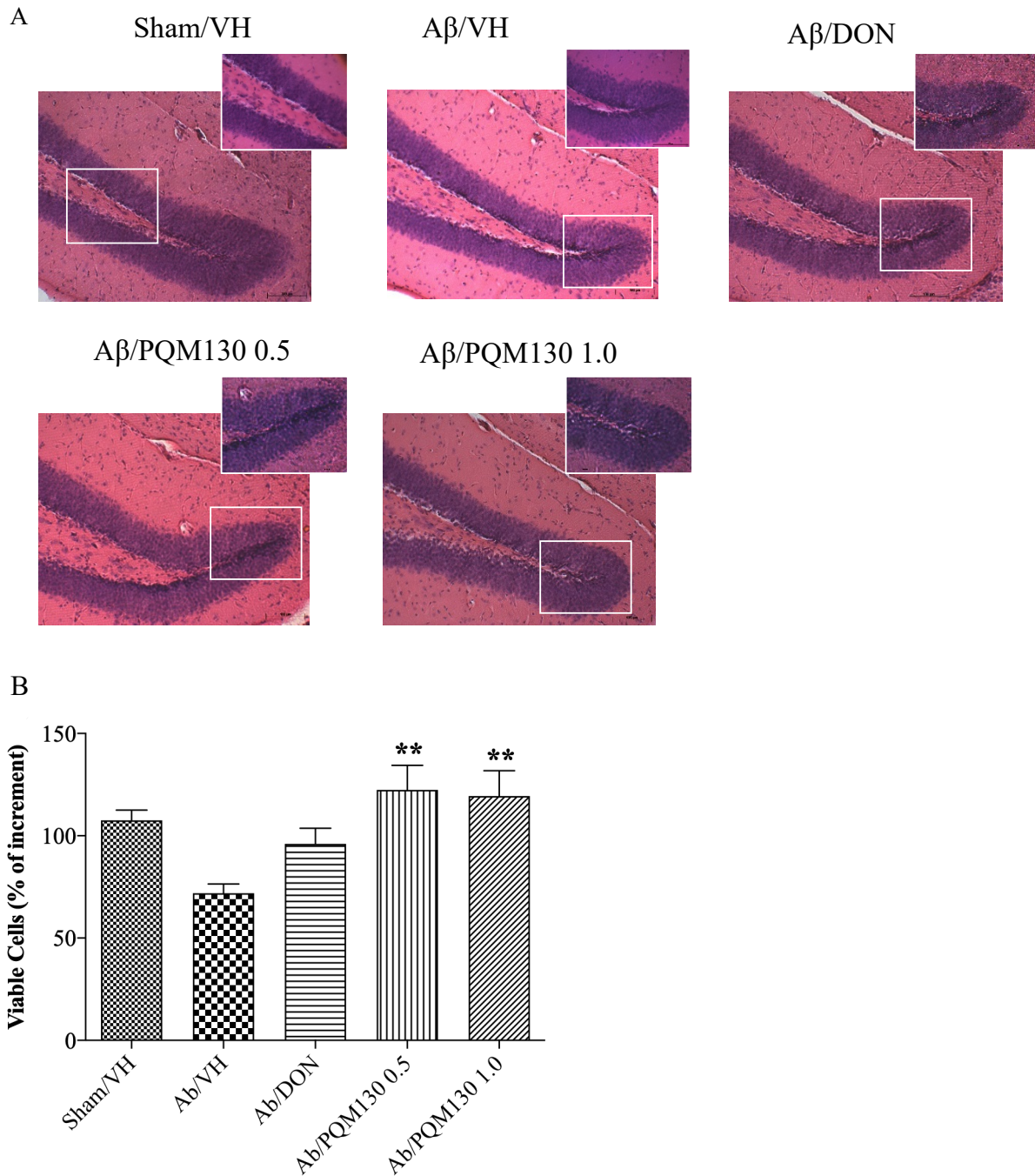


Figure 14 Effects of donepezil and PQM130 treatments (0.5 or 1.0 mg/kg) on neuronal cell death after  $A\beta_{1-42}O$  injection. Representative H&E staining of coronal sections containing the hippocampus. Magnification 20x and 40x, scale bar 100  $\mu\text{m}$  (A). Quantitative analysis of H&E staining (B). Values are expressed as mean of fold increase  $\pm$  SEM ( $n=10$ ) of the density of each experimental group compared to Sham/VH group (b: \*\* $p<0.01$  vs.  $A\beta/VH$ ; ANOVA, post hoc test Bonferroni).

The p53 pathway is targeted to respond to various intrinsic and extrinsic stress signals that monitor DNA replication, chromosome segregation, and cell division. In AD, increased tp53 level was detected in various parts of patient brains<sup>170</sup> compared to healthy individuals' brains. Equally, data from *in vivo* AD models showed an increase in tp53 level in affected neurons.<sup>171</sup> In this study,  $A\beta$  treatment induced the up-

regulation of tp53 mRNA level. On the contrary, PQM-130 but not donepezil significantly down-regulated tp53 expression ( $p < 0.05$ , Figure 15).

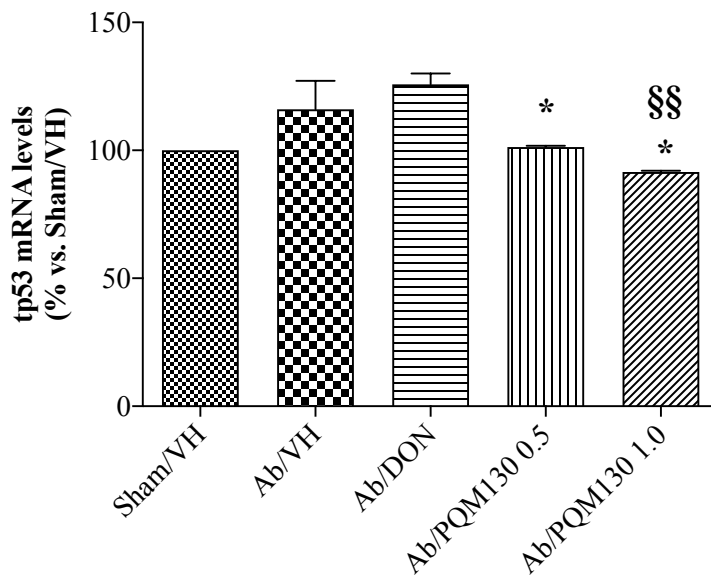


Figure 15 Effects of donepezil and PQM130 treatments (0.5 or 1.0 mg/kg) on tp53 mRNA relative expression in  $A\beta_{1-42}O$ -injected mice. The pc53 mRNA relative expression was determined in hippocampal samples through the  $2^{-\Delta\Delta C_t}$  method and represented as percentage vs. Sham/VH group. ACTB was used as control housekeeping gene. (\* $p < 0.05$  vs.  $A\beta/VH$ , §§ $p < 0.01$  vs.  $A\beta/DON$ ; ANOVA, post hoc test Bonferroni).

To study the underlying mechanisms of the mitigation of PQM130 on  $A\beta$ -induced neuronal damage caspase-9 and -3 activations were detected. Caspase-9 is involved in the intrinsic signaling apoptotic pathway. This protease is known as a biomarker of oxidative stress-induced cell death, so we further investigated the effect of PQM130 on its activation.

The activated caspase-9 successively cleaves and activates the downstream effector procaspase-3, contributing to caspase-dependent apoptosis. As shown in Figure 16, the activation of caspase-9 and -3 increased significantly in the hippocampal samples of the  $A\beta_{1-42}O$  treated group compared to the sham group ( $p < 0.05$ ). However, PQM130 was shown to be useful to reduce the activation of both caspases, returned to levels comparable to those of sham group treatment, especially at the maximum dose ( $p < 0.05$  and  $p < 0.01$ , correspondingly), while donepezil was only effective for caspase-3 activation ( $p < 0.05$ ).

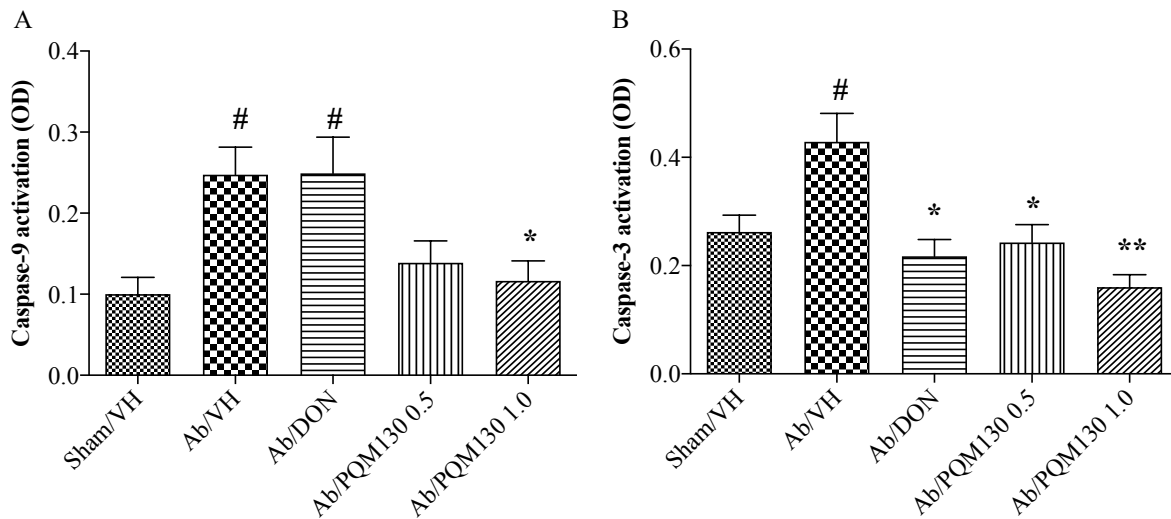


Figure 16 Effects of donepezil and PQM130 treatments (0.5 or 1.0 mg/kg) on caspase-9 (B) and -3 (C) activations in  $A\beta_{1-42}$ -injected mice. Caspase-9 and -3 activations were determined using a specific chromogenic substrate in hippocampal samples. Values are expressed as mean  $\pm$  SEM ( $n=10$ ) of optical density (OD) of each experimental group (A: #  $p<0.05$  vs. Sham/VH, \* $p<0.05$  vs.  $A\beta$ /VH; B: # $p<0.05$  vs. Sham/VH, \* $p<0.05$  and \*\* $p<0.01$  vs.  $A\beta$ /VH; ANOVA, post hoc test Bonferroni).

### 6.3 PQM130 antagonizes oxidative stress in mice

Evidence suggests that in the early stages of AD pathogenesis,  $A\beta$  reaches the mitochondria and causes the development of ROS and oxidative stress, and ROS generation may be involved in the deposition of senile plaques in AD brains.<sup>172,173</sup>

Cellular antioxidants such as GSH counteract oxidative stress-mediated damage. GSH plays a crucial role in the detoxification of ROS and regulation of intracellular redox environment.<sup>174</sup> Brain cells are vulnerable to oxidative stress; compounds able to modulate GSH level may contribute to developing a new treatment strategy.  $A\beta_{1-42}$ O injection caused apparent oxidant stress in mice brain as indicated by significant increased ROS formation ( $p<0.001$ , Figure 17A) and reduced GSH levels in the hippocampus compared to the sham group (Figure 17B). Nevertheless, the administration of PQM130, not donepezil, resulted in a significant decrease of ROS compared with the sham group ( $p<0.001$  and  $p<0.01$ , Figure 17A). Furthermore, PQM130 treatments increase GSH levels in the hippocampal samples of  $A\beta_{1-42}$ O injected mice close to the sham group levels, mainly with the 0.5 mg/kg dose ( $p<0.01$ , Figure 17B).

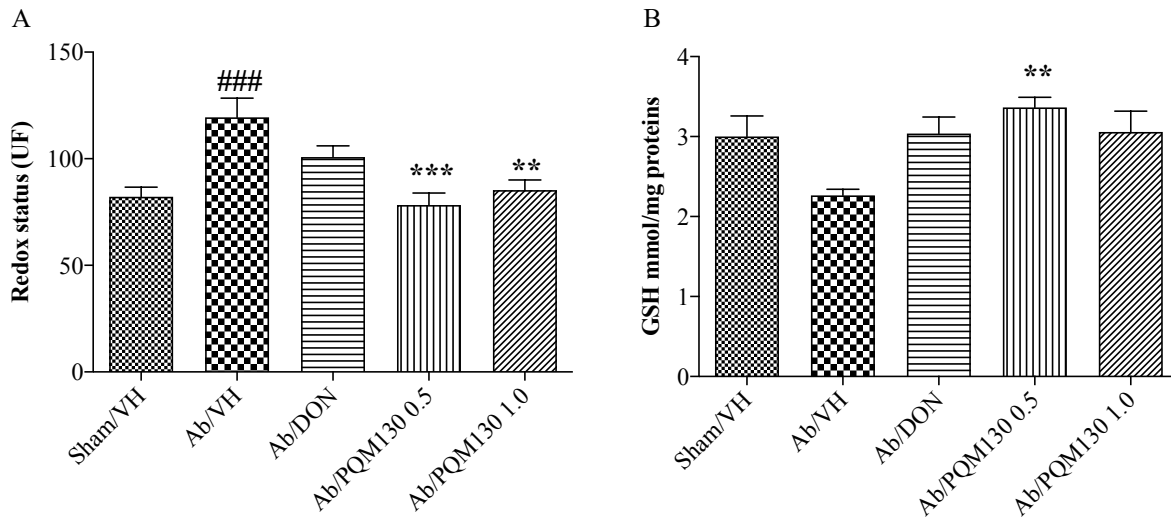


Figure 17 Effects of donepezil and PQM130 treatments (0.5 or 1.0 mg/kg) on cellular redox status after  $A\beta_{1-42}O$  injection. Redox status was evaluated in hippocampal samples based on DCF's fluorescence emission at 535 nm after excitation at 485 nm. Values are expressed as mean  $\pm$  SEM ( $n=10$ ) of fluorescence intensity arbitrary units (UF) of each experimental group (A). GSH content was measured using a colorimetric assay in hippocampal samples. Values are calculated using a standard calibration curve and expressed as mean  $\pm$  SEM ( $n=10$ ) of mmol GSH/mg protein (B). (A: ### $p<0.001$  vs. Sham/VH, \*\* $p<0.01$  and \*\*\* $p<0.001$  vs.  $A\beta/VH$ ; B: \*\* $p<0.01$  vs.  $A\beta/VH$  group)

Besides, gene expression has also been used as a useful biomarker to identify cellular stress. The Nrf2-ARE pathway involves a battery of antioxidative and anti-inflammatory genes that remove oxidized proteins and prevent  $A\beta$  protein aggregate formation.<sup>175</sup> We examined whether PQM130 treatment could alter the Nrf2 activation and GR levels in mice's hippocampus. Gene expression analysis was performed for GR enzyme showing that  $A\beta$  injection reduced GR mRNA expression levels, while donepezil and PQM130 (0.5 mg/kg) significantly improved GR mRNA levels ( $p<0.01$  and  $p<0.05$ , respectively; Figure 18A). GR restores intracellular GSH by reducing glutathione disulfide. As expected, the Nrf2 expression was found to be significantly decreased in the hippocampi of  $A\beta/VH$  mice ( $p<0.001$ ), contrariwise PQM130 (0.5 mg/kg) treatment up-regulated the mRNA levels of Nrf2, compared to  $A\beta/VH$  mice ( $p<0.001$ , Figure 18B) and  $A\beta/DON$  1 mice ( $p<0.01$ , Figure 18B).

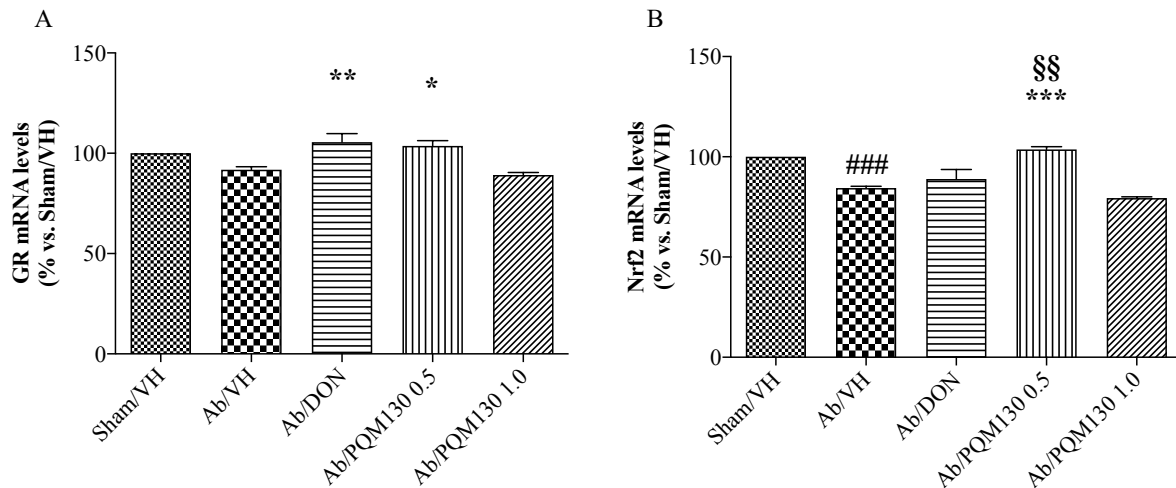


Figure 18 GR and Nrf2 mRNA relative expressions (A-B) were determined through the  $2^{-\Delta\Delta Ct}$  method and presented as percentage vs. Sham/VH group. ACTB was used as control housekeeping gene. (A: \* $p < 0.05$  and \*\* $p < 0.01$  vs.  $A\beta$ /VH group; B: \*\*\* $p < 0.001$  vs. sham groups, §§ $p < 0.01$  vs.  $A\beta$ /DON; ANOVA, post hoc test Bonferroni).

## 6.4 PQM130 regulates GSK3 $\beta$ and ERK1/2 protein expressions in mice

MAPK/ERK1/2 signaling pathway is involved in the transcriptional regulation of neuronal apoptosis and has been shown to play a crucial role in AD,<sup>168</sup> the phosphorylation of ERK1/2 was also found in the present study. Data revealed that  $A\beta_{1-42}O$  injection aroused the phosphorylation of ERK1/2 compared with the sham group ( $p < 0.001$ , Figure 19A). However, treatment with PQM-130 and donepezil remarkably blocked the phosphorylation of ERK1/2 induced by  $A\beta_{1-42}O$  ( $p < 0.05$ , Figure 19A), suggesting that the dephosphorylation of ERK1/2 contributed to the antiapoptotic effect of PQM130.

Increasing evidence suggests that the GSK3 activity is directly impacted by  $A\beta_{1-42}O$  exposure, and it is altered in AD brains.<sup>176</sup> The phosphorylation level of GSK3 $\beta$  (Ser9) was assessed by western blot studies to study its potential connection with the PQM130 mechanism of neuroprotection. As shown in Figure 19B, the phosphorylated GSK3 $\beta$  was diminished, although not significantly, in the  $A\beta$ /VH group. The treatment with 0.5 mg/kg PQM130 significantly increased the phosphorylated GSK3 $\beta$  protein ( $p < 0.05$ ).

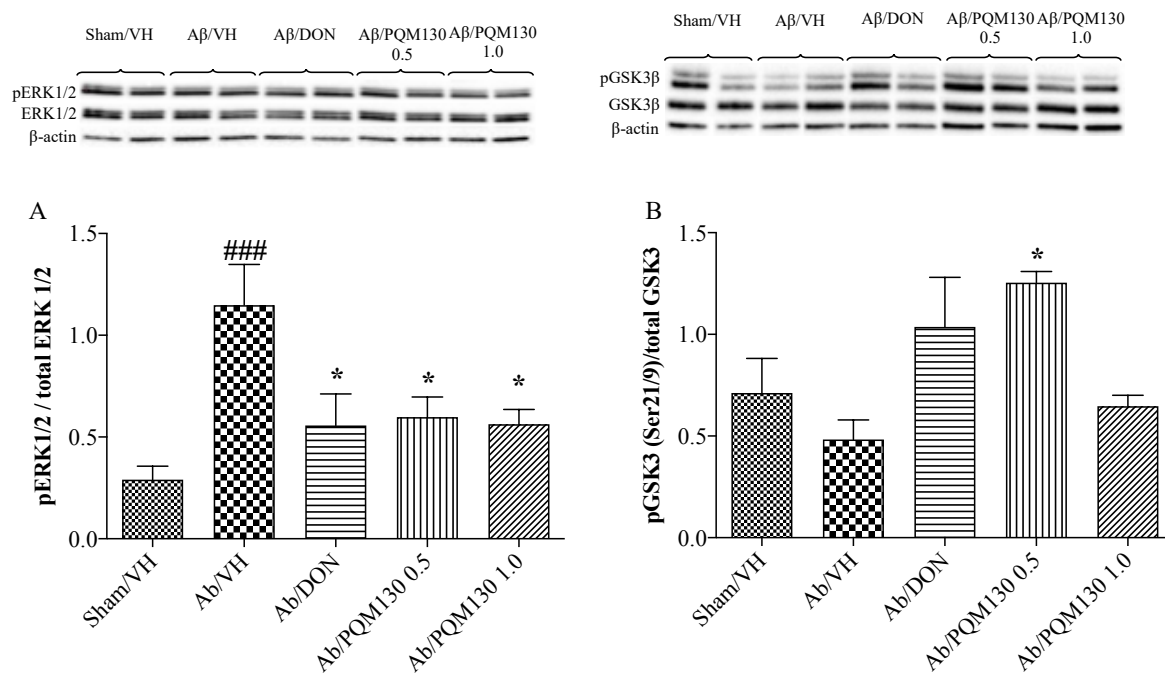


Figure 19 Effects of donepezil and PQM130 treatments (0.5 or 1.0 mg/kg) on ERK1/2 (A) and GSK3 (B) phosphorylation (pERK1/2 and pGSK3 $\beta$  Ser21/9 residue) in A $\beta$ <sub>1-42</sub>O-injected mice. pGSK3 $\beta$  and pERK1/2 were determined by Western Blotting in hippocampal samples at 46 kDa and 42/44 kDa respectively, and using total GSK3, total ERK1/2 and  $\beta$ -actin (42 kDa) as loading control. Top: representative images of pERK1/2, ERK1/2 and  $\beta$ -actin (A) and pGSK3 $\beta$ , GSK3,  $\beta$ -actin (B) expressions in hippocampus. Bottom: quantitative analysis of the Western Blotting results for the pERK1/2 (A) and pGSK3 $\beta$  Ser21/9 (B) levels. The graphs show densitometry analysis of the bands pertaining to the protein of interest. Values are expressed as mean  $\pm$  SEM (n=10) of each group. (A: \*p<0.01 vs. A $\beta$ /VH group; B: ###p<0.001 vs. Sham/VH, \*p<0.05 vs. A $\beta$ /VH group; ANOVA, post hoc test Bonferroni).

## 6.5 PQM130 reduces neuroinflammation and astrocytic activation in mice

Neuroinflammatory reactions mediated by microglia and astrocytes have been shown to play a key role in the early progression of AD. Several studies have demonstrated that neurons exacerbate local inflammatory reactions by producing inflammatory mediators and act as an essential contributor in the pathogenesis of AD<sup>177</sup>. Activated astrocytes facilitate A $\beta$  clearance and mediate inflammation via the production of proinflammatory cytokines and immunostimulatory molecules<sup>178</sup>. Glial fibrillary acidic protein (GFAP) is a specific marker for activated astrocytes.

Immunohistochemical staining for astrogliosis (GFAP) in hippocampal regions revealed a significant increase in GFAP (p<0.01) reactive cells in the A $\beta$ /VH group compared to sham mice. However, the PQM130-treated mice (1 mg/kg) showed a significant decrease in GFAP-positive areas compared with the A $\beta$ /VH mice group (p<0.01,

Figure 20B). These results suggested that PQM130 treatment alleviated the neuroinflammation induced by  $A\beta_{1-42}O$  in the AD brain.

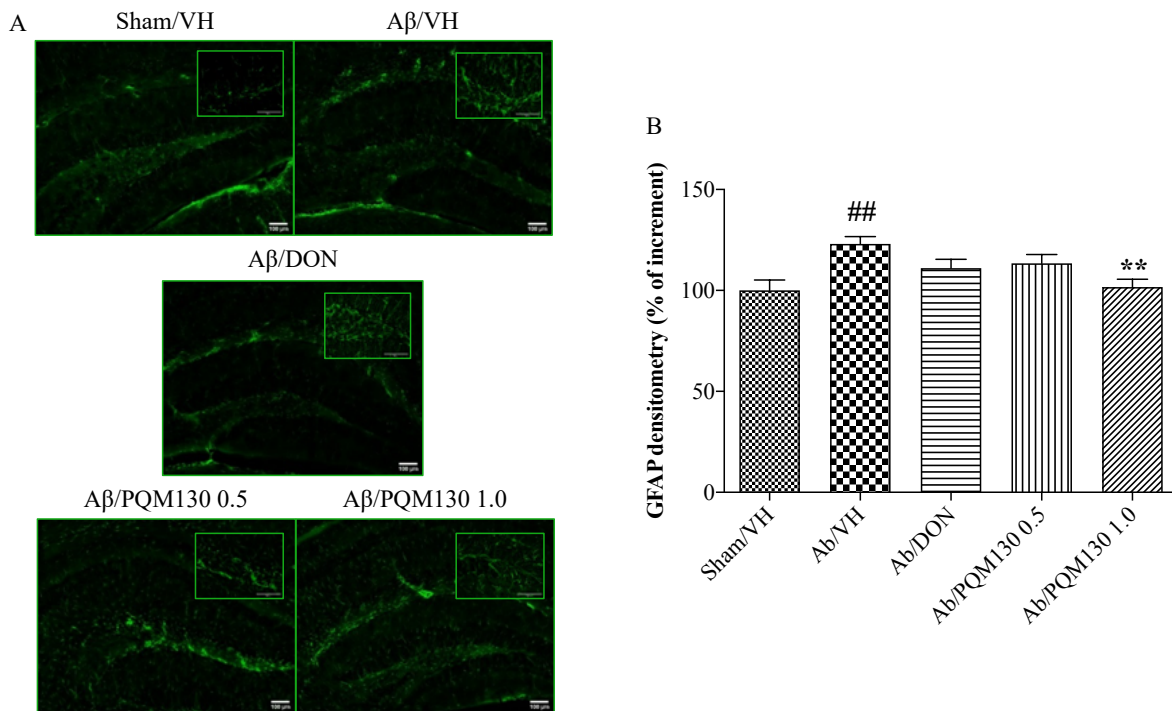


Figure 20 Effects of donepezil and PQM130 treatments (0.5 or 1.0 mg/kg) on astrocyte activation in  $A\beta_{1-42}O$ -injected mice. Representative photomicrographs (A) of immunostaining for GFAP in brain coronal sections containing hippocampal structure of each experimental group. Magnification 10x and 40x, scale bar 100  $\mu$ m. Quantitative analysis of GFAP immunostaining (B). Values are expressed as mean of % of increment  $\pm$  SEM ( $n = 10$ ) of the fluorescent intensity of each experimental group compared to the Sham/VH group (B: ## $p < 0.01$  vs. Sham/VH, \*\* $p < 0.01$  vs.  $A\beta/VH$ ; ANOVA, post hoc test Bonferroni).

## 6.6 PQM130 modulates synaptic plasticity in mice

Classic effects of BDNF include promoting neuronal viability, differentiation, migration, and dendritic arborization. As a first step, we investigated the effect of PQM130 on total BDNF gene expression, and the results did not indicate any significant difference among the different experimental groups (Figure 21A). To obtain further information about the different responsiveness to PQM130, some neurotrophin transcripts' expression profiles as long 3' UTR BDNF, exons IV, and VI were considered (Figure 21B-D). In deep, PQM130 (0.5 mg/kg) increased significantly the

expression of long 3' UTR BDNF ( $p < 0.05$ , Figure 21B) and isoform IV ( $p < 0.05$ , Figure 21C), whereas no changes were found in the other experimental groups.

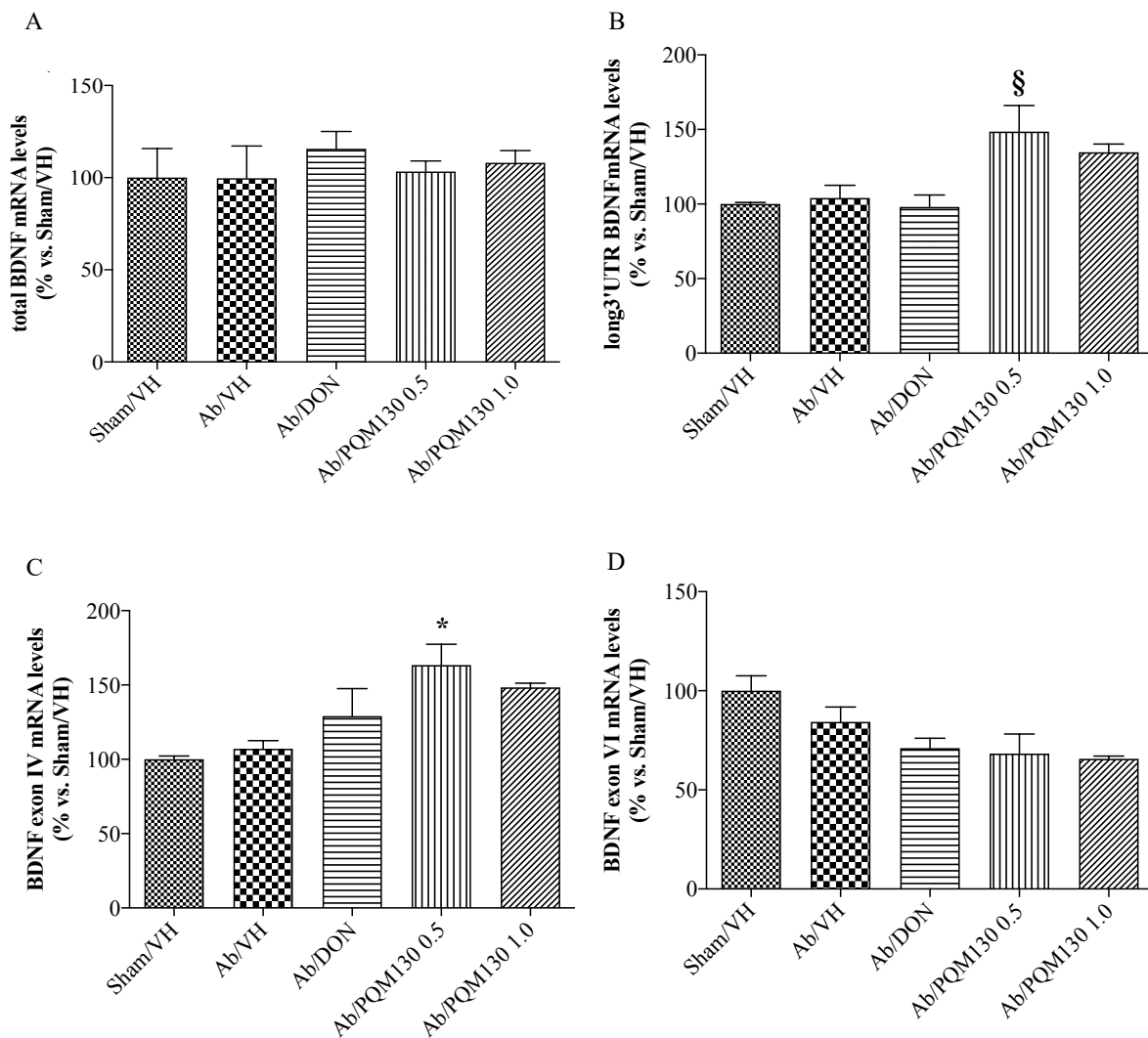


Figure 21 Effects of donepezil and PQM130 treatments (0.5 or 1.0 mg/kg) on the total BDNF (A), long 3' UTR BDNF (B), BDNF exon IV (C), and BDNF exon VI (D) mRNA relative expressions in  $A\beta_{1-42}$ -injected mice. The mRNA relative expressions were determined in hippocampal samples through the  $2^{-\Delta\Delta C_t}$  method and represented as percentage vs. Sham/VH group. ACTB was used as control housekeeping gene. (B: § $p < 0.05$  vs.  $A\beta$ /DON; C: \* $p < 0.05$  vs.  $A\beta$ /VH; ANOVA, post hoc test Bonferroni).

In addition to well-known actions, it seems that BDNF has an essential role at the synapse level, where it affects the development, function, and plasticity.<sup>179</sup> Consequently, the effect of PQM130 on the pre-synaptic protein synaptophysin was next explored. As shown in Figure 22A, there is a small reduction in synaptophysin mRNA levels in the  $A\beta$ /VH and  $A\beta$ /DON groups, while the mRNA expression in the PQM130 groups was kept at the sham group levels. Even more impressive, the western

blot analysis (Figure 22B) revealed an evident decrease of synaptophysin expression in the A $\beta$ /VH and A $\beta$ /DON hippocampal groups. However, after PQM130 treatment with the highest dose, synaptophysin expression was significantly increased compared to the A $\beta$ /VH group ( $p < 0.05$ ).

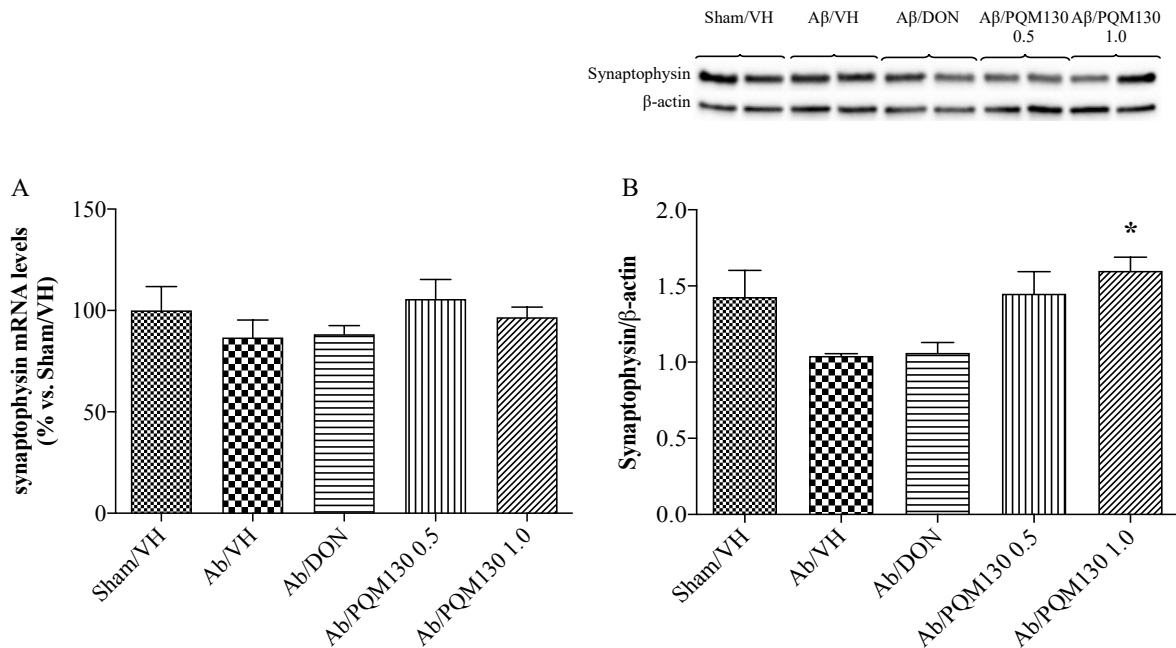


Figure 22 Effects of donepezil and PQM130 treatments (0.5 or 1.0 mg/kg) on synaptophysin levels in A $\beta_{1-42}$ O-injected mice. Synaptophysin mRNA relative expressions in hippocampal samples (A). The mRNA relative expressions were determined through the  $2^{-\Delta\Delta C_t}$  method and represented as percentage vs. Sham/VH group. ACTB was used as control housekeeping gene. Synaptophysin activation was determined by Western Blotting in hippocampal samples at 33 kDa using  $\beta$ -actin (42 kDa) as loading control (B). Top: representative images of synaptophysin and  $\beta$ -actin expressions in hippocampus. Bottom: quantitative analysis of the Western Blotting results for the synaptophysin levels. Values are expressed as mean  $\pm$  SEM ( $n=10$ ) of each experimental group. (B: \* $p < 0.001$  vs. A $\beta$ /VH; ANOVA, post hoc test Bonferroni).

## 7 Discussion

Patients with mild to moderately severe AD are currently treated with AChE inhibitors, and among these, the first-line symptomatic drug is donepezil. Given the widely recognized concept of AD as a dynamic pathological network, intense efforts are being made to try to find new therapies that can reach many of the network's biological features, including AChE, at the same time. Considering the decades-long preclinical period associated with AD, it is also crucial to identify drugs that could be used at the initial stages of AD pathology.

In this view, the present study focused on evaluating the efficacy of the feruloyl-donepezil hybrid PQM130 on the AD neurodegenerative process, trying to compare it with donepezil activity.

Dias et al. have already shown the *in vitro* metal chelator activity and neuroprotective activity against oxidative stress and *in vivo* anti-inflammatory activity of PQM130.

The multifactorial effects of PQM130, such as decreased neuronal death and oxidative stress, increased neurotrophic activity, decreased inflammation, and improved spatial memory formation compared to the A $\beta$ <sub>1-42</sub>O treated group, were demonstrated by research results acquired from the present work. Neuroprotective and neurotrophic strategies could be a winning approach because, on the one hand, they delay the progression of neurodegeneration; on the other hand, they improve the disease condition.

To investigate the neuroprotective activities of PQM130, we used a mouse A $\beta$ <sub>1-42</sub> model. The i.c.v. A $\beta$ -injection model is a useful mouse model for developing and evaluating therapeutic approaches to AD pathology because it can reproduce different peculiar mechanisms of AD, neuroinflammation, synaptotoxicity, apoptosis, and neurodegeneration. Moreover, the i.c.v. A $\beta$ -injection model simplifies behavioral studies in a reasonably short timeframe.

Thanks to the MWM test is possible to evaluate two main aspects: the first one is that the mice should develop specific behavioral tactics, essential to managing the stressful situation like learning to swim and recognize that the hidden platform is the only escape

route; the second aspect is the spatial learning component, which means that the mice must learn the precise position of the platform and swim to reach it from the randomly chosen starting point within a minute.<sup>180</sup>

In this study, a gradual enhancement in the spatial memory was found as there was a significant reduction in escape latency time in the donepezil and PQM130 treated mice compared to A $\beta$ /VH mice when evaluated on the fourth and fifth days during the training. This improved performance in the MWM test may be because PQM130 could increase cholinergic neuronal transmission by reducing oxidative stress and alleviating AChE activity. A $\beta$ /DON group had equivalent swimming performance as that of higher doses of PQM130. This effect of donepezil may be correlated with its AChE inhibition.<sup>181</sup> However, during the probe trial in which the escape platform is removed to assess the memory aspect, the latency was not implemented significantly, only the time spent in the opposite quadrant markedly decreased after PQM130 and donepezil treatments. Thus, the reduced escape latency time in PQM130 treated group proves its promising effect on spatial learning capacity.

It has been previously reported that working memory can be compromised at an early stage of AD.<sup>182,183</sup> Spontaneous alternation behavior is considered as a reflection of working memory in the Y-maze test. The continuous spontaneous alternation in the Y-maze test has the advantage of providing memory and locomotor evaluation, simultaneously eluding redundant stressful handling of animals.<sup>184</sup> We observed a compromised working memory in A $\beta$ <sub>1-42</sub>O injected mice, and the deleterious effect was reverted by PQM130 dose-dependent treatment. The compound can enhance the percent of alternation behavior in the Y-maze, and the highest dose of PQM130 has effects comparable to those of donepezil. Our findings were consistent with previous reports that donepezil significantly improves alternation deficits in the Y-maze test in the A $\beta$ -injected mice.<sup>185,186</sup>

Apoptosis is toughly related to the memory and cognitive decline in AD,<sup>187</sup> and it is known as programmed cell death involving mitochondrial dysfunction, caspases activation, and DNA fragmentation.<sup>188</sup> It is known that A $\beta$  leads to vast and extensive neuronal cell death, one of AD's significant hallmarks, along with NFTs and amyloid

plaques<sup>189</sup>. Previous studies have shown that neuronal apoptosis is a crucial factor leading to neuronal loss<sup>190</sup>. The caspase family plays a crucial role in modulating the apoptosis pathway, caspase-9 is an initiator caspase that activates the executioner caspases, such as caspase-3, which brings cells to apoptosis. It has been proved that caspases mediate the apoptosis of cortical and hippocampal neurons of AD<sup>191</sup>, and relate with A $\beta$ <sup>192</sup>, APP<sup>193</sup>, and NFTs<sup>194</sup>. Finding compounds able to inhibit or reduce the activity of caspases may be a successful strategy for preventing and treating AD<sup>195</sup>. Our results demonstrated that PQM130 markedly overturned the hippocampal injury and caspase-9 and -3 activations in A $\beta$ -injected mice. Meanwhile, donepezil did not show the same efficiency in reducing apoptosis and neuronal damage. Also, increased p53 level is detectable in brain areas damaged by AD, animal models, and neuronal cells isolated from AD brains.<sup>196</sup> Interestingly, PQM130 reduced the expression of p53, validating its antiapoptotic activity.

GSK3 $\beta$  is involved in tau phosphorylation, memory impairment, increased amyloid production, inflammation, and neuronal death. P53 directly binds and increases the activity of GSK3 $\beta$ , besides inhibition of nuclear GSK3 $\beta$  attenuated p53-dependent transcription.<sup>197</sup>

The link between p53 and GSK3 $\beta$  is undoubtedly more complicated; however, in this study, it has been found that decreased p53 expression after PQM130 treatment is most likely reflected in phosphorylation, and therefore deactivation of GSK3 $\beta$ , leading to protection against neuronal death induced by A $\beta$ <sub>1-42</sub>O.

All pathological changes caused by A $\beta$  oligomers are linked with oxidative stress and inflammation, and both can lead to neuronal injury<sup>198,199</sup>. Therefore, we hypothesized that alleviation of oxidative stress and inflammation might attenuate the toxicity of A $\beta$ <sub>1-42</sub>O. GSH is an intracellular antioxidant that protects against endogenous oxygen radicals. GSH neutralize ROS by directly reacting with them and prevents hydrogen peroxide-induced hydroxyl radical formation. GSH level is the first indicator for oxidative stress in the brain<sup>200</sup>. In this study, the ROS levels, significantly higher, and the GSH, lower, in the A $\beta$ /VH group than those in the sham group, demonstrated that A $\beta$ <sub>1-42</sub>O induced oxidative stress and the antioxidant defenses were not able to respond.

PQM130 and not donepezil significantly ameliorates oxidative damage as confirmed by decreased ROS levels as well as increased GR and restored GSH content in brain tissues, confirming the similar evidence recorded by PQM130 in neuronal SH-SY5Y cells.<sup>156</sup> Another endogenous defense against oxidative stress involves the Nrf2 pathway, which engages the Nrf2 activation and the subsequent amplified expression of the downstream cytoprotective proteins<sup>201</sup>. Branca et al.<sup>202</sup> removed the Nrf2 gene from APP/PS1 mice and found that the absence of Nrf2 significantly exacerbates cognitive deficits in APP/PS1 mice, suggesting a link between Nrf2 and AD. This hypothesis is supported by the findings from several laboratories reporting that Nrf2 activity decreases with aging.<sup>203</sup> Additionally, *in vitro* and *in vivo* studies demonstrated that Nrf2 pathway activation by pharmacological activators plays a protective role against A $\beta$ -induced toxicity.<sup>204–206</sup> In our model, exposure to A $\beta$ <sub>1-42</sub>O caused a marked decrease in Nrf2 activation, and only PQM130 significantly increase its expression, probably due to the presence of ferulic acid in this hybrid molecule. In this regard, the  $\alpha$ ,  $\beta$ -unsaturated carbonyl system in PQM130 is responsible for initiating Nrf2 cascade through a Michael addition reaction.<sup>207</sup> Thus, the reduction PQM130-mediated of oxidative stress could be useful to explain the protective effect of PQM130 on apoptotic cell death and memory impairment A $\beta$ <sub>1-42</sub>O-induced.

Studies on postmortem human brains indicated the Ras-MAPK pathway as an early driver of AD pathology development<sup>208,209</sup>. It has been proved that phosphorylation of ERK1/2 contributes to apoptosis response in neurons<sup>210,211</sup>. Blocking its phosphorylation generates subsequent inhibition of apoptosis through the regulation of caspase-3 activity.<sup>212,213</sup> The activity of ERK1/2 is also regulated by ROS.<sup>214–217</sup> In fact, it has been reported that the reduction of ROS accumulation decreased ERK1/2 activation in an AD model.<sup>218</sup> The ERK pathway is fundamental to memory formation and hippocampal synaptic plasticity. The balance between phosphorylated and not phosphorylated ERK is essential for normal hippocampal-related functions.<sup>219</sup> In our model A $\beta$ <sub>1-42</sub>O contributed to abnormal activation of ERK1/2, and there was a pronounced decrease of p-ERK1/2 levels by PQM130 administration.

Excessive activation of ERK has also been revealed in astrocytes, which influence A $\beta$  generation through ROS formation.<sup>220</sup> It is clear as compounds able to inactivate ERK phosphorylation could also be responsible for the reduction of A $\beta$  generation and thus to the prevention or inhibition of neuronal damage in the AD brain<sup>221,222</sup> Astrocytes and their resident protein GFAP modulate synaptic activity and process neuronal input, and signals related to learning and memory by the formation of cytoskeletal filaments.<sup>223</sup> Our results suggest that PQM130 and not donepezil might alleviate reactive gliosis since this treatment reduced levels of GFAP in the hippocampus of A $\beta$ <sub>1-42</sub>O-lesioned mice.

BDNF exerts substantial protective effects on crucial neuronal circuitry involved in AD.<sup>224</sup> The transcription of the BDNF gene is intricate. At least eight differentially promoters give rise to multiple mRNA transcripts, each of which contains a distinct 5' exon spliced to a common 3' coding exon, and all of which encode an identical BDNF protein.<sup>225</sup>

We examined total BDNF mRNA expression, two 5' exon-specific transcripts (IV and VI), and BDNF mRNA transcripts with an extended 3'untranslated region (3'UTR) in the hippocampal samples. BDNF mRNA transcripts with long 3'UTRs are reported to play important roles in dendritic spine morphology and long-lasting synaptic plasticity.<sup>226</sup> We found that even if these transcripts' expression was not reduced by A $\beta$ <sub>1-42</sub>O injection, PQM130 markedly increased long 3'UTR and exon IV. Interestingly, the increased level of BDNF in the hippocampus was supplemented by an up-regulated expression of synaptophysin. So, assembling these results, PQM130 may activate the BDNF signaling pathway, which regulates the expression of its downstream signaling components, including synaptic plasticity proteins, to improve cognitive deficits in mice.

## SECTION TWO

## 8 Aim of the study

Investigating AD mechanisms can provide new insights into the disease's pathogenesis, diagnosis, and treatment. However, it is not easy to assess putative associations with genetic risk factors due to features, such as comorbidities variables and diversity in genetic background. Despite lower incidence, AD studies have long been focused on EOAD cases due to the A $\beta$  peptides and causative mutations, such as PS1 and PS2, and studied with a neuron-centric view. However, recent large-scale genetic studies have identified numerous risk genes primarily expressed in non-neuronal cell types, such as astrocyte and microglia, as significant risk factors for LOAD, suggesting the importance of regulating the balance between production and clearance of A $\beta$  peptide from the brain.<sup>227,228</sup>

The involvement of ABC transporters has been associated with AD, where different transporters, like ABCA1, ABCA7, and many others, have been evaluated for their roles in the transportation of different biological substrates. Adenosine triphosphate (ATP) hydrolysis controls substrate passage within the cells through ABCA transports.<sup>229</sup> ABC transporters protect against toxic endogenous and exogenous entities, exhibiting significant roles in maintaining the neuronal microenvironment.<sup>229</sup> ABC transporters are crucial in regulating the levels of neuronal A $\beta$  peptides, and AD risks can be enhanced in case of functional changes of these transporter proteins.<sup>230</sup>

The ABCA subfamily of transporters seems strictly correlated with AD. The ABCA family of transporters includes 12 members, which play essential roles in the transportation and metabolism of lipids.

Among all ABCA subtypes ABCA7 was identified as a robust AD-associated gene by GWAS studies.<sup>231</sup> ABCA7 gene is located on human chromosome 19p13.3 and is highly expressed in the brain.<sup>232</sup> ABCA7 has been reported to be expressed in neurons, astrocytes, oligodendrocyte precursor cells (OPCs), and microglia in the mouse brain (Figure 23), though expression data in human cells is less clear.<sup>232</sup>

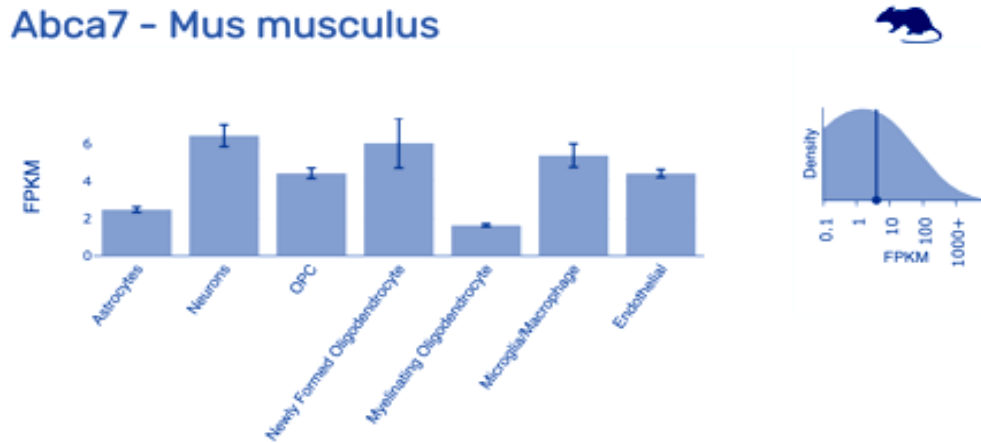


Figure 23. *ABCA7* mRNA expression from Barres Lab data sets. FPKM (fragments per kilobase of transcript per Million mapped read) mean  $\pm$  SD.

Decreased *ABCA7* expression is associated with increased AD risk, while increased expression is associated with reduced AD risk.<sup>233</sup> Loss of function variants in *ABCA7* are also related to the risk of AD.<sup>155</sup>

While much effort has been made on understanding the mechanisms of AD driven by EOAD mutations, specific impacts of *ABCA7* on LOAD remain much less clear. Most studies on the effect of *ABCA7* on LOAD have relied on a knockout mouse model and non-brain cell lines, such as HEKs.<sup>152,234</sup> *ABCA7* knockout mouse studies have shown that cerebral amyloid  $\beta$  plaque load was exacerbated.<sup>152</sup> Besides, results from *in vitro* cellular models suggest that *ABCA7* may affect phagocytic activities,<sup>235,236</sup> but the role of *ABCA7* in phagocytosis is not entirely clear. Despite these studies, the cell type-specific effects leading to pathological phenotypes have not been directly tested.

Moreover, studies involving animal models have drawn a lot of attention and concerns about humans' translatability due to species differences.<sup>237</sup> Similarly, current *in vitro* studies have revealed limitations caused by the inaccessibility to the relevant cell types such as neurons and glial cells and by failure to build a complex disease model. To further investigate the role of *ABCA7* in AD pathogenesis and functional changes induced by the *ABCA7* mutation in human brain cells, an isogenic iPSC line harboring rare homozygous mutant alleles (Y622\*) from healthy parental control cells has been created. A rare variant was selected instead of a common variant because the rare one presents a stronger association with LOAD than the common variant with a weaker

association with AD. The study aimed to evaluate if iPSC carrying the ABCA7 variant could present AD's pathological hallmarks in brain cells, such as astrocytes. Because ABCA7 could significantly impact the production and deposition of A $\beta$  plaques, promoting the development of neurotoxic A $\beta$  oligomers and aggregates, we evaluated the uptake capability of A $\beta$  oligomers in iPSC derived astrocytes with ABCA7 Y622\* mutation. It has been postulated that ABCA7 acts as a regulator of phagocyte function, so we investigated a dysregulation in phagocytosis.

Due to the significance of balanced cholesterol concentration in the maintenance of CNS functions, dysregulation of ABCA could cause brain degenerative disorders.<sup>238</sup> In fact, these transporter families have been reported to contribute to AD's pathophysiology, exhibiting functions related to cholesterol trafficking within the cells.<sup>239</sup>

To confirm an alteration of lipid homeostasis and cholesterol transport, several assays have been executed to show how this mutation could be responsible for lipids process dysregulation, leading to an increased risk of AD development.

Although additional research is needed to clarify ABC transporters' roles in AD, increasing evidence suggests that several of them, especially ABCA7, are key players in protecting the CNS against A $\beta$  neurotoxicity.

Shortly, new diagnostic instruments and therapeutic approaches can emerge based on this mechanism to early detect and improve amyloid pathology in the brain of AD patients by modulating the expression and/or activity of specific ABC transporters.

This project proposes new evidence regarding multiple roles of ABCA7 in AD development, showing a model for mechanistic studies on ABCA7 dependent pathogenesis and insights into therapeutic interventions for AD.

## 9 Materials and Methods

### 9.1 ABCA7 Isogenic iPSC Lines Generation

The CRISPR/Cas9-ABCA7 sgRNA plasmid was prepared followed by the published protocol. Briefly summarizing, a sgRNA sequence within 10 nucleotides from the target site corresponding to amino acid 120 was designed. The oligomer pairs (forward: 5'-CACCGCCCCTACAGCCACCCGGGCG-3' and reverse: 5'-AAACCGCCCGGGTGGCTGTAGGGGC-3') were annealed and cloned into pSpCas9-2A-GFP (PX458) plasmid (Addgene #48138). Plasmid DNA was submitted for Sanger sequencing to confirm correct ABCA7 sgRNA sequence. Furthermore, single-strand oligonucleotides (ssODN) was designed to create the non-sense mutation on ABCA7:

5'GGTGCGCGCCCCAGGCCAATCCAGGAGCTGCACCCTAAGCTCCCGTTGCCTCTCAC  
AGCTGGGAGACATCCTCCCCTAGAGCCACCCGGGCGTCGTCTTCTGTTCTTGGCAGC  
CTTCGCGGTGGCCACGGTGACCCAGAGCTTCTTGCTCAGCGCCTTCTTCTCCCGCGCCA  
ACCTGG-3'.

For electroporation, 80% confluent iPSCs of healthy line (#AG09173 and #AG08379) were dissociated with 20 minutes-long accutase treatment (Thermo Fisher Scientific) supplemented with 10  $\mu$ M ROCK inhibitor (Tocris). About 5 million cells were subject to electroporation using Amaxa and Human Stem Cell Nucleofector Kit I (Lonza) according to the manufacturer's instructions. In short, cells were resuspended in 100  $\mu$ l of reaction buffer from the kit supplemented with 7.5  $\mu$ g of CRISPR/Cas9-ABCA7 sgRNA plasmid and 15  $\mu$ g of ssODN. This mixture was nucleofected with program A-23, then resuspended with hES media supplemented with 10  $\mu$ M ROCK inhibitor and seeded on MEF plates. To screen the cells having successful integration of CRISPR/Cas9-ABCA7 sgRNA plasmid into host genome, fluorescence-activated cell sorting (FACS) was performed two days after the electroporation. In brief, cells were accutased and filtered through Falcon polystyrene test tubes (Corning #352235). Filtered cell suspensions were

transferred to Falcon polypropylene test tubes (Corning #352063) and sorted by BD FACS Aria IIU in FACS Facility at the Whitehead Institute. After sorting, cells were resuspended in hES media supplemented with 1X Penicillin-Streptomycin (P/S, Gemini Bio-products) and 10  $\mu$ M ROCK inhibitor, and seeded on 6 wells MEF plates.

### 9.1.1 Colony inspection

Each colony grown out of FACS-performed single cells was transferred to one well of gelatin-coated 12-well plate covered with MEFs and maintained till the colony grew big enough for another transfer. A part of each colony was transferred to 12-well plate while the rest of iPSCs in the original plate were collected and used to extract genomic DNA. Using primers (5'-CTGGTTCTGGTGCTCAAG-3' and 5'-CCTACGGCAGACGTCTTCAG-3'), DNA in ABCA7 gene was amplified and its PCR products were submitted to GENEWIZ for Sanger sequencing.

### 9.1.2 Karyotyping

In order to assess any abnormalities in chromosomes of iPSCs, we performed karyotyping after inspecting colonies. Cells cultured on Matrigel (Corning) in mTESR™1 media (Stem Cell Technologies) were prepared, and then sent to Cell Line Genetics for the analysis.

### 9.1.3 Genomic variant analysis for genome-edited iPSCs

The sequencing core facility of the Broad Institute of MIT and Harvard handled submitted samples and generated exome-seq data (76-bp paired-end). Our data was processed based on “GATK Best Practices” followed by Broad GATK team guidelines. The raw fastq files were mapped to human hg19 assembly using BWA mapper (version 7, mem option) and elimination of PCR duplicates were employed by MarkDuplicates function of Picard software package (<http://broadinstitute.github.io/picard>). Next, local

realignment and recalibration were executed using RealignerTargetCreator, IndelRealigner, and BaseRecalibrator modules of GATK tools. Using haplotypeCaller of GATK tools, variants in exonic regions with stand\_emit\_conf of 10 and stand\_call\_conf of 30 were called. INDEL variants were chosen using SelectVariants of GATK tools. Genomic variants from genome-edited iPSCs were compared to the variants from their parental lines, resulting in identifying unique variants to genome-edited iPSCs. Variants overlapping with repeatmasker regions and one with low DP were further removed, and then QUAL scores were calculated before functional annotation of exomic variants using ANNOVAR package. All potential unique variants resulted from the pipeline described above were manually examined by overlaying bam traces of genome-edited iPSCs with their parental lines in IGV browser.

## 9.2 Astrocyte Differentiation

iPSCs were prepared, cultured in mTeSR<sup>TM</sup>1 media on Matrigel coated plate until 100% confluent. As of this point, cells were cultured with neural media (1:1 mixture of DMEM/F12 GlutaMax, Neurobasal) supplemented with 1X N-2, 1X B-27, 1X NEAA, 1X GlutaMax, 1X P/S, 5 µg/ml insulin, 100 µM 2-mercaptoethanol instead of mTeSR<sup>TM</sup>1 media. For induction, 1 µM Dorsomorphin and 10 µM SB431542 were added into neural media for 12 days. Then cells were accutased and passaged to new Matrigel-coated plates. Once the neural rosette structure was identified under the microscope on day 16-24, another passage was performed with four million cells/well seeding density. A day after the passage, 20 ng/ml FGF2 and 10 ng/ml Bone Morphogenetic Protein 4 (BMP4, Peprotech) were added into neural media for maintenance. Full media change was performed every other day for 28 days. Using GLAST antibody (Miltenyi Biotec), astrocytes were purified from the mixed population by FACS. After sorting, purified astrocytes were cultured in astrocyte media (Sciencell) every other day for 7 days, and were FACS-sorted again for further purification with GLAST surface marker antibody.

## 9.3 RNA-seq analysis of iPSC-derived cell lines

Extracted total RNA was subject to QC using an Advanced Analytical-fragment Analyzer before library preparation using Illumina Neoprep stranded RNA-seq library preparation kit. Libraries were pooled for sequencing using Illumina NextSeq500 platforms at the MIT Biomicro Center. The raw fastq data were aligned to human hg19 assembly using STAR 2.4.0 RNA-seq aligner. Mapped RNA-seq reads covering the edited ABCA7 site were used to validate data genotypes. Gene raw counts were generated from the mapped data using featureCounts tool. The mapped reads were also processed by Cufflinks2.2 with hg19 reference gene annotation to estimate transcript abundances. Gene differential expression test between control and ABCA7-Y622\* groups was performed using Cuffdiff module with adjusted q-value < 0.05 for statistical significance. Geometric method was chosen as the library normalization method for Cuffdiff. Gene raw count matrix was processed by edgeR package to generate logCPM values (CPM counts per million) for data clustering analysis. Phylogenetic tree was constructed based on Euclidean distance of logCPM values of group average count values and ward.D2 option of hclust tool. Gene ontology was performed using Broad GSEA tool<sup>240</sup> and TOPPGENE tool<sup>110</sup>.

## 9.4 Amyloid $\beta$ up-take

Oligomerized A $\beta$ <sub>42</sub> was used for iPSC-derived astrocyte. A $\beta$ <sub>42</sub> peptide (AnaSpec) was dissolved in 1% NH<sub>4</sub>OH with 1 mg/ml concentration, and sonicated. Lysophilized A $\beta$ <sub>42</sub> was dissolved in water, filtered and incubated at 37 °C for 1 day before any usage. Astrocytes (30,000 cells/well) were seeded in 24-well plates for 2 days and treated with oligomerized A $\beta$ <sub>42</sub> (250 ng/ml) for another 2 days. Self-degradation levels were measured from oligomerized A $\beta$ <sub>42</sub>-treated media without astrocytes. The levels of A $\beta$ <sub>42</sub> in cultured media were measured by human A $\beta$ <sub>42</sub> ELISA kit (Invitrogen) following the manufacturer's instructions. Reduced levels of oligomerized A $\beta$ <sub>42</sub> by astrocytes were calculated by subtracting remaining A $\beta$ <sub>42</sub> and self-degradation from total A $\beta$ <sub>42</sub>. A $\beta$ <sub>42</sub>

uptake level was calculated from dividing reduced levels of A $\beta$ <sub>42</sub> by the number of cells measured by Cell Titer-Glo cell viability assay (Promega).

## 9.5 Cholesterol Assay

Cholesterol levels in iPSC-derived astrocytes were measured using cholesterol assay kits (Abcam). To measure cholesterol levels in iPSC-derived astrocytes media, cells were prepared in 24-well plates. The day after passaging, media were fully changed. Two days later, media were collected and secreted cholesterol levels were measured using cholesterol assay kits following the manufacturer's instructions and an EnSpire plate reader (Perkin Elmer). For the pHrodo LDL uptake assay cells were incubated with labeled LDL solution (pHrodo™ Green-LDL, Thermo Fischer) and using an incucyte we were able to perform a live-cell analysis monitoring the fluorescence increase during time.

## 9.6 Transferrin and EGF uptake assay

Astrocytes were seeded at a density of 10,000 cells per well of a 96-well glass-bottom plate (IBIDI). Then cells were grown to 80/90% of confluence. Cells were kept 2h in astrocyte media without FBS. After starvation the cells were then placed on ice for 5 minutes to halt endocytic processes, and either EGF conjugated to AlexaFluor555 (Thermo Fischer Scientific E35350) or transferrin conjugated to AlexaFluor647 (Thermo Fischer Scientific T23366) was added to the media at a concentration of 100 ng/mL or 25 ug/mL and the cells were incubated at 37°C for 5 minutes. Cells were then washed three times with cold PBS and fixed with 4% paraformaldehyde for 20 minutes at room temperature. The cells were then washed with PBS three times and Hoechst 33342 was added at a final concentration of 2 mM to each well and imaged using a Zeiss LSM 880 Laser Scanning Confocal Microscope taking 1 um sections of 10-15 um Z stacks and analyzed using Imaris (Bitplane) and Fiji.

## 9.7 Lipid droplet analysis

To assay the number of lipid droplets in astrocytes, equal number of cells were plated on the 96-well  $\mu$ -Plate (Ibidi, 89626) in astrocyte medium. After 12-14 days cells were stained with Phalloidin, Hoechst and LipidTox (ThermoFisher/Molecular Probes) according to manufacturer's protocols. Lipid droplet count was performed with Imaris (Bitplane) software after confocal imaging.

## 9.8 Immunostaining analysis

After DPBS wash-out, cells were fixed with 4% paraformaldehyde in PBS for 15 minutes. After fixation, cells were permeabilized with blocking solution containing 0.1% Triton X-100, 10% donkey serum, 2% BSA and 1 M glycine in PBS for 1 hour at room temperature. Next, cells were incubated with appropriate antibodies overnight at 4 °C and then were treated with fluorescence-conjugated secondary antibodies including Hoechst 33342 (Invitrogen) for 1 hour at room temperature.

## 9.9 Fluorescence microscopy

For all iPSC-derived cell type imaging, images were acquired using a Nikon Plan Apo 63x oil objective (NA 1.4) using a Nikon Eclipse Ti-E inverted microscope and a CCD camera (Andor technology) or a Zeiss LSM710 inverted confocal microscope with a 40x water immersion objective and Z-stacks with a stack height of 0.5 $\mu$ m. Imaging was analyzed using Imaris (Bitplane) and Fiji.

## 9.10 Quantification and statistical analysis

GraphPad Prism software was used to process data, calculate statistics and prepare graphs. For determining statistical significance, we used the unpaired versions of t-tests, unless stated otherwise. FlowJo was used to process FACS data. Images were processed using Imaris and Fiji <sup>241</sup>.

# 10 Results

## 10.1 Generation of human isogenic ABCA7 Y622\* iPSCs

It has been used CRISPR/Cas9 genome editing technologies to generate isogenic ABCA7 cell lines harboring the ABCA7-Y622\* mutation (Figure 24A), to evaluate the impacts of rare ABCA7 variants on AD-related phenotypes in each brain cell type.

The CRISPR/Cas9 plasmid and a single guide RNA (sgRNA) were inserted to ABCA7 control cells, targeting the region of ABCA7 based on the selected rare variant with the strongest odd ratio<sup>155</sup>, and a repair template, single-stranded oligodeoxynucleotides (ssODNs) was introduced to direct precise edits of ABCA7. After that, a DNA extraction procedure was executed from single colonies originated from a single cell after the transformation, and Sanger sequencing was performed to measure the success of editing by checking a point mutation corresponding to the Tyrosine-622 in ABCA7. Instead of the codon TAC, coding for a tyrosine, we obtained a TAG, which is a stop codon in exon 15 generating the ABCA7 Y622\* line (Figure 24B).

Moreover, it has also been generated a new cell line from a different healthy subject, AG 08379, to create another isogenic mutant iPSC line harboring a loss of function variant, ABCA7 Y622\*, in order to validate the results shown in the first clone. This independent line is crucial for determining that the results are due to defects in ABCA7 and independent from the genetic background. The second line will ensure that these findings can be translated to all the patients with this mutation in ABCA7 mutation (Figure 24C).

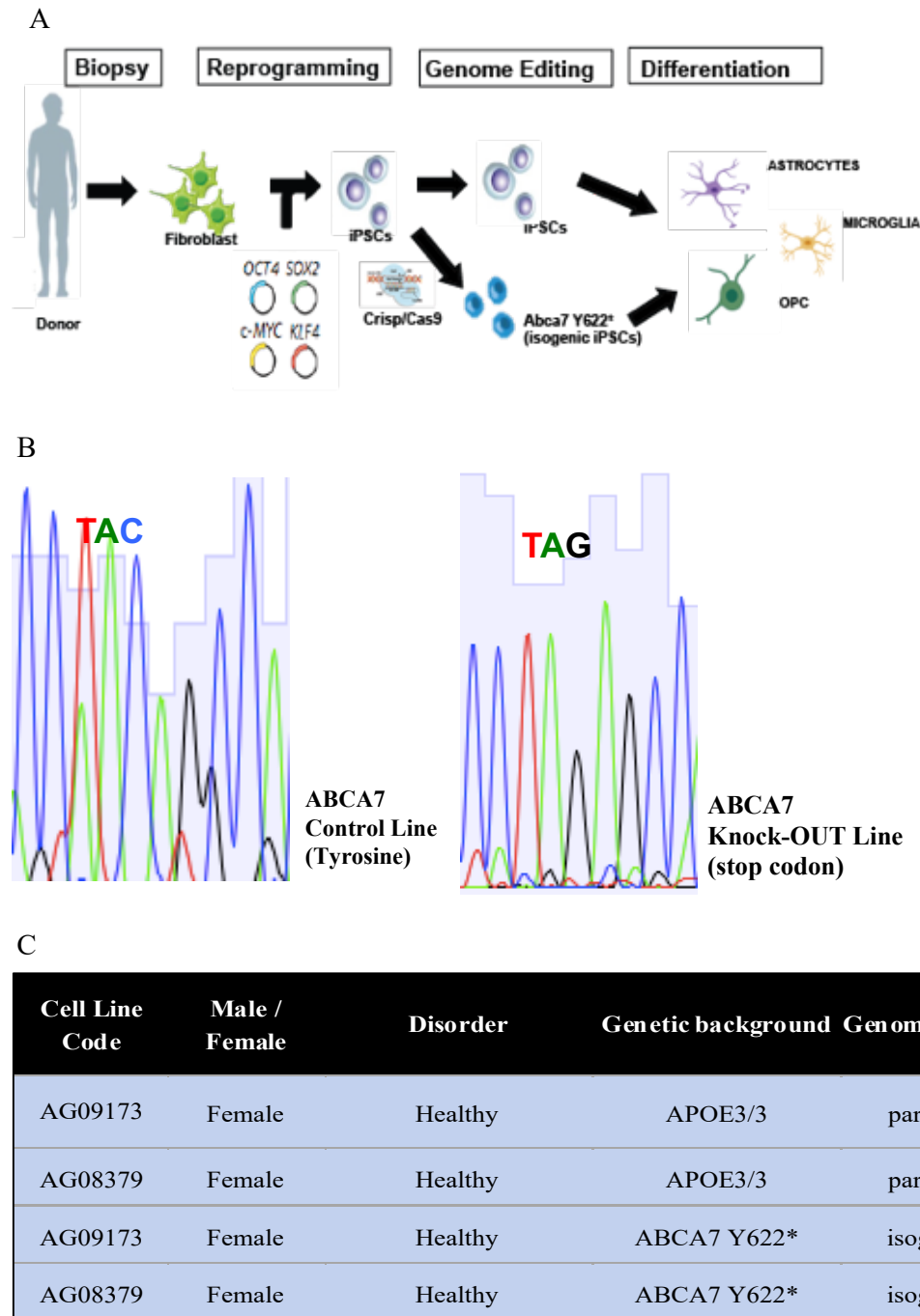


Figure 24 Generation of isogenic ABCA7 lines from healthy donor. A) Schematic overview of iPSC derived Alzheimer's disease (AD) model; B) Sanger sequencing confirmation on targeted mutagenesis. Single nucleotide replacement from Cytosine to Guanine was made, resulting in conversion from Tyrosine 622 to stop codon; C) Information of donors.

## 10.2 Generation of ABCA7 Y622\* astrocytes

Astrocytes are well known to play an important role in neurodegenerative diseases and regulate neurons' synaptic development.<sup>242,243</sup> But, the effects of ABCA7 on astrocyte's activities remain mostly unknown.

To generate astrocytes, a two-step differentiating process have been performed: first, making neural progenitor cells (NPCs) using two growth factors, SB431542 and Dorsomorphin, then deriving NPCs to astrocytes with an additional growth factor, BMP-4 and FGF-2 (Figure 25A).<sup>244</sup> The derived cell type was selected by FACS with GLAST antibody to increase the purity of astrocyte cultures confirmed (Figure 25B), then, by the immunostaining with the antibody against S100b and GFAP, astrocyte marker (Figure 26).

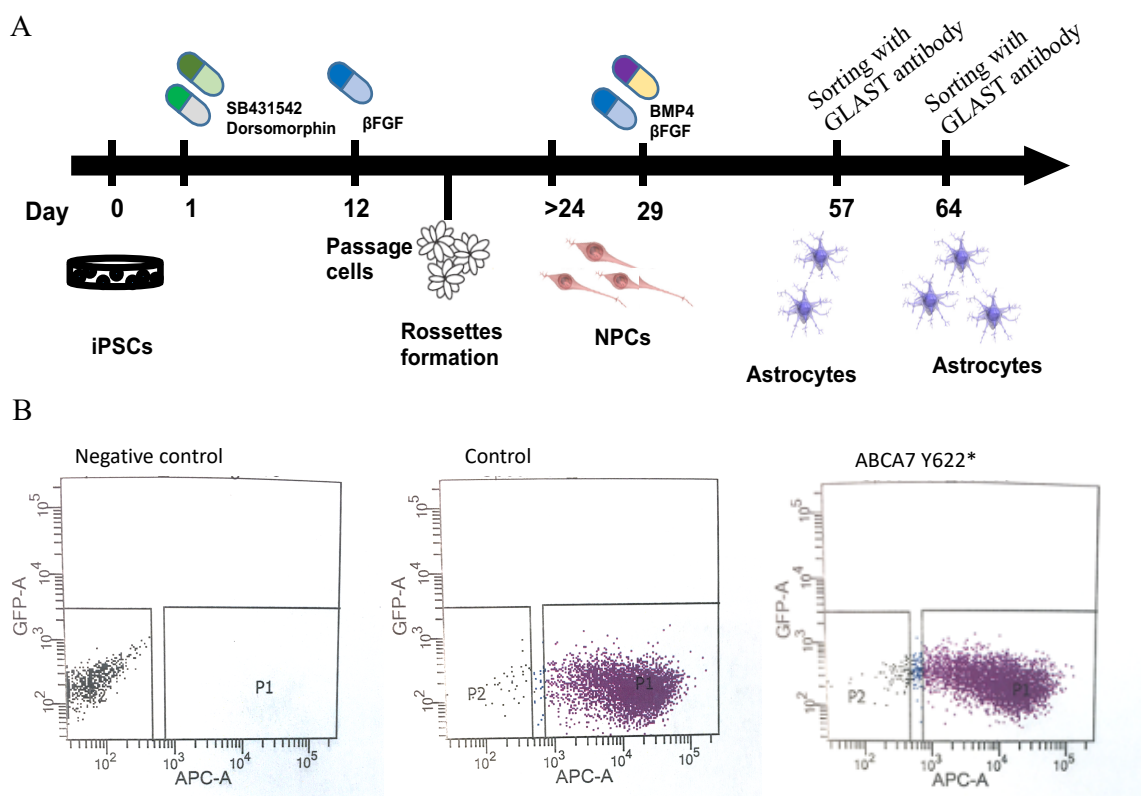


Figure 25 Differentiation of iPSCs into astrocytes. A) schematics for two-steps astrocyte inducing procedure using growth factors. iPSCs were driven to NPCs first as an intermediate cell type, then differentiated into astrocytes. B) Plots from fluorescence-assisted cell cytometry of iPSC-derived astrocytes stained with anti-GLAST antibody or an unlabeled control.

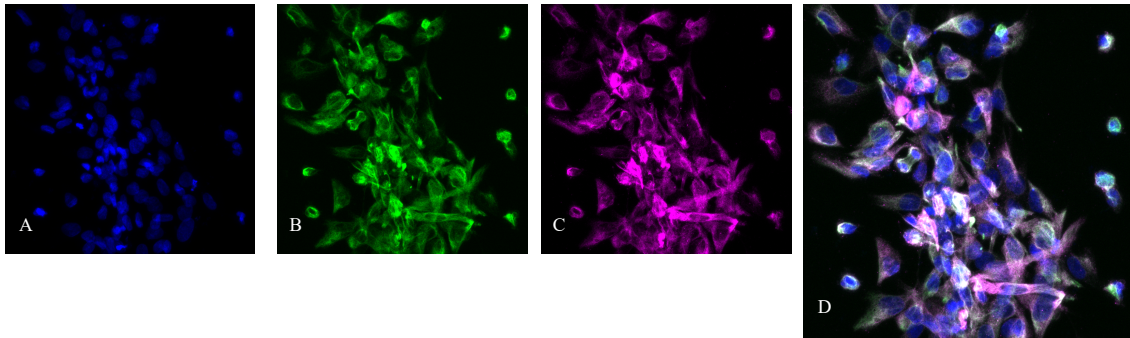


Figure 26 Representative fluorescent microscopy images of astrocytes stained with DAPI(A), antibodies against S100 $\beta$  (B), and GFAP (C) merged image (D) Scale bar represents 100  $\mu$ m.

### 10.3 Gene expression and Gene set enrichment analysis of ABCA7 Y622\* astrocytes

RNA-seq data were generated and revealed 4597 significantly differentially expressed genes (2054 up-regulated genes; 2543 downregulated genes) in ABCA7 Y622\* compared to control astrocytes (Figure 27).

Expression data were analyzed for genes associated by Gene set enrichment analysis (GSEA) using parameters recommended for expression datasets that contain a sample with less than seven replicates: dataset and gene sets were converted into gene symbols, redundant probe sets were collapsed using probe medians, a Signal2Noise metric was used for ranking genes, and the weighted enrichment statistic and 1000 gene set permutations were employed. GSEA revealed that genes linked to ECM organization, ECM components, muscle contraction, and cell to cell interaction were mainly downregulated in ABCA7 Y622\* astrocytes (Figure 28). Besides, genes known to be involved in lipid metabolism, cholesterol biosynthesis, adipogenesis, and transport were up-regulated in astrocytes harboring ABCA7 mutation (Figure 29, Figure 30, Figure 31). Gene ontology was performed using the Broad GSEA tool.

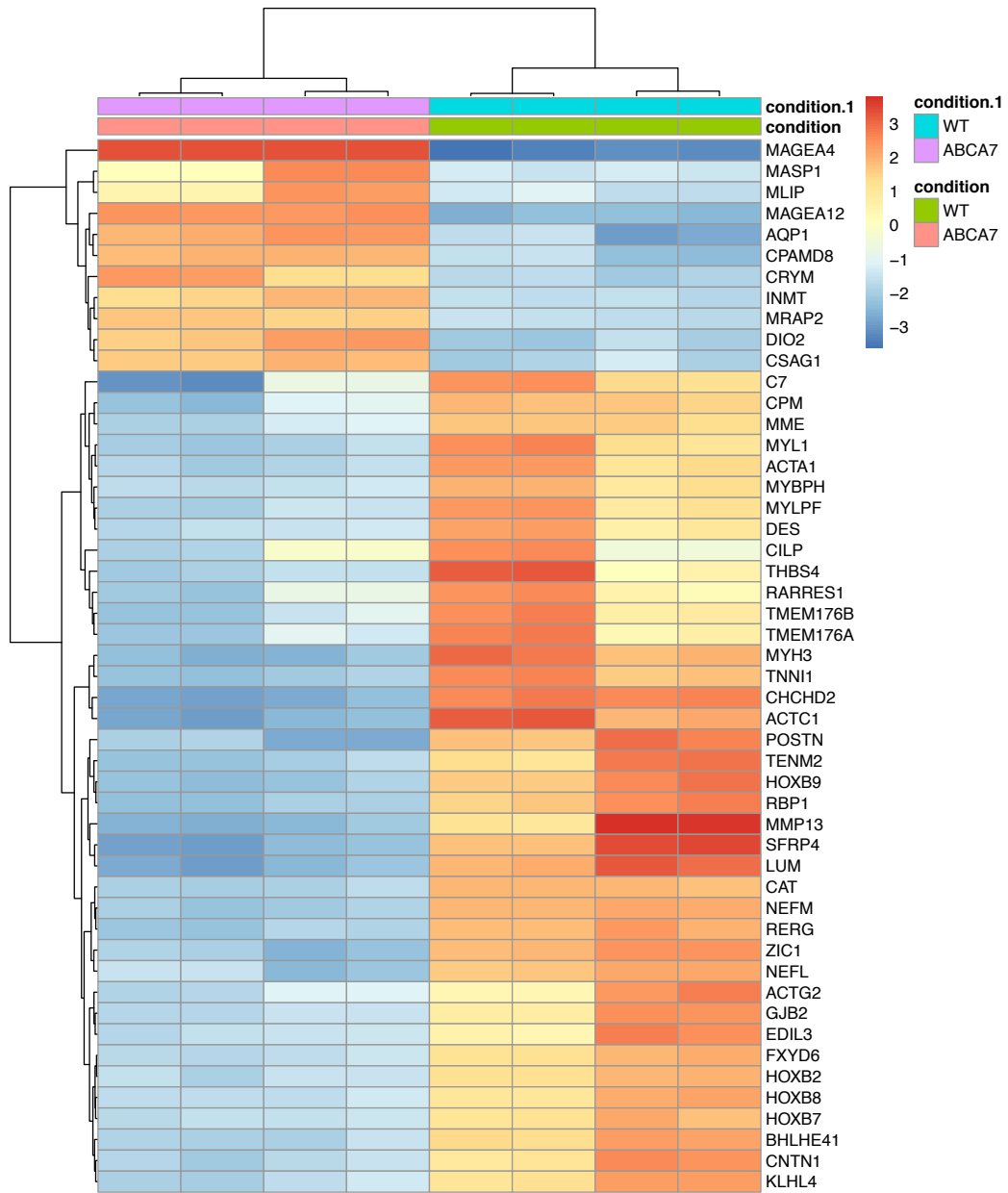


Figure 27 first 50 up and down regulated genes in Rna-seq analysis

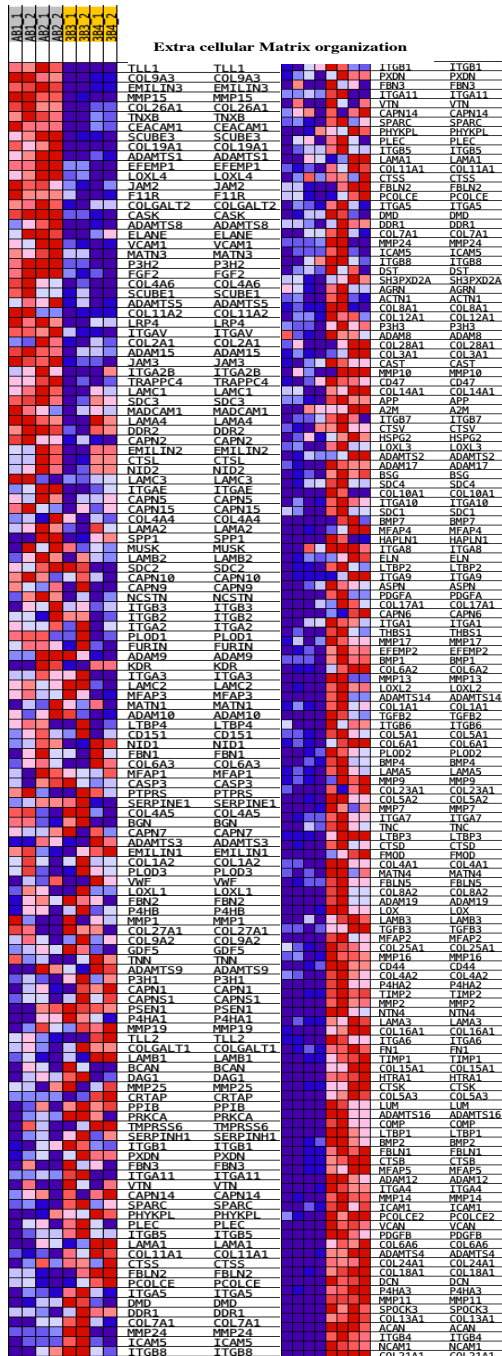
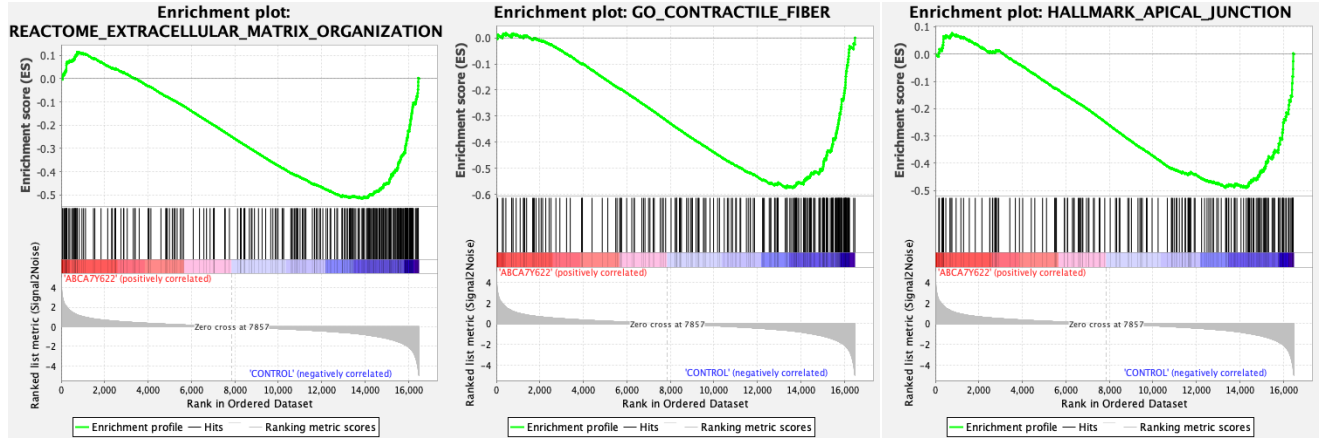


Figure 28 Enrichment plots and heat maps for core enrichment genes were generated by GSEA using the REACTOME (NES -1.91, nominal p-value 0, FDR 0.01), GO (NES -2.11, nominal p-value 0.0, FDR 1.91), and HALLMARK (NES -1.75, nominal p-value 0.0, FDR 0.0028) gene sets. Comparison of ABCA7 Y622\* versus control astrocytes identifies downregulation of the “extracellular matrix organization”, “skeletal system development” and “apical junction” gene set in ABCA7 Y622\* ASTROCYTES compared to control group.

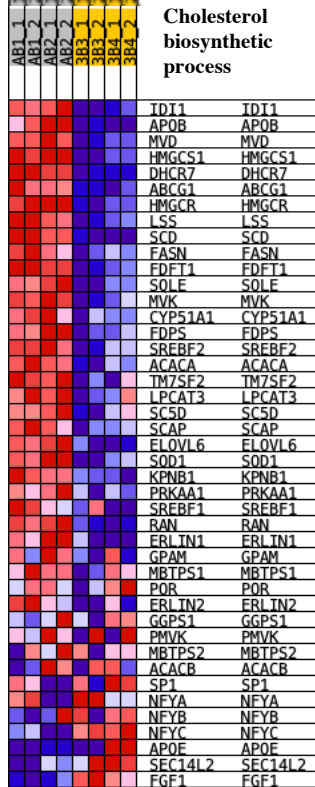
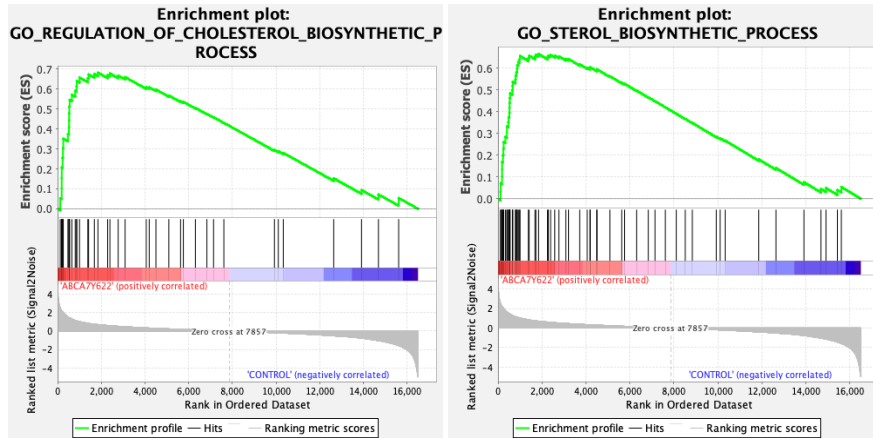


Figure 29 Enrichment plots and heat maps for core enrichment genes were generated by GSEA using the GO gene set. (NES 2.43, nominal p-value 0.0, FDR 0.0), (NES 2.54, nominal p-value 0.0, FDR 0.0). Comparison of ABCA7 Y622\* versus control astrocytes identifies upregulation of the “regulation of cholesterol biosynthetic process” and “sterol biosynthetic process” gene set in ABCA7 Y622\* ASTROCYTES compared to control group.

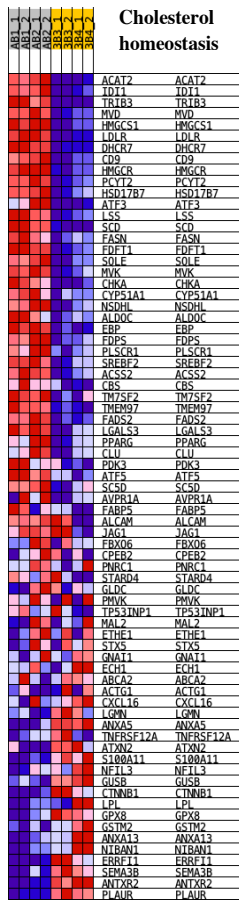
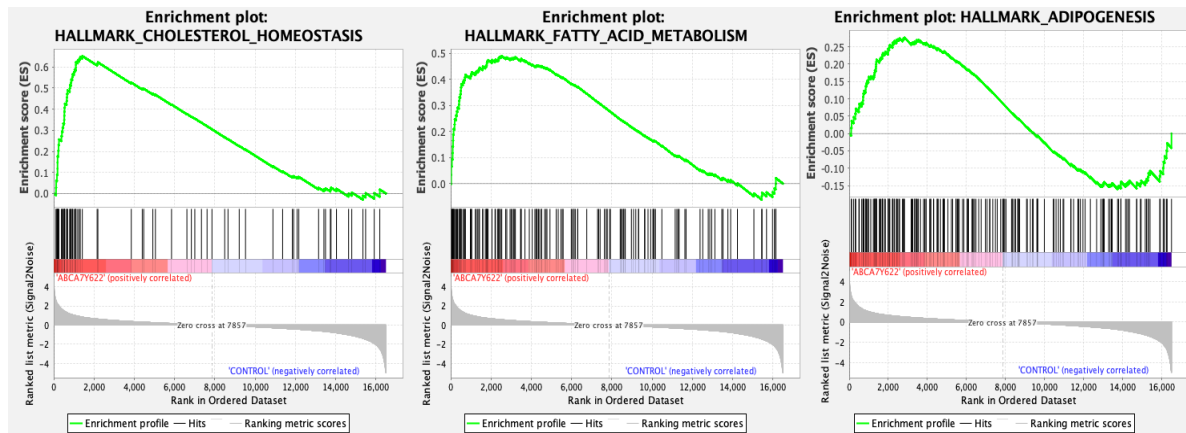


Figure 30 Enrichment plots and heat maps for core enrichment genes were generated by GSEA using the HALLMARK gene set. (NES 2.49, nominal p-value 0.0, FDR 0.0), (NES 2.06, nominal p-value 0.0, FDR 0.0), (NES 1.29, nominal p-value 0.04, FDR 0.180). Comparison of ABCA7 Y622\* versus control astrocytes identifies upregulation of the “cholesterol homeostasis” and “fatty acid metabolism” and “adipogenesis” gene set in ABCA7 Y622\* ASTROCYTES compared to control group.

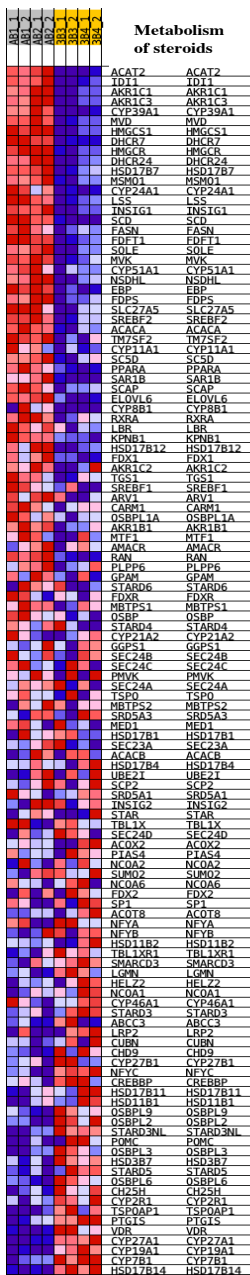
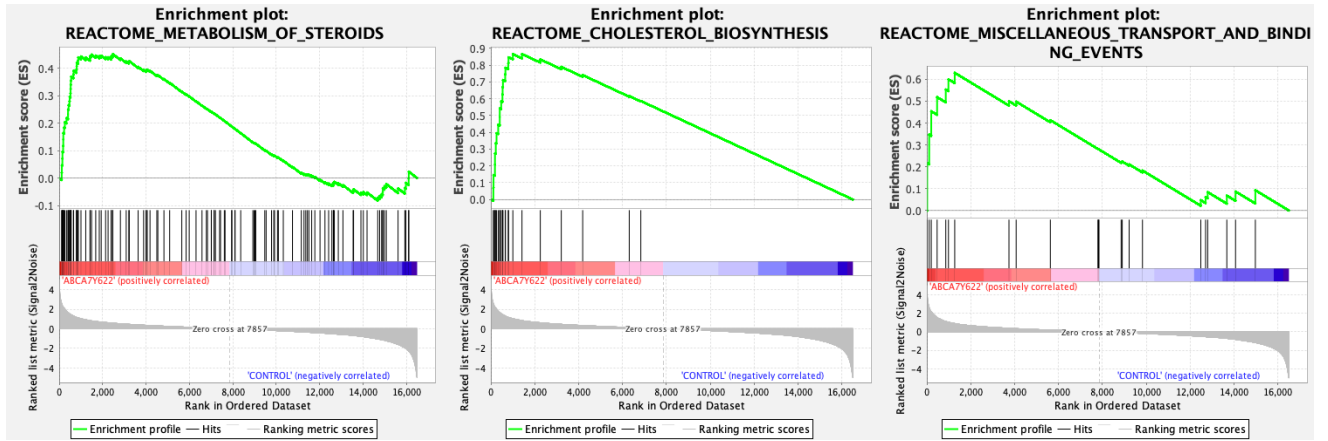


Figure 31 Enrichment plots and heat maps for core enrichment genes were generated by GSEA using the REACTOME gene set. (NES 1.87, nominal p-value 0.0, FDR 0.03), (NES 2.59, nominal p-value 0.0, FDR 0.0), (NES 1.91, nominal p-value 0.0, FDR 0.02),. Comparison of ABCA7 Y622\* versus control astrocytes identifies upregulation of the “metabolism of steroids” and “cholesterol biosynthesis” and “miscellaneous transport and binding events” gene set in ABCA7 Y622\* ASTROCYTES compared to control group.

## 10.4 Effects of ABCA7 Y622\* mutation on A $\beta$ clearance capacity

Astrocytes are known to provide neuroprotective functions in AD by clearing oligomeric/fibrillar A $\beta_{1-42}$  *in vitro* and *in vivo*, resulting in preventing the detrimental effects of amyloid accumulation<sup>245-247</sup>. Thus, it has been determined whether the ABCA7 variant affected the ability to internalize A $\beta$ . In order to address this question, it has been evaluated the A $\beta$  clearance ability of astrocytes. Considering the relatively slow internalization rate of astrocytes, synthetic A $\beta_{1-42}$  oligomers were administered at a known concentration for two days, and the A $\beta_{1-42}$  leftover was measured by ELISA. For the quantification, an uptake index to estimate the fraction of oligomeric A $\beta_{1-42}$  left in the media was used. Data showed that ABCA7 Y622\* is less efficient than the control in internalizing A $\beta_{1-42}$  from the media, the level of A $\beta_{1-42}$  is significantly higher in the isogenic line compare to the control (Figure 32).

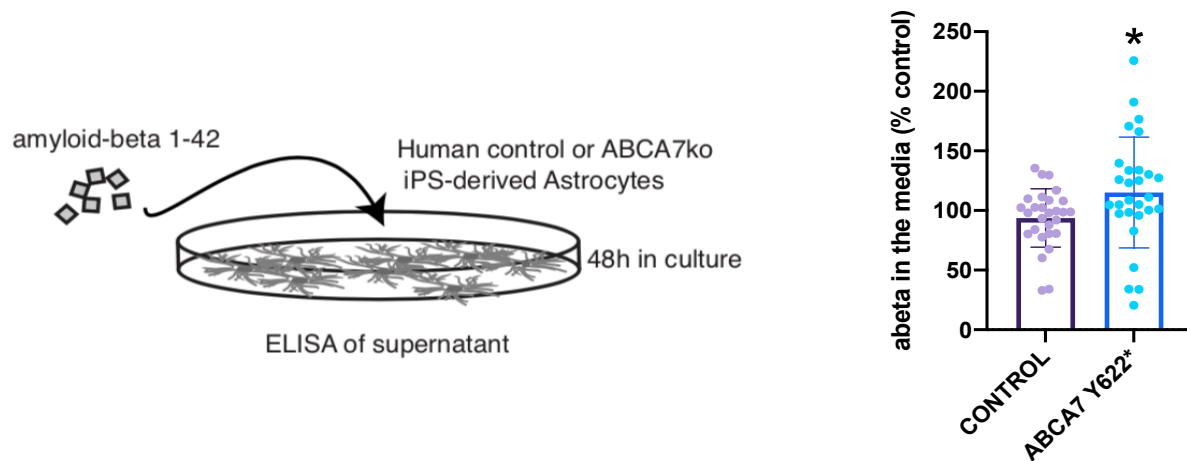


Figure 32 Altered A $\beta$  up-take capability of astrocytes. Oligomerized synthetic A $\beta_{1-42}$  were administered into astrocytes, and residual A $\beta$  levels were measured by ELISA after 48 hours. Schematic overview on the left. ABCA7 Y622\* astrocytes contain more A $\beta$  in the media compare to control, indicating impaired A $\beta$  take-up capacity (right). Values are expressed as mean  $\pm$  SEM of each experimental group (\* $p < 0.05$  vs. control, Unpaired T-test).

## 10.5 Effects of ABCA7 Y622\* mutation on early endocytosis

Because of the important role that ABCA7 plays in the transport system, it has been investigated if the loss of expression of ABCA7 could alter clathrin-mediated early endocytosis. Following serum starvation, the cells were treated with fluorescently tagged EGF or transferrin for five minutes, after that, cells were immediately fixed the cells. Analyzing the intensity of fluorescence of EGF and transferrin in the cells, we identified increased uptake in the ABCA7 Y622\* astrocytes compared to the control (\* $p < 0.05$  \*\*\*\* $p < 0.0001$ , Figure 33).

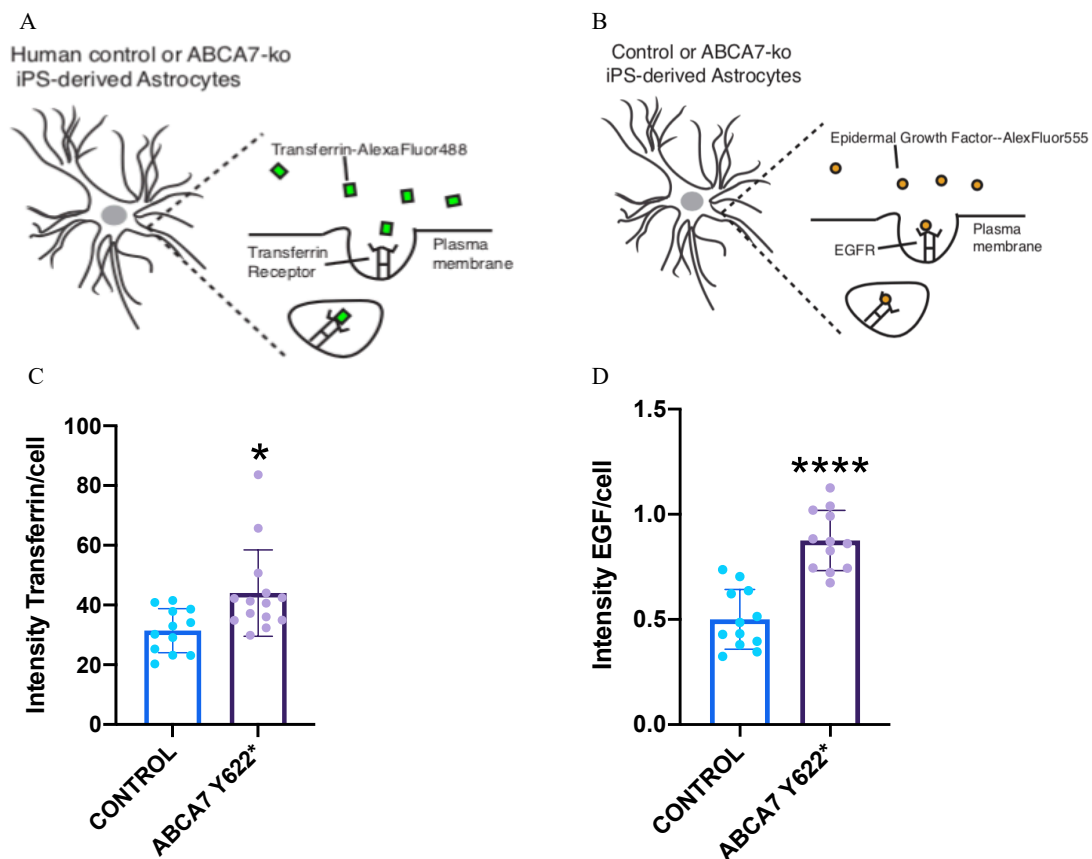


Figure 33 Altered transferrin and EGF up-take capability of astrocytes. Schematic overview of experimental procedure (A,B). Increased uptake of transferrin (C) and EGF (D) by ABCA7 Y622\* astrocytes. Values are expressed as mean  $\pm$  SEM (n=12-14) of each experimental group (\* $p < 0.05$ , \*\*\*\* $p < 0.0001$  vs. control; Unpaired T-test)

## 10.6 Effects of ABCA7 Y622\* mutation on lipids transport

Astrocytes are a significant source of cholesterol for neurons, required for a wide range of normal physiological functions, and the transport of cholesterol from astrocytes to neurons is primarily mediated by APOE and ABCA proteins. Serum cholesterol levels are lower in ABCA7 KO mice,<sup>152</sup> and ABCA7 deficiency alters the lipid profile in the mouse brain<sup>248</sup>. Therefore, it has been investigated whether any difference could be detected in cholesterol levels in the media of ABCA7 mutant astrocytes. Indeed, an accumulation of cholesterol in the media of ABCA7 Y622\* astrocytes compared to the isogenic control line was observed (Figure 34C).

Cholesterol and other lipids are packaged into lipoprotein particles to be trafficked, most of which are low-density lipoproteins, or LDLs.<sup>249</sup> To further confirm our data suggesting dysfunction in lipid transport, we used a pH-sensitive dye pHrodo conjugated to human low-density lipoprotein (LDL), wherein we measured internalization of pHrodoLDL by observing increased pHrodo fluorescence in low pH organelles. Using this technique, a significant decrease in internalized pHrodoLDL was measured in ABCA7 Y622\* astrocytes compared to their control (Figure 34D). Together these data suggest that ABCA7 mutation in astrocytes likely alters lipid transport.

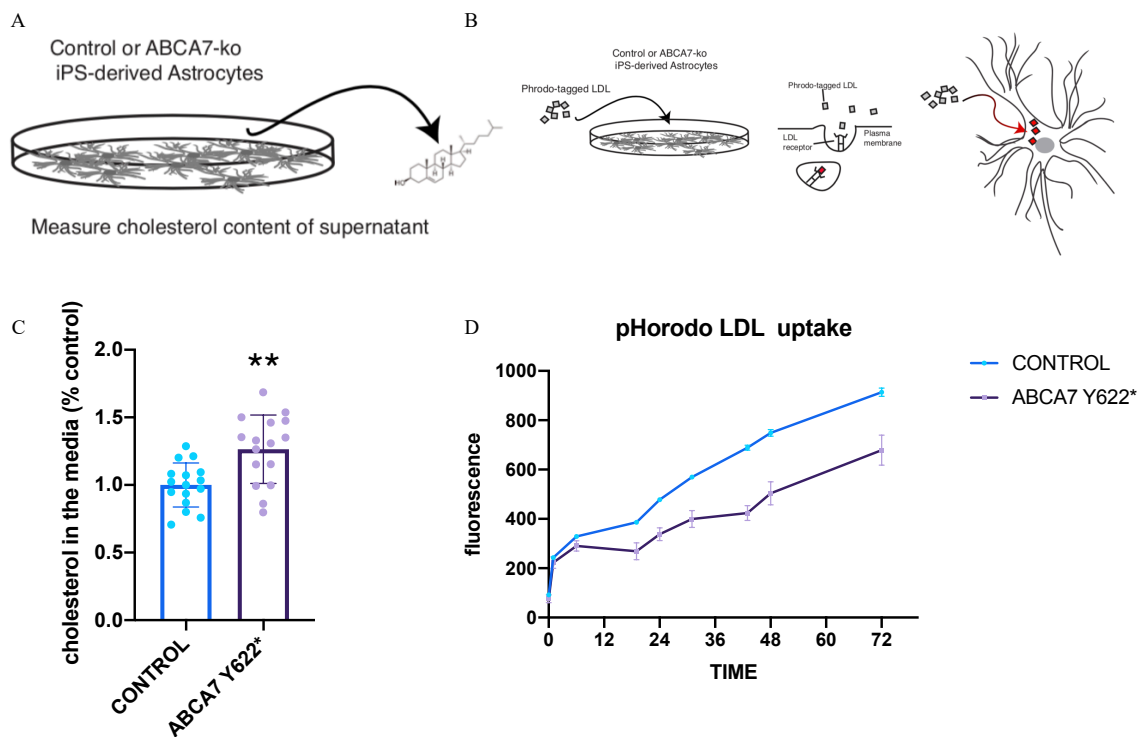


Figure 34 ABCA7 Y622\* mutant astrocytes alter lipid transport. Schematic overview of experimental procedure (A,B). Extracellular cholesterol levels were measured in media from ABCA7 Y622\* isogenic astrocyte cultures and control astrocyte cultures. (\*\*:  $p < 0.01$ , Unpaired T-test) (C). Timecourse showing reduced pHrodo-LDL uptake in ABCA7 Y622\* astrocytes (D). Values are expressed as mean  $\pm$  SEM of each experimental group.

## 10.7 Effects of ABCA7 Y622\* mutation on intracellular lipid homeostasis

Lipid droplets are storage organelles at the center of lipid and energy homeostasis. They have a unique architecture consisting of a hydrophobic core of neutral lipids, which is enclosed by a phospholipid monolayer, decorated by a specific set of proteins. Lipid droplets formation and degradation and their interactions with other organelles are strictly linked to cellular homeostasis and are necessary to control the levels of toxic lipids.<sup>250</sup>

To identify if there was an alteration in lipid droplets formation or accumulation, the astrocytes were stained with the LipidTOX™ red, a neutral lipid stain with a too high affinity for neutral lipid droplets and can be detected by fluorescence microscopy. A significant increase in lipid droplets of the ABCA7 Y622\* astrocytes compared to their

controls has been observed, suggesting that they are more sensitive to stress conditions (Figure 35).

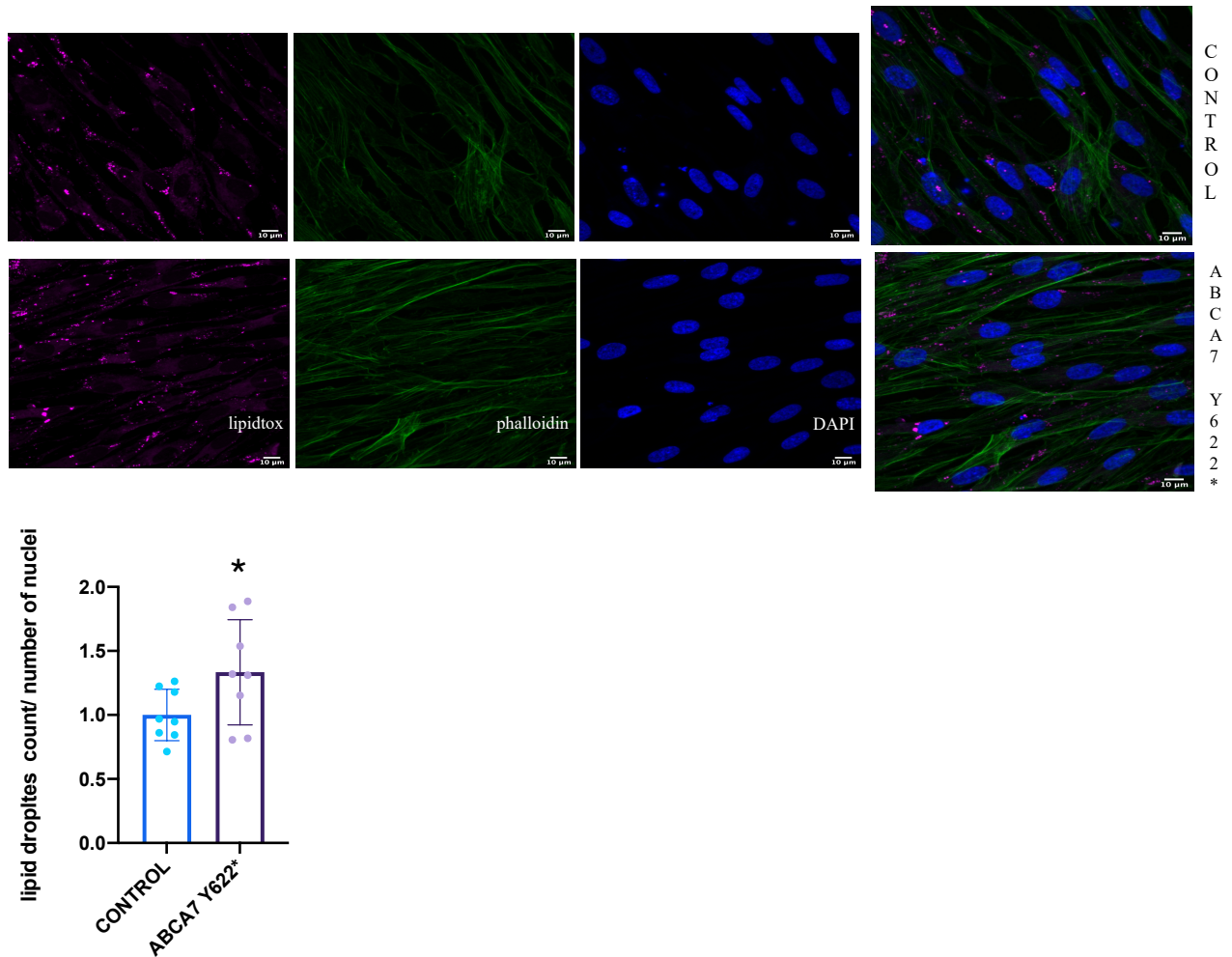


Figure 35. ABCA7 Y622\* mutant astrocytes present an altered lipid intracellular condition. Top: Fluorescent microscopy images of the iPSC-derived astrocytes stained with LipidTox. Bottom: quantification of the lipid droplet number per cell (each point (n) is an average of four wells with at least 20 cells analyzed). Data are represented as mean  $\pm$  SEM (t-test, \*  $p \leq 0.05$ ). (scale bar 10  $\mu$ m).

# 11 Discussion

Over the last ten years, a new AD research field emerged with a focus on ABC transporters in the blood-brain barrier and in other cells of the CNS. ABC transporters consume ATP to move their substrates across membranes of organelles, cells, and tissues. Cholesterol, sterols, lipids, peptides, metabolites, and xenobiotics and drugs are only some of the substrates of ABC transporters involved in AD. Therefore, ABC transporters are an essential component of several physiological processes and biochemical pathways and play a significant role in preserving the body's homeostasis by extruding metabolites and reducing xenobiotic intake. Researchers have recently found that ABC carriers also contribute to diseases when ABC carriers' mechanisms and networks are altered. For some ABC transporters, including ABCA7, such a role is emerging in AD and other CNS disorders associated with high A $\beta$  brain levels. If, and how exactly, ABC transporters contribute to AD pathophysiology is unknown. This lack of understanding creates opportunities for groundbreaking discoveries and, far more importantly, intends to reveal disease mechanisms and identify targets that could assist in developing new AD therapeutic strategies.<sup>239</sup>

Recent GWAS revealed that ABCA7 is strongly associated with LOAD.<sup>154,155</sup> However, the biological role that ABCA7 have in AD pathogenesis remains unclear. A possible role related to phagocytosis has been reported in *in vitro* studies in macrophages and other cell types. The level of ABCA7 expression is negatively correlated with the clearance function of macrophages.<sup>235,236</sup> In terms of cerebral A $\beta$ , when ABCA7 was suppressed in a mouse model of AD, A $\beta$  plaque load was significantly exacerbated,<sup>152</sup> providing further evidence of the importance of ABCA7 function in A $\beta$  pathology. Based on such evidence, we hypothesized that ABCA7 Y622\* mutation could modulate a phenotype related to AD pathology because ABCA7 disruptions may significantly affect astrocytes' critical roles in lipid homeostasis, trafficking, and A $\beta$  clearance in the brain.

Glial cells are deeply involved in the cellular uptake of A $\beta$ .<sup>251</sup> Several studies showed that a cell's phagocytic function could be impaired by downregulated ABCA7.<sup>235,236,252</sup> Other *in vivo* studies showed that ABCA7 deficiency exacerbates A $\beta$  plaque burden.<sup>248</sup> Deficits in A $\beta$  uptake and transport could lead to facilitate A $\beta$  aggregation, confirming evidence already reported. These data reveal that the ABCA7 Y622\* mutation significantly impaired the capability to uptake A $\beta$  in astrocytes and highlighted that ABCA7 predominantly modulates A $\beta$  clearance.

Regarding A $\beta$  production, endocytic trafficking plays a critical role in A $\beta$  processing because A $\beta$  is proteolytically cleaved from APP by a series of enzymatic activities in early endosomes.<sup>253</sup> For APP to be processed, the APP's internalization is necessary and is the most critical step.<sup>149</sup> Several studies also showed that modulating the expression of ABCA7 can affect the amount of A $\beta$  generation.<sup>254,255</sup>

While the APP endocytosis is a significant step for A $\beta$  production, impairment in endocytosis can modulate astrocyte phagocytic capability because endocytosis is one type of phagocytic activity. Therefore, our results are consistent with previous reports, supporting that ABCA7 can induce dysfunctional endocytic trafficking, thereby impairing both A $\beta$  generation and A $\beta$  clearance. Further studies are required to determine whether ABCA7 can directly affect APP and A $\beta$  endocytosis or indirectly modulate trafficking through other proteins.

Because of the ABCA7 crucial role in maintaining lipid compositions and considering that lipids can play a role in endocytosis as a mediator<sup>256</sup>, and as a modifier;<sup>257</sup> it seems clear that an alteration in this composition could directly modify endocytic trafficking systems<sup>258</sup>. Also, considering the lipid composition of each organelle's membrane, alteration in ABCA7 activities could modulate endocytosis at multiple levels. Endocytosis is critical for normal APP processing, and synaptic activity and neurotransmitter release are disrupted in AD.

It has been performed an assay to investigate early endocytosis modulation by ABCA7 Y622\* mutation, using transferrin and EGF fluorescently tagged.

The significant increase in transferrin and EGF uptake in ABCA7 Y622\* astrocytes could promote substrates accumulation in the early endocytic compartment, potentially

resulting in earlier saturation of this compartment compared to the control. This hypothesis should be pursued by analyzing markers representing each phase of endocytosis, recycling, and trafficking across lysosomes.

Many studies investigating the ABCA7 role in trafficking have focused mainly on the trafficking of specific AD-associated proteins like APP and its cleavage product, A $\beta$ . Here, it has been shown that ABCA7 mutations can alter endocytosis independently of APP or A $\beta$ . Minor disruption to endocytosis can drastically alter the intracellular dynamics of many substrates in neuronal and glial cell types in which endocytic trafficking is critical to cellular function. Chronic dysfunction over an individual's life of trafficking pathways could relate to a cellular environment susceptible to disease, aggravated by other environmental or other genetic factors. Endocytic disruption may manifest with different phenotypic outcomes in different cell types or brain regions, could be useful to indagate better ABCA7 function on endocytosis in different brain cells type. ABCA7 Y622\* alteration could be responsible for endocytosis dysfunction that could generate AD-related alterations.

As predicted from its structure, the primary function of ABCA7 is likely to regulate lipid metabolism. It has been reported that ABCA7 can alter phospholipid profile in the mouse brain.<sup>248</sup> Also, several studies indicate that lipid composition in lipoproteins can impair endocytosis of extracellular A $\beta$ .<sup>259,260</sup> Besides, many *in vitro* studies highlighted that ABCA7 expression could modulate cells' lipid profile.<sup>261-264</sup> Moreover, loss of ABCA7 expression causes the disruption of lipid rafts on the plasma membrane of thymocytes and antigen-presenting cells in mice, which is associated with the compromised development and function of natural killer T cells.<sup>265</sup> Together, these findings suggest that ABCA7 plays a role in maintaining intracellular lipid metabolism, thereby regulating cellular homeostasis.

Gene expression analysis and gene set enrichment analysis of ABCA7 Y622\* astrocytes show dysregulation in cholesterol homeostasis, fatty acid metabolism, cholesterol biosynthesis, sterol biosynthesis, metabolism of steroids, and transport through the cell's membrane. One of the fascinating phenotypes found was an accumulation of extracellular cholesterol and altered uptake of LDL in ABCA7-Y622\* mutated

astrocyte cultures. The cholesterol level in the media was measured through an ELISA assay able to identify a significant increase of cholesterol in ABCA7 Y622\* astrocytes compared to control. Since cholesterol and lipids are packed in lipoprotein particles to be transported, it has also been tested if ABCA7 Y622\* astrocytes uptake less pHrodoLDL. The slower increase of fluorescence in ABCA7 Y622\* astrocytes means a reduced and slow uptake of pHrodo conjugate LDL.

ABCA7 Y622\* astrocytes are characterized by significant impairment in cholesterol transport and uptake. Because of the crucial role of cholesterol and lipids in synapsis, neurons, astrocytes, and basal brain function, alteration in its metabolism or transport appears to be associated with multiple pathological phenotypes in various neurodegenerative disorders. Previous studies reported that any impaired lipid regulation promoted by abnormal ABCA7 activities can cause cell cycle arrest and that ABCA7 reduction can disrupt cellular development and function.<sup>265,266</sup> Therefore, our data also propose that ABCA7 can contribute to AD pathologies by disrupting cellular homeostasis. To investigate cellular homeostasis and alteration in lipid metabolism, we also analyzed the lipid droplets formation. Lipid droplets are storage organelles that regulate lipid metabolism and energy homeostasis. They are made up of a hydrophobic core of neutral lipids and a phospholipid monolayer containing a specific set of proteins. Lipid droplets' interactions with other organelles are linked to cellular metabolism and are critical to balance the levels of toxic lipid species like fatty acid.<sup>250</sup> Based on the results, it has been confirmed that ABCA7 plays a crucial role in maintaining lipid compositions, thus regulating endocytic trafficking, which can significantly contribute to AD pathologies.

This study revealed the effects of ABCA7 loss on astrocytes; ABCA7 Y622\* affect not only amyloid accumulation and clearance but also other aspects of AD pathogenesis, such as lipid dysregulation and cell homeostasis, all changes that could bring to synaptic susceptibility and neurodegeneration. These results provide a better understanding of the role of ABCA7 in AD and suggest potential therapeutic strategies for ABCA7-associated AD pathology or AD itself.

Even if further investigations are needed to evaluate whether ABCA7 can directly affect AD-related phenotypes or other pathologies related to ABCA7; reported findings suggest that ABCA7-Y622\* mutation could induce AD pathological features.

## 12 Conclusion

Dementia is one of the 21st century's most significant public health issues, largely due to the dramatic lifespan increase. AD is the most common type of dementia. AD is a fatal neurodegenerative disease that begins with brain changes many years before clinical symptoms appear. This multifaceted disease is characterized by A $\beta$  accumulation in amyloid plaques, tau aggregation in neurofibrillary tangles, brain atrophy caused by loss of neurons and synapses, and neuroinflammation. Though AD progression is closely linked to A $\beta$  aggregation, years of research suggest that several other factors are likely related to AD development and progression, like loss of cholinergic transmission, progressive oxidative damage, excitotoxicity, and neuroinflammatory processes. There is currently no cure for AD. Unfortunately, the A $\beta$ -targeted trials in AD patients to date have not been successful, addressing the need to, on one side, change AD models to better reproduce the disease and its feature, on the other to focus on alternative therapeutic approaches based on other pivotal early events, including synaptic dysfunction, oxidative stress or the initial steps of neuroinflammation.

It is likely reasonable to argue that complex multifactorial diseases, such as AD, cannot be efficiently treated by modulating a single target, but they will require multitarget drug treatment to address different pathological side of this disease.

In the first part of this study, a novel feruloyl-donepezil hybrid compound, PQM130, was synthesized and evaluated as a multitarget drug in an AD's murine model. PQM130 proved to be a nootropic, neuroprotective, and neurotrophic in our AD mouse model. In particular, the inhibition of AChE activity and the modulation of neuronal survival pathways, and the improvement of the spatial memory formation, can be related to the nootropic effect. The neuroprotection could be attributed to its strong antioxidant activities, inhibitory role on apoptotic death, and decreased astrogliosis. PQM130 also increases BDNF and synaptophysin levels in the hippocampus, thus leading to a neurotrophic function. Compared to the first-line treatment donepezil, PQM130 appears a more attractive multipotent therapeutic molecule. Our findings demonstrate that

PQM130 is a promising neuroprotective compound and a candidate to be screened further in neurodegenerative disorders, such as but not limited to AD.

Besides the urgent need to identify novel multitarget drugs, as PQM130, there is also the crucial necessity to better understand the genetic contribution to the pathophysiology of LOAD, which will help to understand the course of disease progression and treatment options.

Recent large GWAS confirmed that the ABCA7 locus is strongly associated with AD. This study supports a robust biological association between a loss of function mutation of ABCA7 and AD susceptibility. ABCA7 is a member of the ABCA transporter specializing in transporting lipids across cell membranes and regulating brain lipid homeostasis. Mutations in the ABCA subfamily members are known to cause disorders characterized by lipid dysregulation and abnormal accumulation of lipids in cells. It has been derived iPSC from a healthy individual and created an isogenic line harboring ABCA7-Y622\* mutation introduced via CRISPR/Cas9 technology.

Astrocytes express physiological properties essential for the accurate modulation of neural and synaptic plasticity and synaptic adaptation and homeostasis. Astrocytes are essential for supporting synaptogenesis (axonal and dendritic spines sprouting) and regulating synaptic robustness. It is well-established that astrocytes take part in aberrant molecular pathways that, ultimately, reflect AD pathomechanistic alterations, like brain proteinopathies, synaptic failure, loss of brain plasticity, neuroinflammation, axonal damage, and neurodegeneration. Considering the increasing importance that non neuronal cells are acquiring in AD development and valuated the crucial role and function of astrocytes, control and ABCA7-Y622\* iPSCs have been differentiated to astrocytes. It has been reported that in vitro ABCA7-Y622\* astrocytes are a cell model able to mimics multiple critical features of the AD pathology: impaired A $\beta$  uptake; impaired cholesterol and lipoprotein uptake capability; aberrant early endocytic trafficking phenotype. Therefore, these findings provide a more in-depth understanding of ABCA7's function in AD and propose additional treatment for AD pathology.

Though further experimental studies are needed to confirm the PQM130 neuroprotective role and ABCA7 function in AD. The results presented in this study

provide a better understanding of AD's pathophysiology, show a new therapeutic approach to treat AD and illustrate an innovative and different methodology for studying the disease.

# 13 Bibliography

1. Solanki, I., Parihar, P. & Parihar, M. S. Neurodegenerative diseases: From available treatments to prospective herbal therapy. *Neurochem. Int.* 95, 100–108 (2016).
2. Parihar, M. S., Parihar, A., Fujita, M., Hashimoto, M. & Ghafourifar, P. Mitochondrial association of alpha-synuclein causes oxidative stress. *Cell. Mol. Life Sci.* 65, 1272–1284 (2008).
3. Wyss-Coray, T. Ageing, neurodegeneration and brain rejuvenation. *Nature* 539, 180–186 (2016).
4. Chambon, C., Wegener, N., Gravius, A. & Danysz, W. Behavioural and cellular effects of exogenous amyloid- $\beta$  peptides in rodents. *Behav. Brain Res.* 225, 623–641 (2011).
5. Hou, Y. et al. Ageing as a risk factor for neurodegenerative disease. *Nature Reviews Neurology* 15, 565–581 (2019).
6. Goedert, M. & Spillantini, M. G. A century of Alzheimer's disease. *Science* 314, 777–781 (2006).
7. Cummings, J. L. & Cummings, J. L. Alzheimer's disease. *N. Engl. J. Med.* 351, 56–67 (2004).
8. Mar, J., Soto-Gordoa, M., Arrospide, A., Moreno-Izco, F. & Martínez-Lage, P. Fitting the epidemiology and neuropathology of the early stages of Alzheimer's disease to prevent dementia. *Alzheimer's Res. Ther.* 7, (2015).
9. Albert, M. S. et al. The diagnosis of mild cognitive impairment due to Alzheimer's disease: Recommendations from the National Institute on Aging-Alzheimer's Association workgroups on diagnostic guidelines for Alzheimer's disease. *Alzheimer's Dement.* 7, 270–279 (2011).
10. Jack, C. R. et al. NIA-AA Research Framework: Toward a biological definition of Alzheimer's disease. *Alzheimer's and Dementia* 14, 535–562 (2018).
11. Yiannopoulou, K. G. & Papageorgiou, S. G. Current and Future Treatments in Alzheimer Disease: An Update. *J. Cent. Nerv. Syst. Dis.* 12, 117957352090739 (2020).
12. Sabbagh, M. N., Hendrix, S. & Harrison, J. E. FDA position statement “Early Alzheimer's disease: Developing drugs for treatment, Guidance for Industry.” *Alzheimer's and Dementia: Translational Research and Clinical Interventions* 5, 13–19 (2019).
13. Therapeutics | ALZFORUM. Available at: <https://www.alzforum.org/therapeutics>. (Accessed: 28th November 2020)
14. Ferri, C. P. et al. Global prevalence of dementia: a Delphi consensus study. *Lancet* 366, 2112–2117 (2005).
15. Van Oyen, H. et al. Gender differences in healthy life years within the EU: An exploration of the “health-survival” paradox. *Int. J. Public Health* 58, 143–155 (2013).
16. Alzheimer's Disease Facts and Figures 2020. On the Front Lines: Primary Care Physicians and Alzheimer's Care in America.
17. Brookmeyer, R., Abdalla, N., Kawas, C. H. & Corrada, M. M. Forecasting the

- prevalence of preclinical and clinical Alzheimer's disease in the United States. *Alzheimer's Dement.* 14, 121–129 (2018).
18. Alzheimer's Association. 2016 Alzheimer's disease facts and figures. *Alzheimers. Dement.* 12, 459–509 (2016).
  19. Reitz, C. & Mayeux, R. Alzheimer disease: Epidemiology, diagnostic criteria, risk factors and biomarkers. *Biochemical Pharmacology* 88, 640–651 (2014).
  20. Champion, D. et al. Early-onset autosomal dominant Alzheimer disease: prevalence, genetic heterogeneity, and mutation spectrum. *Am. J. Hum. Genet.* 65, 664–70 (1999).
  21. Tedde, A. et al. Identification of new presenilin gene mutations in early-onset familial Alzheimer disease. *Arch. Neurol.* 60, 1541–4 (2003).
  22. Oyama, F., Shimada, H., Oyama, R. & Ihara, Y. Apolipoprotein E genotype, Alzheimer's pathologies and related gene expression in the aged population. *Brain Res. Mol. Brain Res.* 29, 92–8 (1995).
  23. Blacker, D. et al. ApoE-4 and age at onset of Alzheimer's disease: The NIMH genetics initiative. *Neurology* 48, 139–147 (1997).
  24. Meyer, M. R. et al. APOE genotype predicts when-not whether-one is predisposed to develop Alzheimer disease [2]. *Nature Genetics* 19, 321–322 (1998).
  25. Shinohara, M. et al. APOE2 eases cognitive decline during Aging: Clinical and preclinical evaluations. *Ann. Neurol.* 79, 758–774 (2016).
  26. Holtzman, D. M. et al. Apolipoprotein E isoform-dependent amyloid deposition and neuritic degeneration in a mouse model of Alzheimer's disease. *Proc. Natl. Acad. Sci. U. S. A.* 97, 2892–7 (2000).
  27. Andrews, S. J., Fulton-Howard, B. & Goate, A. Interpretation of risk loci from genome-wide association studies of Alzheimer's disease. *The Lancet Neurology* 19, 326–335 (2020).
  28. Marioni, R. E. et al. GWAS on family history of Alzheimer's disease. *Transl. Psychiatry* 8, (2018).
  29. Kunkle, B. W. et al. Genetic meta-analysis of diagnosed Alzheimer's disease identifies new risk loci and implicates A $\beta$ , tau, immunity and lipid processing. *Nat. Genet.* 51, 414–430 (2019).
  30. Jansen, I. E. et al. Genome-wide meta-analysis identifies new loci and functional pathways influencing Alzheimer's disease risk. *Nat. Genet.* 51, 404–413 (2019).
  31. Pimenova, A. A., Raj, T. & Goate, A. M. Untangling Genetic Risk for Alzheimer's Disease. *Biological Psychiatry* 83, 300–310 (2018).
  32. Mawuenyega, K. G. et al. Decreased clearance of CNS beta-amyloid in Alzheimer's disease. *Science* 330, 1774 (2010).
  33. Khachaturian, A. S. et al. Antihypertensive medication use and incident Alzheimer disease: the Cache County Study. *Arch. Neurol.* 63, 686–92 (2006).
  34. Plassman, B. L. et al. Documented head injury in early adulthood and risk of Alzheimer's disease and other dementias. *Neurology* 55, 1158–66 (2000).
  35. Mawuenyega, K. G. et al. Decreased clearance of CNS  $\beta$ -amyloid in Alzheimer's disease. *Science* (80-. ). 330, 1774 (2010).
  36. Perl, D. P. Neuropathology of Alzheimer's Disease. *Mt. Sinai J. Med. A J. Transl. Pers. Med.* 77, 32–42 (2010).

37. Bierer, L. M. et al. Neocortical Neurofibrillary Tangles Correlate with Dementia Severity in Alzheimer's Disease. *Arch. Neurol.* 52, 81–88 (1995).
38. Nishiyama, E., Iwamoto, N., Ohwada, J. & Arai, H. Distribution of apolipoprotein E in senile plaques in brains with Alzheimer's disease: Investigation with the confocal laser scan microscope. *Brain Res.* 750, 20–24 (1997).
39. Hansen, L. A., DeTeresa, R., Davies, P. & Terry, R. D. Neocortical morphometry, lesion counts, and choline acetyltransferase levels in the age spectrum of Alzheimer's disease. *Neurology* 38, 48–54 (1988).
40. Visser, P. J., Scheltens, P. & Verhey, F. R. J. Do MCI criteria in drug trials accurately identify subjects with predementia Alzheimer's disease? *J. Neurol. Neurosurg. Psychiatry* 76, 1348–54 (2005).
41. Marasco, R. A. Current and Evolving Treatment Strategies for the Alzheimer Disease Continuum. *Am. J. Manag. Care* 26, S167–S176 (2020).
42. Canter, R. G., Penney, J. & Tsai, L. H. The road to restoring neural circuits for the treatment of Alzheimer's disease. *Nature* 539, 187–196 (2016).
43. Owens, D. K. et al. Screening for Cognitive Impairment in Older Adults: US Preventive Services Task Force Recommendation Statement. *JAMA - J. Am. Med. Assoc.* 323, 757–763 (2020).
44. HA, F. et al. Diagnosis and Treatment of Clinical Alzheimer's-Type Dementia: A Systematic Review [Internet]. *Diagnosis and Treatment of Clinical Alzheimer's-Type Dementia: A Systematic Review* (2020).
45. Johnson, K. A. et al. Appropriate use criteria for amyloid PET: a report of the Amyloid Imaging Task Force, the Society of Nuclear Medicine and Molecular Imaging, and the Alzheimer's Association. *Alzheimers. Dement.* 9, (2013).
46. Janelidze, S. et al. Plasma P-tau181 in Alzheimer's disease: relationship to other biomarkers, differential diagnosis, neuropathology and longitudinal progression to Alzheimer's dementia. *Nat. Med.* 26, 379–386 (2020).
47. Haass, C., Kaether, C., Thinakaran, G. & Sisodia, S. Trafficking and proteolytic processing of APP. *Cold Spring Harb. Perspect. Med.* 2, a006270–a006270 (2012).
48. Vassar, R. et al.  $\beta$ -Secretase cleavage of Alzheimer's amyloid precursor protein by the transmembrane aspartic protease BACE. *Science* (80-. ). 286, 735–741 (1999).
49. Voytyuk, I., De Strooper, B. & Chávez-Gutiérrez, L. Modulation of  $\gamma$ - and  $\beta$ -Secretases as Early Prevention Against Alzheimer's Disease. *Biological Psychiatry* 83, 320–327 (2018).
50. Cirrito, J. R. et al. Endocytosis Is Required for Synaptic Activity-Dependent Release of Amyloid- $\beta$  In Vivo. *Neuron* 58, 42–51 (2008).
51. Verges, D. K., Restivo, J. L., Goebel, W. D., Holtzman, D. M. & Cirrito, J. R. Opposing synaptic regulation of amyloid- $\beta$  metabolism by NMDA receptors in vivo. *J. Neurosci.* 31, 11328–11337 (2011).
52. Long, J. M. & Holtzman, D. M. Alzheimer Disease: An Update on Pathobiology and Treatment Strategies. doi:10.1016/j.cell.2019.09.001
53. Chen, G. F. et al. Amyloid beta: Structure, biology and structure-based therapeutic development. *Acta Pharmacologica Sinica* 38, 1205–1235 (2017).

54. Hardy, J. A. & Higgins, G. A. Alzheimer's disease: the amyloid cascade hypothesis. *Science* 256, 184–5 (1992).
55. Selkoe, D. J. & Hardy, J. The amyloid hypothesis of Alzheimer's disease at 25 years. *EMBO Mol. Med.* 8, 595–608 (2016).
56. Tcw, J. & Goate, A. M. Genetics of  $\beta$ -Amyloid Precursor Protein in Alzheimer's Disease. *Cold Spring Harbor perspectives in medicine* 7, (2017).
57. Martiskainen, H. et al. Decreased plasma  $\beta$ -amyloid in the Alzheimer's disease APP A673T variant carriers. *Ann. Neurol.* 82, 128–132 (2017).
58. Verghese, P. B. et al. ApoE influences amyloid- $\beta$  ( $A\beta$ ) clearance despite minimal apoE/ $A\beta$  association in physiological conditions. *Proc. Natl. Acad. Sci. U. S. A.* 110, (2013).
59. Nelson, P. T. et al. Correlation of alzheimer disease neuropathologic changes with cognitive status: A review of the literature. *Journal of Neuropathology and Experimental Neurology* 71, 362–381 (2012).
60. De Strooper, B. & Karran, E. The Cellular Phase of Alzheimer's Disease. *Cell* 164, 603–615 (2016).
61. Palop, J. J. & Mucke, L. Amyloid-B-induced neuronal dysfunction in Alzheimer's disease: From synapses toward neural networks. *Nature Neuroscience* 13, 812–818 (2010).
62. Labbadia, J. & Morimoto, R. I. The biology of proteostasis in aging and disease. *Annual Review of Biochemistry* 84, 435–464 (2015).
63. Nixon, R. A. The role of autophagy in neurodegenerative disease. *Nature Medicine* 19, 983–997 (2013).
64. Karch, C. M. & Goate, A. M. Alzheimer's disease risk genes and mechanisms of disease pathogenesis. *Biological Psychiatry* 77, 43–51 (2015).
65. Burda, J. E. & Sofroniew, M. V. Reactive gliosis and the multicellular response to CNS damage and disease. *Neuron* 81, 229–248 (2014).
66. Dixit, R., Ross, J. L., Goldman, Y. E. & Holzbaur, E. L. F. Differential regulation of dynein and kinesin motor proteins by tau. *Science* (80-. ). 319, 1086–1089 (2008).
67. Marcelli, S. et al. The Involvement of Post-Translational Modifications in Alzheimer's Disease. *Curr. Alzheimer Res.* 15, 313–335 (2017).
68. Guo, T., Noble, W. & Hanger, D. P. Roles of tau protein in health and disease. *Acta Neuropathologica* 133, 665–704 (2017).
69. Mandelkow, E., Von Bergen, M., Biernat, J. & Mandelkow, E. M. Structural principles of tau and the paired helical filaments of Alzheimer's disease. in *Brain Pathology* 17, 83–90 (Brain Pathol, 2007).
70. Hoover, B. R. et al. Tau Mislocalization to Dendritic Spines Mediates Synaptic Dysfunction Independently of Neurodegeneration. *Neuron* 68, 1067–1081 (2010).
71. Crary, J. F. et al. Primary age-related tauopathy (PART): a common pathology associated with human aging. *Acta Neuropathol.* 128, 755–766 (2014).
72. Price, J. L. et al. Neuropathology of nondemented aging: presumptive evidence for preclinical Alzheimer disease. *Neurobiol. Aging* 30, 1026–36 (2009).
73. Hanseeuw, B. J. et al. Association of Amyloid and Tau with Cognition in Preclinical Alzheimer Disease: A Longitudinal Study. *JAMA Neurol.* 76, 915–

- 924 (2019).
74. Frost, B. & Diamond, M. I. Prion-like mechanisms in neurodegenerative diseases. *Nature Reviews Neuroscience* 11, 155–159 (2010).
  75. Iba, M. et al. Synthetic tau fibrils mediate transmission of neurofibrillary tangles in a transgenic mouse model of Alzheimer's-like tauopathy. *J. Neurosci.* 33, 1024–1037 (2013).
  76. DeVos, S. L. et al. Tau reduction prevents neuronal loss and reverses pathological tau deposition and seeding in mice with tauopathy. *Sci. Transl. Med.* 9, (2017).
  77. Huynh, T. P. V., Davis, A. A., Ulrich, J. D. & Holtzman, D. M. Apolipoprotein E and Alzheimer's disease: The influence of apolipoprotein E on amyloid- $\beta$  and other amyloidogenic proteins. *Journal of Lipid Research* 58, 824–836 (2017).
  78. Namba, Y., Tomonaga, M., Kawasaki, H., Otomo, E. & Ikeda, K. Apolipoprotein E immunoreactivity in cerebral amyloid deposits and neurofibrillary tangles in Alzheimer's disease and kuru plaque amyloid in Creutzfeldt-Jakob disease. *Brain Res.* 541, 163–166 (1991).
  79. Basak, J. M., Verghese, P. B., Yoon, H., Kim, J. & Holtzman, D. M. Low-density lipoprotein receptor represents an apolipoprotein E-independent pathway of A $\beta$  uptake and degradation by astrocytes. *J. Biol. Chem.* 287, 13959–13971 (2012).
  80. Heckmann, B. L. et al. LC3-Associated Endocytosis Facilitates  $\beta$ -Amyloid Clearance and Mitigates Neurodegeneration in Murine Alzheimer's Disease. *Cell* 178, 536-551.e14 (2019).
  81. Castellano, J. M. et al. Low-density lipoprotein receptor overexpression enhances the rate of brain-to-blood A $\beta$  clearance in a mouse model of  $\beta$ -amyloidosis. *Proc. Natl. Acad. Sci. U. S. A.* 109, 15502–15507 (2012).
  82. Giannoni, P. et al. Cerebrovascular pathology during the progression of experimental Alzheimer's disease. *Neurobiol. Dis.* 88, 107–117 (2016).
  83. Golia, M. T. et al. Interplay between inflammation and neural plasticity: Both immune activation and suppression impair LTP and BDNF expression. *Brain. Behav. Immun.* 81, 484–494 (2019).
  84. Jayaraj, R. L., Azimullah, S., Beiram, R., Jalal, F. Y. & Rosenberg, G. A. Neuroinflammation: Friend and foe for ischemic stroke. *Journal of Neuroinflammation* 16, 142 (2019).
  85. De Sousa Rodrigues, M. E. et al. Targeting soluble tumor necrosis factor as a potential intervention to lower risk for late-onset Alzheimer's disease associated with obesity, metabolic syndrome, and type 2 diabetes. *Alzheimer's Res. Ther.* 12, (2019).
  86. Sivandzade, F., Prasad, S., Bhalerao, A. & Cucullo, L. NRF2 and NF- $\kappa$ B interplay in cerebrovascular and neurodegenerative disorders: Molecular mechanisms and possible therapeutic approaches. *Redox Biology* 21, (2019).
  87. Baierle, M., Nascimento, S., Moro, A. & Al., E. Relationship between inflammation and oxidative stress and cognitive decline in the institutionalized elderly. *Oxid Med Cell Longev* 2015, (2015).
  88. Butterfield, D. A. & Keller, J. N. Antioxidants and antioxidant treatment in disease. *Biochim. Biophys. Acta - Mol. Basis Dis.* 1822, 615 (2012).
  89. Deshmukh, P., Unni, S., Krishnappa, G. & Padmanabhan, B. The Keap1–Nrf2 pathway: promising therapeutic target to counteract ROS-mediated damage in

- cancers and neurodegenerative diseases. *Biophys. Rev.* 9, 41–56 (2017).
90. Qin, J.-J., Cheng, X.-D., Zhang, J. & Zhang, W.-D. Dual roles and therapeutic potential of Keap1-Nrf2 pathway in pancreatic cancer: a systematic review. *Cell Commun. Signal.* 17, 121 (2019).
  91. Morganti-Kossmann, M. C., Satgunaseelan, L., Bye, N. & Kossmann, T. Modulation of immune response by head injury. *Injury* 38, 1392–1400 (2007).
  92. Davalos, D. et al. ATP mediates rapid microglial response to local brain injury in vivo. *Nat. Neurosci.* 8, 752–758 (2005).
  93. Block, M. L. & Hong, J.-S. Microglia and inflammation-mediated neurodegeneration: multiple triggers with a common mechanism. *Prog. Neurobiol.* 76, 77–98 (2005).
  94. Zhang, D., Hu, X., Qian, L., O’Callaghan, J. P. & Hong, J. S. Astrogliosis in CNS pathologies: Is there a role for microglia? in *Molecular Neurobiology* 41, 232–241 (Humana Press, 2010).
  95. Zhao, Z. et al. Overexpression of glial cell line-derived neurotrophic factor in the CNS rescues motoneurons from programmed cell death and promotes their long-term survival following axotomy. *Exp. Neurol.* 190, 356–72 (2004).
  96. Cohen-Cory, S., Kidane, A. H., Shirkey, N. J. & Marshak, S. Brain-derived neurotrophic factor and the development of structural neuronal connectivity. *Developmental Neurobiology* 70, 271–288 (2010).
  97. Liu, Q. R. et al. Human brain derived neurotrophic factor (BDNF) genes, splicing patterns, and assessments of associations with substance abuse and Parkinson’s disease. *Am. J. Med. Genet. - Neuropsychiatr. Genet.* 134 B, 93–103 (2005).
  98. Pattabiraman, P. P. et al. Neuronal activity regulates the developmental expression and subcellular localization of cortical BDNF mRNA isoforms in vivo. *Mol. Cell. Neurosci.* 28, 556–570 (2005).
  99. Gonzalez, A., Moya-Alvarado, G., Gonzalez-Billaut, C. & Bronfman, F. C. Cellular and molecular mechanisms regulating neuronal growth by brain-derived neurotrophic factor. *Cytoskeleton* 73, 612–628 (2016).
  100. Kumar, V., Zhang, M. X., Swank, M. W., Kunz, J. & Wu, G. Y. Regulation of dendritic morphogenesis by Ras-PI3K-Akt-mTOR and Ras-MAPK signaling pathways. *J. Neurosci.* 25, 11288–11299 (2005).
  101. Reichardt, L. F. Neurotrophin-regulated signalling pathways. *Philosophical Transactions of the Royal Society B: Biological Sciences* 361, 1545–1564 (2006).
  102. Junhee Seok et al. Genomic responses in mouse models poorly mimic human inflammatory diseases. *Proc. Natl. Acad. Sci. U. S. A.* 110, 3507–3512 (2013).
  103. Li, X., Bao, X. & Wang, R. Experimental models of Alzheimer’s disease for deciphering the pathogenesis and therapeutic screening (Review). *Int. J. Mol. Med.* 37, 271–83 (2015).
  104. Neha, Sodhi, R. K., Jaggi, A. S. & Singh, N. Animal models of dementia and cognitive dysfunction. *Life Sci.* 109, 73–86 (2014).
  105. Jean, Y. Y., Baleriola, J., Fà, M., Hengst, U. & Troy, C. M. Stereotaxic Infusion of Oligomeric Amyloid-beta into the Mouse Hippocampus. *J. Vis. Exp.* 52805 (2015).
  106. Morroni, F., Sita, G., Tarozzi, A., Rimondini, R. & Hrelia, P. Early effects of A $\beta$ 1-42 oligomers injection in mice: Involvement of PI3K/Akt/GSK3 and

- MAPK/ERK1/2 pathways. *Behav. Brain Res.* 314, 106–115 (2016).
107. Takahashi, K., Okita, K., Nakagawa, M. & Yamanaka, S. Induction of pluripotent stem cells from fibroblast cultures. *Nat. Protoc.* 2, 3081–3089 (2007).
  108. Bellin, M., Marchetto, M. C., Gage, F. H. & Mummery, C. L. Induced pluripotent stem cells: the new patient? *Nat. Rev. Mol. Cell Biol.* 13, 713–726 (2012).
  109. Sander, J. D. & Joung, J. K. CRISPR-Cas systems for editing, regulating and targeting genomes. *Nat. Biotechnol.* 32, 347–355 (2014).
  110. Chen, A. E. et al. Optimal Timing of Inner Cell Mass Isolation Increases the Efficiency of Human Embryonic Stem Cell Derivation and Allows Generation of Sibling Cell Lines. *Cell Stem Cell* 4, 103–106 (2009).
  111. Tomoda, K. et al. Derivation Conditions Impact X-Inactivation Status in Female Human Induced Pluripotent Stem Cells. *Cell Stem Cell* 11, 91–99 (2012).
  112. Ohi, Y. et al. Incomplete DNA methylation underlies a transcriptional memory of somatic cells in human iPS cells. *Nat. Cell Biol.* 13, 541–549 (2011).
  113. Boulting, G. L. et al. A functionally characterized test set of human induced pluripotent stem cells. *Nat. Biotechnol.* 29, 279–286 (2011).
  114. Bock, C. et al. Reference Maps of human ES and iPS cell variation enable high-throughput characterization of pluripotent cell lines. *Cell* 144, 439–52 (2011).
  115. Ding, Q. et al. A TALEN genome-editing system for generating human stem cell-based disease models. *Cell Stem Cell* 12, 238–51 (2013).
  116. Veres, A. et al. Low Incidence of Off-Target Mutations in Individual CRISPR-Cas9 and TALEN Targeted Human Stem Cell Clones Detected by Whole-Genome Sequencing. *Cell Stem Cell* 15, 27–30 (2014).
  117. Cruchaga, C. et al. GWAS of Cerebrospinal Fluid Tau Levels Identifies Risk Variants for Alzheimer’s Disease. *Neuron* 78, 256–268 (2013).
  118. Jia, P., Wang, L., Meltzer, H. Y. & Zhao, Z. Common variants conferring risk of schizophrenia: a pathway analysis of GWAS data. *Schizophr. Res.* 122, 38–42 (2010).
  119. Identification of risk loci with shared effects on five major psychiatric disorders: a genome-wide analysis. *Lancet* 381, 1371–1379 (2013).
  120. Haque, A., Engel, J., Teichmann, S. A. & Lönnberg, T. A practical guide to single-cell RNA-sequencing for biomedical research and clinical applications. *Genome Med.* 9, 75 (2017).
  121. Di Giorgio, F. P., Carrasco, M. A., Siao, M. C., Maniatis, T. & Eggan, K. Non-cell autonomous effect of glia on motor neurons in an embryonic stem cell-based ALS model. *Nat. Neurosci.* 10, 608–14 (2007).
  122. Lobsiger, C. S. & Cleveland, D. W. Glial cells as intrinsic components of non-cell-autonomous neurodegenerative disease. *Nat. Neurosci.* 10, 1355–1360 (2007).
  123. Singh, S. K., Grimaud, R., Hoskins, J. R., Wickner, S. & Maurizi, M. R. Unfolding and internalization of proteins by the ATP-dependent proteases ClpXP and ClpAP. *Proc. Natl. Acad. Sci. U. S. A.* 97, 8898–903 (2000).
  124. Vodyanik, M. A., Thomson, J. A. & Slukvin, I. I. Leukosialin (CD43) defines hematopoietic progenitors in human embryonic stem cell differentiation cultures. *Blood* 108, 2095–105 (2006).
  125. Bartus, R. T., Dean, R. L., Beer, B. & Lippa, A. S. The cholinergic hypothesis of

- geriatric memory dysfunction. *Science* 217, 408–417 (1982).
126. Birks, J. Cholinesterase inhibitors for Alzheimer's disease. *Cochrane Database of Systematic Reviews* (2006). doi:10.1002/14651858.CD005593
  127. Livingston, G. et al. Dementia prevention, intervention, and care. *The Lancet* 390, 2673–2734 (2017).
  128. McShane, R., Areosa Sastre, A. & Minakaran, N. Memantine for dementia. *Cochrane Database Syst. Rev.* (2006). doi:10.1002/14651858.cd003154.pub5
  129. Winslow, B. T., Onysko, M. K., Stob, C. M. & Hazlewood, K. A. Treatment of Alzheimer disease. *Am. Fam. Physician* 83, 1403–12 (2011).
  130. Hrelia, P. et al. Common Protective Strategies in Neurodegenerative Disease: Focusing on Risk Factors to Target the Cellular Redox System. *Oxidative Medicine and Cellular Longevity* 2020, (2020).
  131. Moosavi, F., Hosseini, R., Saso, L. & Firuzi, O. Modulation of neurotrophic signaling pathways by polyphenols. *Drug Design, Development and Therapy* 10, 23–42 (2015).
  132. Gustafson, D. R. et al. New Perspectives on Alzheimer's Disease and Nutrition. in *Journal of Alzheimer's Disease* 46, 1111–1127 (IOS Press, 2015).
  133. Blennow, K., de Leon, M. J. & Zetterberg, H. Alzheimer's disease. *Lancet* (London, England) 368, 387–403 (2006).
  134. Mattila, P. & Kumpulainen, J. Determination of free and total phenolic acids in plant-derived foods by HPLC with diode-array detection. *J. Agric. Food Chem.* 50, 3660–3667 (2002).
  135. Zduńska, K., Dana, A., Kolodziejczak, A. & Rotsztein, H. Antioxidant properties of ferulic acid and its possible application. *Skin Pharmacology and Physiology* 31, 332–336 (2018).
  136. Tee-Ngam, P., Nunant, N., Rattanarat, P., Siangproh, W. & Chailapakul, O. Simple and rapid determination of ferulic acid levels in food and cosmetic samples using paper-based platforms. *Sensors (Switzerland)* 13, 13039–13053 (2013).
  137. Rice-Evans, C. A., Miller, N. J. & Paganga, G. Antioxidant properties of phenolic compounds. *Trends in Plant Science* 2, 152–159 (1997).
  138. Lodovici, M., Guglielmi, F., Meoni, M. & Dolaro, P. Effect of natural phenolic acids on DNA oxidation in vitro. *Food Chem. Toxicol.* 39, 1205–1210 (2001).
  139. Doody, R. S., Tariot, P. N., Pfeiffer, E., Olin, J. T. & Graham, S. M. Meta-analysis of six-month memantine trials in Alzheimer's disease. *Alzheimers Dement* 3, 7–17 (2007).
  140. Schmitt, B., Bernhardt, T., Moeller, H. J., Heuser, I. & Frölich, L. Combination Therapy in Alzheimer's Disease. *CNS Drugs* 18, 827–844 (2004).
  141. Ismaili, L. et al. Multitarget compounds bearing tacrine- and donepezil-like structural and functional motifs for the potential treatment of Alzheimer's disease. *Progress in Neurobiology* 151, 4–34 (2017).
  142. Luo, Z. et al. Synthesis and evaluation of multi-target-directed ligands against Alzheimer's disease based on the fusion of donepezil and ebselen. *J. Med. Chem.* 56, 9089–9099 (2013).
  143. Benchekroun, M. et al. Donepezil-ferulic acid hybrids as anti-Alzheimer drugs. *Future Med. Chem.* 7, 15–21 (2015).

144. Xie, S. S. et al. Design, synthesis and biological evaluation of novel donepezil-coumarin hybrids as multi-target agents for the treatment of Alzheimer's disease. *Bioorganic Med. Chem.* 24, 1528–1539 (2016).
145. Chen, S. Y. et al. Design, synthesis, and biological evaluation of curcumin analogues as multifunctional agents for the treatment of Alzheimer's disease. *Bioorganic Med. Chem.* 19, 5596–5604 (2011).
146. Fang, L., Gou, S., Liu, X., Cao, F. & Cheng, L. Design, synthesis and anti-Alzheimer properties of dimethylaminomethyl- substituted curcumin derivatives. *Bioorganic Med. Chem. Lett.* 24, 40–43 (2014).
147. Ono, K., Hasegawa, K., Naiki, H. & Yamada, M. Curcumin Has Potent Anti-Amyloidogenic Effects for Alzheimer's  $\beta$ -Amyloid Fibrils In Vitro. *J. Neurosci. Res.* 75, 742–750 (2004).
148. Dias, K. S. T. et al. Design, synthesis and evaluation of novel feruloyl-donepezil hybrids as potential multitarget drugs for the treatment of Alzheimer's disease. *Eur. J. Med. Chem.* 130, 440–457 (2017).
149. LaFerla, F. M., Green, K. N. & Oddo, S. Intracellular amyloid- $\beta$  in Alzheimer's disease. *Nat. Rev. Neurosci.* 8, 499–509 (2007).
150. Hamaguchi, T., Ono, K. & Yamada, M. REVIEW: Curcumin and Alzheimer's disease. *CNS Neurosci Ther* 16, 285–97 (2010).
151. Sgarbossa, A., Giacomazza, D. & di Carlo, M. Ferulic Acid: A Hope for Alzheimer's Disease Therapy from Plants. *Nutrients* 7, 5764–82 (2015).
152. Kim, W. S. et al. Deletion of Abca7 Increases Cerebral Amyloid- Accumulation in the J20 Mouse Model of Alzheimer's Disease. *J. Neurosci.* 33, 4387–4394 (2013).
153. Aikawa, T., Holm, M. L. & Kanekiyo, T. ABCA7 and pathogenic pathways of Alzheimer's disease. *Brain Sciences* 8, 27 (MDPI AG, 2018).
154. Hollingworth, P. et al. Common variants at ABCA7, MS4A6A/MS4A4E, EPHA1, CD33 and CD2AP are associated with Alzheimer's disease. *Nat. Genet.* 43, 429–436 (2011).
155. Steinberg, S. et al. Loss-of-function variants in ABCA7 confer risk of Alzheimer's disease. *Nat. Genet.* 47, 445–447 (2015).
156. Dias, K. S. T. et al. Design, synthesis and evaluation of novel feruloyl-donepezil hybrids as potential multitarget drugs for the treatment of Alzheimer's disease. *Eur J Med Chem* 130, 440–457 (2017).
157. Furukawa-Hibi, Y. et al. Butyrylcholinesterase inhibitors ameliorate cognitive dysfunction induced by amyloid- $\beta$  peptide in mice. *Behav Brain Res* 225, 222–229 (2011).
158. Tarozzi, A. et al. Cyanidin 3-O-glucopyranoside protects and rescues SH-SY5Y cells against amyloid-beta peptide-induced toxicity. *Neuroreport* 19, 1483–6 (2008).
159. Hong, H. S. et al. Combining the rapid MTT formazan exocytosis assay and the MC65 protection assay led to the discovery of carbazole analogs as small molecule inhibitors of A $\beta$  oligomer-induced cytotoxicity. *Brain Res* 1130, 223–234 (2007).
160. Maezawa, I. et al. Congo red and thioflavin-T analogs detect A $\beta$  oligomers. *J Neurochem* 104, 457–468 (2008).

161. Morroni, F. et al. Neuroprotective effect of caffeic acid phenethyl ester in a mouse model of Alzheimer's disease involves Nrf2/HO-1 pathway. *Aging Dis* (2018). doi:10.14336/AD.2017.0903
162. Sarter, M., Bodewitz, G. & Stephens, D. N. Attenuation of scopolamine-induced impairment of spontaneous alteration behaviour by antagonist but not inverse agonist and agonist beta-carbolines. *Psychopharmacology (Berl)*. 94, 491–5 (1988).
163. Lopes, I. S. et al. Riparin II ameliorates corticosterone-induced depressive-like behavior in mice: Role of antioxidant and neurotrophic mechanisms. *Neurochem Int* 120, 33–42 (2018).
164. Bradford, M. M. A rapid and sensitive method for the quantitation of microgram quantities of protein utilizing the principle of protein-dye binding. *Anal Biochem* 72, 248–54 (1976).
165. Movsesyan, V. A., Yakovlev, A. G., Dabaghyan, E. A., Stoica, B. A. & Faden, A. I. Ceramide induces neuronal apoptosis through the caspase-9/caspase-3 pathway. *Biochem Biophys Res Commun* 299, 201–207 (2002).
166. Morroni, F., Sita, G., Tarozzi, A., Cantelli-Forti, G. & Hrelia, P. Neuroprotection by 6-(methylsulfinyl)hexyl isothiocyanate in a 6-hydroxydopamine mouse model of Parkinson's disease. *Brain Res.* 1589, 93–104 (2014).
167. Morroni, F. et al. Protective effects of 6-(methylsulfinyl)hexyl isothiocyanate on A $\beta$ 1-42-induced cognitive deficit, oxidative stress, inflammation, and apoptosis in mice. *Int. J. Mol. Sci.* 19, 2083 (2018).
168. Morroni, F., Sita, G., Tarozzi, A., Rimondini, R. & Hrelia, P. Early effects of A $\beta$ 1-42 oligomers injection in mice: Involvement of PI3K/Akt/GSK3 and MAPK/ERK1/2 pathways. *Behav Brain Res* 314, 106–115 (2016).
169. Fischer, A. H., Jacobson, K. A., Rose, J. & Zeller, R. Hematoxylin and eosin staining of tissue and cell sections. *Cold Spring Harb Prot* 3, 3–5 (2008).
170. Cenini, G., Sultana, R., Memo, M. & Butterfield, D. A. Elevated levels of pro-apoptotic p53 and its oxidative modification by the lipid peroxidation product, HNE, in brain from subjects with amnesic mild cognitive impairment and Alzheimer's disease. *J Cell Mol Med* 12, 987–994 (2008).
171. Ohyagi, Y. et al. Intracellular A $\beta$ 42 activates p53 promoter: a pathway to neurodegeneration in Alzheimer's disease. *FASEB J* 19, 255–257 (2005).
172. Reddy, P. H. & Beal, M. F. Are mitochondria critical in the pathogenesis of Alzheimer's disease? *Brain Res. Brain Res. Rev.* 49, 618–32 (2005).
173. Chen, J. X. & Yan, S. Du. Amyloid- $\beta$ -induced mitochondrial dysfunction. *J. Alzheimers. Dis.* 12, 177–84 (2007).
174. Dringen, R. Metabolism and functions of glutathione in brain. *Prog. Neurobiol.* 62, 649–71 (2000).
175. Lipton, S. A. et al. Therapeutic advantage of pro-electrophilic drugs to activate the Nrf2/ARE pathway in Alzheimer's disease models. *Cell Death Dis.* 7, e2499 (2016).
176. Liu, X. J., Wei, J., Shang, Y. H., Huang, H. C. & Lao, F. X. Modulation of A $\beta$ PP and GSK3 $\beta$  by endoplasmic reticulum stress and involvement in Alzheimer's disease. *J. Alzheimers. Dis.* 57, 1157–1170 (2017).
177. Li, J. et al. Methyl salicylate lactoside protects neurons ameliorating cognitive

- disorder through inhibiting amyloid beta-induced neuroinflammatory response in Alzheimer's disease. *Front. Aging Neurosci.* 10, 85 (2018).
178. Griffin, W. S. T. Inflammation and neurodegenerative diseases. *Am. J. Clin. Nutr.* 83, 470S-474S (2006).
  179. Kuczewski, N., Porcher, C., Lessmann, V., Medina, I. & Gaiarsa, J. L. Activity-Dependent Dendritic Release of BDNF and Biological Consequences. *Mol Neurobiol* 39, 37–49 (2009).
  180. Broadbent, N. J., Squire, L. R. & Clark, R. E. Spatial memory, recognition memory, and the hippocampus. *P Natl Acad Sci* 101, 14515–14520 (2004).
  181. Ghumatkar, P. J., Patil, S. P., Jain, P. D., Tambe, R. M. & Sathaye, S. Nootropic, neuroprotective and neurotrophic effects of phloretin in scopolamine induced amnesia in mice. *Pharmacol Biochem Behav* 135, 182–191 (2015).
  182. Okamoto, M. et al. Riluzole reduces amyloid beta pathology, improves memory, and restores gene expression changes in a transgenic mouse model of early-onset Alzheimer's disease. *Transl Psychiat* 8, 153 (2018).
  183. Kim, H. G. et al. Donepezil inhibits the amyloid-beta oligomer-induced microglial activation in vitro and in vivo. *Neurotoxicology* 40, 23–32 (2014).
  184. Kirshenbaum, G. S., Dachtler, J., Roder, J. C. & Clapcote, S. J. Characterization of cognitive deficits in mice with an alternating hemiplegia-linked mutation. *Behav Neurosci* 129, 822–31 (2015).
  185. Meunier, J., Ieni, J. & Maurice, T. The anti-amnesic and neuroprotective effects of donepezil against amyloid beta<sub>25-35</sub> peptide-induced toxicity in mice involve an interaction with the sigma<sub>1</sub> receptor. *Br J Pharmacol* 149, 998–1012 (2006).
  186. Hu, D. et al. Deoxyschizandrin Isolated from the Fruits of *Schisandra chinensis* Ameliorates Aβ<sub>1-42</sub>-induced Memory Impairment in Mice. *Planta Med* 78, 1332–1336 (2012).
  187. Obulesu, M. & Lakshmi, M. J. Apoptosis in Alzheimer's Disease: An Understanding of the Physiology, Pathology and Therapeutic Avenues. *Neurochem Res* 39, 2301–2312 (2014).
  188. Ramalho, R. M., Viana, R. J. S., Low, W. C., Steer, C. J. & Rodrigues, C. M. P. Bile acids and apoptosis modulation: an emerging role in experimental Alzheimer's disease. *Trends Mol Med* 14, 54–62 (2008).
  189. Klein, W. Synaptotoxic amyloid-β oligomers: a molecular basis for the cause, diagnosis, and treatment of Alzheimer's disease? *J. Alzheimers. Dis.* 33 Suppl 1, S49-65 (2013).
  190. Yuan, J. & Yankner, B. A. Apoptosis in the nervous system. *Nature* 407, 802–9 (2000).
  191. Yu, W., Mechawar, N., Krantic, S. & Quirion, R. Evidence for the involvement of apoptosis-inducing factor-mediated caspase-independent neuronal death in Alzheimer disease. *Am. J. Pathol.* 176, 2209–2218 (2010).
  192. Tarozzi, A. et al. Guanosine protects human neuroblastoma cells from oxidative stress and toxicity induced by Amyloid-beta peptide oligomers. *J. Biol. Regul. Homeost. Agents* 24, 297–306 (2010).
  193. Cheng, N., Jiao, S., Gumaste, A., Bai, L. & Belluscio, L. APP Overexpression Causes Aβ-Independent Neuronal Death through Intrinsic Apoptosis Pathway. *eNeuro* 3, 1–12 (2016).

194. de Calignon, A. et al. Caspase activation precedes and leads to tangles. *Nature* 464, 1201–4 (2010).
195. Galimberti, D. & Scarpini, E. Disease-modifying treatments for Alzheimer's disease. *Ther. Adv. Neurol. Disord.* 4, 203–16 (2011).
196. Szybińska, A. & Leśniak, W. P53 Dysfunction in Neurodegenerative Diseases - The Cause or Effect of Pathological Changes? *Aging Dis* 8, 506–518 (2017).
197. Watcharavit, P. et al. Direct, activating interaction between glycogen synthase kinase-3 and p53 after DNA damage. *P Natl Acad Sci* 99, 7951–7955 (2002).
198. Markesbery, W. R. Oxidative stress hypothesis in Alzheimer's disease. *Free Radic. Biol. Med.* 23, 134–47 (1997).
199. Philippens, I. H. et al. Acceleration of amyloidosis by inflammation in the amyloid-beta Marmoset monkey model of Alzheimer's disease. *J. Alzheimers. Dis.* 55, 101–113 (2017).
200. Zhong, S.-Z., Ge, Q. H., Li, Q., Qu, R. & Ma, S. P. Peoniflorin attenuates A $\beta$ (1-42)-mediated neurotoxicity by regulating calcium homeostasis and ameliorating oxidative stress in hippocampus of rats. *J. Neurol. Sci.* 280, 71–8 (2009).
201. Bonet-Costa, V., Pomatto, L. C. D. & Davies, K. J. A. The proteasome and oxidative stress in Alzheimer's disease. *Antioxid. Redox Signal.* 25, 886–901 (2016).
202. Branca, C. et al. Genetic reduction of Nrf2 exacerbates cognitive deficits in a mouse model of Alzheimer's disease. *Hum. Mol. Genet.* 26, 4823–4835 (2017).
203. Suh, J. H. et al. Decline in transcriptional activity of Nrf2 causes age-related loss of glutathione synthesis, which is reversible with lipoic acid. *P Natl Acad Sci* 101, 3381–3386 (2004).
204. Kim, H. V. et al. Amelioration of Alzheimer's disease by neuroprotective effect of sulforaphane in animal model. *Amyloid* 20, 7–12 (2013).
205. Chiang, M. C., Nicol, C. J. & Cheng, Y. C. Resveratrol activation of AMPK-dependent pathways is neuroprotective in human neural stem cells against amyloid-beta-induced inflammation and oxidative stress. *Neurochem. Int.* 115, 1–10 (2018).
206. Rong, H., Liang, Y. & Niu, Y. Rosmarinic acid attenuates  $\beta$ -amyloid-induced oxidative stress via Akt/GSK-3 $\beta$ /Fyn-mediated Nrf2 activation in PC12 cells. *Free Radic. Biol. Med.* 120, 114–123 (2018).
207. de Freitas Silva, M. et al. The Keap1/Nrf2-ARE Pathway as a Pharmacological Target for Chalcones. *Molecules* 23, 1803 (2018).
208. Arendt, T., Holzer, M., Grossmann, A., Zedlick, D. & Brückner, M. K. Increased expression and subcellular translocation of the mitogen activated protein kinase and mitogen-activated protein kinase in Alzheimer's disease. *Neuroscience* 68, 5–18 (1995).
209. Gärtner, U., Holzer, M., Heumann, R. & Arendt, T. Induction of p21ras in Alzheimer pathology. *Neuroreport* 6, 1441–4 (1995).
210. Kim, S. W. et al. Extracellular HMGB1 released by NMDA treatment confers neuronal apoptosis via RAGE-p38 MAPK/ERK signaling pathway. *Neurotox. Res.* 20, 159–69 (2011).
211. Musgrove, R. E. J., King, A. E. & Dickson, T. C.  $\alpha$ -Synuclein protects neurons

- from apoptosis downstream of free-radical production through modulation of the MAPK signalling pathway. *Neurotox. Res.* 23, 358–69 (2013).
212. Ito, Y., Oh-Hashi, K., Kiuchi, K. & Hirata, Y. p44/42 MAP kinase and c-Jun N-terminal kinase contribute to the up-regulation of caspase-3 in manganese-induced apoptosis in PC12 cells. *Brain Res.* 1099, 1–7 (2006).
  213. Knowles, H. et al. Transient Receptor Potential Melastatin 2 (TRPM2) ion channel is required for innate immunity against *Listeria monocytogenes*. *Proc. Natl. Acad. Sci. U. S. A.* 108, 11578–83 (2011).
  214. Zhu, X., Lee, H., Raina, A. K., Perry, G. & Smith, M. A. The Role of Mitogen-Activated Protein Kinase Pathways in Alzheimer's Disease. *Neurosignals* 11, 270–281 (2002).
  215. Gan, X. et al. Inhibition of ERK-DLP1 signaling and mitochondrial division alleviates mitochondrial dysfunction in Alzheimer's disease cybrid cell. *Biochim biophys Acta* 1842, 220–31 (2014).
  216. Chang, K. W. et al. Activation of  $\alpha 7$  nicotinic acetylcholine receptor alleviates A $\beta$ 1-42-induced neurotoxicity via downregulation of p38 and JNK MAPK signaling pathways. *Neurochem Int* 120, 238–250 (2018).
  217. Chong, Y. H. et al. ERK1/2 Activation Mediates A $\beta$  Oligomer-induced Neurotoxicity via Caspase-3 Activation and Tau Cleavage in Rat Organotypic Hippocampal Slice Cultures. *J Biol Chem* 281, 20315–20325 (2006).
  218. Kim, T. I. et al. l-Theanine, an amino acid in green tea, attenuates  $\beta$ -amyloid-induced cognitive dysfunction and neurotoxicity: Reduction in oxidative damage and inactivation of ERK/p38 kinase and NF- $\kappa$ B pathways. *Free Radic Biol Med* 47, 1601–1610 (2009).
  219. Goedert, M. & Spillantini, M. G. A Century of Alzheimer's Disease. *Science* (80-). 314, 777–781 (2006).
  220. Kim, J. & Wong, P. K. Y. Oxidative Stress Is Linked to ERK1/2-p16 Signaling-mediated Growth Defect in ATM-deficient Astrocytes. *J Biol Chem* 284, 14396–14404 (2009).
  221. Lee, Y. K. et al. 4-O-methylhonokiol attenuated  $\beta$ -amyloid-induced memory impairment through reduction of oxidative damages via inactivation of p38 MAP kinase. *J Nutr Biochem* 22, 476–486 (2011).
  222. Butterfield, D. A. Amyloid beta-peptide (1-42)-induced oxidative stress and neurotoxicity: implications for neurodegeneration in Alzheimer's disease brain. A review. *Free Radic. res* 36, 1307–13 (2002).
  223. Konar, A. et al. Protective Role of Ashwagandha Leaf Extract and Its Component Withanone on Scopolamine-Induced Changes in the Brain and Brain-Derived Cells. *PLoS One* 6, e27265 (2011).
  224. Nagahara, A. H. et al. Neuroprotective effects of brain-derived neurotrophic factor in rodent and primate models of Alzheimer's disease. *Nat Med* 15, 331–337 (2009).
  225. Aid, T., Kazantseva, A., Piirsoo, M., Palm, K. & Timmusk, T. Mouse and rat BDNF gene structure and expression revisited. *J Neurosci Res* 85, 525–535 (2007).
  226. An, J. J. et al. Distinct role of long 3' UTR BDNF mRNA in spine morphology and synaptic plasticity in hippocampal neurons. *Cell* 134, 175–187 (2008).

227. Zlokovic, B. V. Neurodegeneration and the neurovascular unit. *Nat. Med.* 16, 1370–1371 (2010).
228. Musiek, E. S. & Holtzman, D. M. Three dimensions of the amyloid hypothesis: time, space and “wingmen”. *Nat. Neurosci.* 18, 800–6 (2015).
229. Löscher, W. & Potschka, H. Blood-brain barrier active efflux transporters: ATP-binding cassette gene family. *NeuroRx* 2, 86–98 (2005).
230. Behl, T. et al. The Interplay of ABC Transporters in A $\beta$  Translocation and Cholesterol Metabolism: Implicating Their Roles in Alzheimer’s Disease. *Molecular Neurobiology* 1–19 (2020). doi:10.1007/s12035-020-02211-x
231. Lambert, J.-C. et al. Meta-analysis of 74,046 individuals identifies 11 new susceptibility loci for Alzheimer’s disease. *Nat. Genet.* 45, 1452–1458 (2013).
232. Kim, W. S., Weickert, C. S. & Garner, B. Role of ATP-binding cassette transporters in brain lipid transport and neurological disease. *J. Neurochem.* 104, 1145–1166 (2008).
233. Vasquez, J. B., Fardo, D. W. & Estus, S. ABCA7 expression is associated with Alzheimer’s disease polymorphism and disease status. *Neurosci. Lett.* 556, 58–62 (2013).
234. Wang, H. et al. One-Step Generation of Mice Carrying Mutations in Multiple Genes by CRISPR/Cas-Mediated Genome Engineering. *Cell* 153, 910–918 (2013).
235. Iwamoto, N., Abe-Dohmae, S., Sato, R. & Yokoyama, S. ABCA7 expression is regulated by cellular cholesterol through the SREBP2 pathway and associated with phagocytosis. *J. Lipid Res.* 47, 1915–1927 (2006).
236. Jehle, A. W. et al. ATP-binding cassette transporter A7 enhances phagocytosis of apoptotic cells and associated ERK signaling in macrophages. *J. Cell Biol.* 174, 547–556 (2006).
237. Calcoen, D., Elias, L. & Yu, X. What does it take to produce a breakthrough drug? *Nat. Rev. Drug Discov.* 14, 161–162 (2015).
238. Pereira, C. D., Martins, F., Wiltfang, J., Da Cruz E Silva, O. A. B. & Rebelo, S. ABC Transporters Are Key Players in Alzheimer’s Disease. *Journal of Alzheimer’s Disease* 61, 463–485 (2017).
239. Wolf, A., Bauer, B. & Hartz, A. M. S. ABC Transporters and the Alzheimer’s Disease Enigma. *Front. Psychiatry* 3, (2012).
240. Subramanian, A. et al. Gene set enrichment analysis: A knowledge-based approach for interpreting genome-wide expression profiles. *Proc. Natl. Acad. Sci. U. S. A.* 102, 15545–15550 (2005).
241. Schindelin, J. et al. Fiji: an open-source platform for biological-image analysis. *Nat. Methods* 9, 676–82 (2012).
242. Sidoryk-Wegrzynowicz, M. et al. Astrocytes in mouse models of tauopathies acquire early deficits and lose neurosupportive functions. *Acta Neuropathol. Commun.* 5, 89 (2017).
243. Farhy-Tselnicker, I. & Allen, N. J. Astrocytes, neurons, synapses: a tripartite view on cortical circuit development. *Neural Dev.* 13, 7 (2018).
244. Lin, Y. T. et al. APOE4 Causes Widespread Molecular and Cellular Alterations Associated with Alzheimer’s Disease Phenotypes in Human iPSC-Derived Brain Cell Types. *Neuron* 98, 1141-1154.e7 (2018).

245. Koistinaho, M. et al. Apolipoprotein E promotes astrocyte colocalization and degradation of deposited amyloid- $\beta$  peptides. *Nat. Med.* 10, 719–726 (2004).
246. Nielsen, H. M. et al. Astrocytic A $\beta$ 1-42 uptake is determined by A $\beta$ -aggregation state and the presence of amyloid-associated proteins. *Glia* 58, n/a-n/a (2010).
247. Wyss-Coray, T. et al. Adult mouse astrocytes degrade amyloid- $\beta$  in vitro and in situ. *Nat. Med.* 9, 453–457 (2003).
248. Sakae, N. et al. ABCA7 Deficiency Accelerates Amyloid- $\beta$  Generation and Alzheimer's Neuronal Pathology. *J. Neurosci.* 36, 3848–59 (2016).
249. Loregger, A. et al. Haploid mammalian genetic screen identifies UBXD8 as a key determinant of HMGCR degradation and cholesterol biosynthesis. *Arterioscler. Thromb. Vasc. Biol.* 37, 2064–2074 (2017).
250. Olzmann, J. A. & Carvalho, P. Dynamics and functions of lipid droplets. *Nat. Rev. Mol. Cell Biol.* 20, 137–155 (2019).
251. Mosher, K. I. & Wyss-Coray, T. Microglial dysfunction in brain aging and Alzheimer's disease. *Biochem. Pharmacol.* 88, 594–604 (2014).
252. Tanaka, N., Abe-Dohmae, S., Iwamoto, N., Fitzgerald, M. L. & Yokoyama, S. Helical apolipoproteins of high-density lipoprotein enhance phagocytosis by stabilizing ATP-binding cassette transporter A7. *J. Lipid Res.* 51, 2591–9 (2010).
253. Haass, C., Kaether, C., Thinakaran, G. & Sisodia, S. Trafficking and Proteolytic Processing of APP. *Cold Spring Harb. Perspect. Med.* 2, a006270–a006270 (2012).
254. Chan, S. L. et al. ATP-binding cassette transporter A7 regulates processing of amyloid precursor protein in vitro. *J. Neurochem.* 106, 793–804 (2008).
255. Satoh, K., Abe-Dohmae, S., Yokoyama, S., St George-Hyslop, P. & Fraser, P. E. ATP-binding cassette transporter A7 (ABCA7) loss of function alters Alzheimer amyloid processing. *J. Biol. Chem.* 290, 24152–65 (2015).
256. Ewers, H. & Helenius, A. Lipid-mediated endocytosis. *Cold Spring Harb. Perspect. Biol.* 3, a004721 (2011).
257. Chakraborty, A. & Jana, N. R. Clathrin to Lipid Raft-Endocytosis via Controlled Surface Chemistry and Efficient Perinuclear Targeting of Nanoparticle. *J. Phys. Chem. Lett.* 6, 3688–3697 (2015).
258. van Meer, G., Voelker, D. R. & Feigenson, G. W. Membrane lipids: where they are and how they behave. *Nat. Rev. Mol. Cell Biol.* 9, 112–124 (2008).
259. Kim, J., Basak, J. M. & Holtzman, D. M. The role of apolipoprotein E in Alzheimer's disease. *Neuron* 63, 287–303 (2009).
260. Liu, C.-C., Liu, C.-C., Kanekiyo, T., Xu, H. & Bu, G. Apolipoprotein E and Alzheimer disease: risk, mechanisms and therapy. *Nat. Rev. Neurol.* 9, 106–18 (2013).
261. Linsel-Nitschke, P. et al. Potential role of ABCA7 in cellular lipid efflux to apoA-I. *J. Lipid Res.* 46, 86–92 (2005).
262. Hayashi, M., Abe-Dohmae, S., Okazaki, M., Ueda, K. & Yokoyama, S. Heterogeneity of high density lipoprotein generated by ABCA1 and ABCA7. *J. Lipid Res.* 46, 1703–1711 (2005).
263. Wang, N. et al. ATP-binding cassette transporter A7 (ABCA7) binds apolipoprotein A-I and mediates cellular phospholipid but not cholesterol efflux. *J. Biol. Chem.* 278, 42906–12 (2003).

264. Abe-Dohmae, S. et al. Human ABCA7 Supports Apolipoprotein-mediated Release of Cellular Cholesterol and Phospholipid to Generate High Density Lipoprotein. *J. Biol. Chem.* 279, 604–611 (2004).
265. Nowyhed, H. N. et al. ATP Binding Cassette Transporter ABCA7 Regulates NKT Cell Development and Function by Controlling CD1d Expression and Lipid Raft Content. *Sci. Rep.* 7, 40273 (2017).
266. Kielar, D. et al. Adenosine Triphosphate Binding Cassette (ABC) Transporters Are Expressed and Regulated During Terminal Keratinocyte Differentiation: A Potential Role for ABCA7 in Epidermal Lipid Reorganization. *J. Invest. Dermatol.* 121, 465–474 (2003).